2012

SYNTHESIS AND BIOLOGICAL EVALUATION OF SECOND GENERATION ANIBAMINE ANALOGUES AS NOVEL ANTI-PROSTATE CANCER AGENTS

Shilpa Singh
Virginia Commonwealth University

SYNTHESIS AND BIOLOGICAL SCREENING OF SECOND GENERATION ANIBAMINE ANALOGUES AS NOVEL ANTI-PROSTATE CANCER AGENTS

A Dissertation submitted in partial fulfillment of the requirements for the degree of Master of Science at Virginia Commonwealth University.

by

SHILPA SINGH
Bachelor of Pharmacy, Mumbai University, India, 2008

Director: DR. YAN ZHANG

ASSOCIATE PROFESSOR OF MEDICINAL CHEMISTRY

Virginia Commonwealth University
Richmond, Virginia
May, 2012

Acknowledgement

This project has been made possible due to contributions made by a lot of people. I would like to start off by expressing deepest gratitude for my advisor and mentor Dr. Yan Zhang. Without his support, guidance and encouragement I would not have been able to complete this project. Right from its inception to its final completion he has provided me endless counseling and supervision. He has shown me great patience and given me the opportunity to work in his lab.

I would like to thank my senior colleague Ms. Kendra Haney who held my hand and walked me through my beginning days. She not only helped me gain footing in the chemistry lab work but also providing me with indispensable help in biological screening. I would also like to sincerely thank Ms. Jiannon Wang and Chris Arnatt for their help in tackling the biological screening of my final compounds and Dr. Yunyun Yuan for her help in performing HPLC and other technical problems that I faced during my research. I would like to especially take time to thank Dr. Feng Zhang for always smiling and providing never ending resourcefulness in the lab. I am also very grateful to Dr. Guo Li for giving me the basic platform to base my research project work on.

It has been a great experience working with my fellow lab mates Soundarya, Orgil, Saheem, Yamini. They made my experience an unforgettable one. I would also like to mention my batch colleagues Atul, Hardik, Harsh, Akul, Ronak, Jigar, Sayali, Soumya for always being ready to help me out and making this journey full of fun. I am also deeply indebted to my two roommates Pinky and Suditi for providing me boundless moral support. And lastly I would like to thank my parents and my sister for their inexhaustible patience and for always being my pillar.

A special mention for Department of Medicinal Chemistry and Virginia Commonwealth University for giving me the opportunity to study here and make my contribution towards cancer research. Thank you to all the people mentioned and those that are not named here for preparing me for this accomplishment and all my future successes too.

Table of Contents

Page

Acknowledgements……ii

List of Tables……..vi

List of Figures……vii

List of Schemes..... viii

Abstract…….....ix

Chapter

1. Introduction……1
2. Background……..4

2.1 Prostate carcinoma……..4

2.1.1 Prostate Gland……4

2.1.2 Prostatic Disorder……....5

2.1.3 Prostate Cancer Cell Lines……..7

2.2 Inflammation and Cancer……..11

2.3 Tumor Microenvironment……14

2.3.1 Chemokines……16

2.3.2 Chemokine Receptors……23

2.4 CCR5……27

2.4.1 Structure and Signaling……..27

2.4.2 CCR5 and HIV……..30

2.4.3 CCR5 and Prostate Cancer……....33

2.5 Natural Product as a CCR5 Antagonist.....37

3. Project Objectives and Design.....41

5.1 Design.....48

5.2 Objectives.....53

4. Results and Discussion.....54

4.1 Chemical Synthesis of Second Generation Anibamine Analogues.....54

4.1.1 Synthesis of Key Intermediate **6**.....54

4.1.2 Synthesis of Key Intermediate **14**.....58

4.1.3 Synthesis of Final Compounds.....61

4.2 Biological Screening.....67

4.2.1 Anti-proliferation Assay.....67

4.2.2 Cytotoxicity Assay.....120

4.2.3 Calcium mobilization Assay.....120

5. Experimental Section.....76

5.1 Chemical Synthesis.....76

5.1.1 Synthesis of Intermediates.....76

5.1.2 Synthesis of Final Compounds.....85

5.2 Biological Screening.....114

5.2.1 Anti-proliferation Assay.....114

5.2.2 Cytotoxicity Assay.....115

5.2.3 Calcium mobilization Assay.....116

6. Conclusions..118

7. References...120

List of Tables

Page

Table 1: Comparison between different prostate cancer cell lines……...…….10

Table 2: Expression of various CCL5 receptors in prostate cancer cell lines……...32

Table 3: CCR5 antagonist in clinical trials……....42

Table 4: Different substituents for R…….52

Table 5: Anti-proliferation data of the ten final compounds…….69

Table 6: Cytotoxicity results of the final compounds ..……72

Table 7: Inhibitory effects on CCL5 induced Ca2+mobilization ……...…74

List of Figures

Page

Figure 1: Normal tissue versus cancerous tissue 13

Figure 2: Inflammation in Cancer.....15

Figure 3: Classification of chemokines.....19

Figure 4: Role of chemokines in the tumor-specific immune response.....21

Figure 5: Chemokine receptor signaling pathway 25

Figure 6: Two dimensional schematic representation of CCR5 receptor 28

Figure 7: The RANTES stimulation of DU-145 prostate tumor cell proliferation.....36

Figure 8: TAK 779 & lead compound used to generate TAK 779.....38

Figure 9: Anibamine 40

Figure 10: Effect on anibamine on prostate tumor growth in mice 44

Figure 11: Binding mode of Maraviroc (purple) in homology model of CCR5.....46

Figure 12: Binding mode of anibamine (orange) in homology model of CCR5. 47

Figure 13: The complete synthetic route of anibamine 49

Figure 14: Anibamine as lead compound 50

Figure 15: List of acids used in coupling reaction.....61

Figure 16: Metabolically driven WST-1 cleavage.....68

Figure 17: Structure of **18d and** lead compound anibamine. 71

List of Schemes

Page

Scheme 1: Two routes for synthesis of intermediate **6** 54

Scheme 2: Route 1 for synthesis of intermediate **6** 55

Scheme 3: Route 2 for synthesis of intermediate **6** 56

Scheme 4: Mechanism of Rosenmund-von Braun reation 57

Scheme 5: Synthesis of intermediate **14** 58

Scheme 6: Synthesis of **16** 59

Scheme 7: Amide coupling reaction 62

Scheme 8: Side reactions of the coupling reaction 63

Scheme 9: Deprotection reaction 64

Scheme 10: Cyclization reaction 65

Abstract

SYNTHESIS AND BIOLOGICAL EVALUATION OF SECOND GENERATION ANALOGUES OF ANIBAMINE AS NOVEL ANTI-PROSTATE CANCER AGENTS

By Shilpa Singh, MS

A Dissertation submitted in partial fulfillment of the requirements for the degree of Master's of in Pharmaceutical Science at Virginia Commonwealth University.

Virginia Commonwealth University, 2012

Major Director: Dr. Yan Zhang

Associate Professor, Department of Medicinal Chemistry

Prostate cancer is the most prevalent non-cutaneous cancer among men. Since the 19th century when Virchow first introduced the concept of inflammation in cancer, chemokines and their receptors have garnered a lot of interest. Chemokine receptor CCR5 has been especially implicated in many disease states and recently found to be over expressed in prostate cancer cell lines. Anibamine, a natural CCR5 antagonist discovered in 2004, has been found to have significant anti-prostate cancer activity at

micromolar level. To optimize this compound and also discover a novel pharmacophore, exploration of the original structure was carried out. Significant modifications were made to the side chain in the original structure and ten different analogues were prepared by altering the original synthetic route. While cytotoxicity assay proved the compounds to be non toxic to normal cells, anti-proliferation assay displayed that having a bulky, hydrophobic group in the side chain of the parent compound is essential for the activity. Looking at this data, the third generation of analogues can be prepared that might generate a better lead compound for the treatment of prostate cancer.

INTRODUCTION

Prostate cancer is currently the most common non-cutaneous neoplasm among men in Western countries. According to the latest statistics, prostate cancer accounts for 28% of the newly diagnosed cases of cancer in men. There have been approximately 217,730 estimated cases of prostate cancer in the United States and around 32,050 deaths[1]. Radical prostatectomy or radiation therapy can be used to treat a more localized prostate cancer. However for more advanced cancers, androgen ablation therapy has shown beneficial effects only for hormone-responsive disease. Apart from these, there are new treatment techniques that are still in clinical trials. These include cryosurgery, chemotherapy, biological therapy etc[2]. Prostate cancer cells that become hormone independent also become highly invasive. They reach clinical stage associated with an increased incidence of skeletal metastases as the disease progresses. Hence, even though diagnosis techniques for early detection have improved, there has been no cure for men suffering from advanced stage metastatic prostate carcinoma[3].

Since the 19th century there has been increased interest in the role of inflammation in neoplastic process. Approximately 20% of all human cancers in adults evolve from chronic inflammatory states and/or chronic inflammation. Prolonged inflammation is believed to potentiate carcinogenesis by providing a microenvironment that is ideal for cancer development and proliferation. This environment which is rich in inflammatory cells, growth factors, activated stroma, and DNA-damage-promoting agents, potentiates or promotes neoplastic risk. This theory led to studying the involvement of chemokines

and chemokine receptors in cancer development and progression. Since the time when novel aspects of 'chemokine receptors and cancer metastasis' were first discussed by Muller *et al.,* chemokine receptors expressed on cancer cells have been discovered to play key roles in cancer progression[29, 34].

Chemokine receptor CCR5 regulates trafficking and effector functions of memory/effector T lymphocytes, immature dendritic cells and macrophages. It has been known to play an important role in pathogenesis of many diseases such as Alzheimer's, atherosclerosis, HIV and in certain cancers like breast, prostate and ovarian. Amongst all these, it's most extensively researched role is that of a co-receptor along with CXCR4 for the entry of R5 strains of Human Immunodeficiency Virus (HIV-1, HIV-2) into the cell. Apart from their use as anti-HIV agents, CCR5 antagonists have also been studied as potential anti- prostate cancer agent. This theory is supported by the fact that CCR5 is found to be over expressed in prostate tumor cells and its substrate CCL5 binds to the receptors on PCa cells to activate cellular responses that are vital to cancer progression[7].

Anibamine, the first and only natural CCR5 antagonist was found to successfully inhibit proliferation of prostate cancer cell lines in *in-vivo* studies at micro molar level. It was successfully synthesized in our lab recently. However due to its poor bioavailability, high log P values and hemolytic tendencies, it proved to be a less ideal drug candidate. Despite that it provided us with a novel structural skeleton compared to other CCR5 antagonists identified through high-throughput screenings carried out by research groups in search for anti-HIV agents[8].

The main goal of this project was to design second generation compounds having structural features of anibamine through "Deconstruction-Reconstruction-Elaboration" approach and to evaluate their biological activity. These analogues were designed in a way to establish a suitable structure-activity relationship and also to verify a novel pharmacophore. The reconstructed analogues were synthesized through two different routes. These newly synthesized antagonists were then tested for their anti-proliferative activity, cytotoxicity and calcium mobilization inhibition ability against PC-3, DU-145 and M12 cell lines. This research may possibly lead to discovery of a clinically relevant CCR5 antagonist.

2. BACKGROUND

2.1 Prostate Carcinoma

2.1.1 Prostate Gland

The word prostate has originated from the Greek word *prostates* meaning "guardian". It is a donut shaped excretory organ unique to male physiology. It is located below the urinary bladder and surrounds urethra. It weighs about 25g and is size of a walnut on complete maturation. It serves the dual function of an accessory sex gland and a urethral gland. Secretions of epithelial cells empty via ducts into urethra forming a vital part of the seminal ejaculate. This alkaline secretion which is milky white in color constitutes 20-30% of the ejaculate. The smooth muscles of the prostate also aid in expulsion of the semen and it has a fibromuscular function to restrict urine flow[4].

Prostate attains its complete mature size and function by the age of 18-20 years and retains this organization for about 10 years. The growth of prostate and its maintenance is stimulated by serum testosterone. In simplest terms, testosterone enters the cell by facilitated diffusion where it is converted to dihydrotestosterone (DHT). DHT from there on binds to cytoplasmic androgen receptor and this hormone-receptor complex undergoes transformation and translocation to the nucleus. This causes activation of RNA polymerase and leads to synthesis of specific protein enzymes in the ribosome. Other than testosterone, adrenal androgens and certain growth factors are also responsible for its normal function and size preservation[5, 6].

At about 30 years of age, the structure and function of prostate begin to deteriorate. At this point the stromal and parenchymal cells are dormant with respect to proliferation. At the age of 45-50 years, due to changed hormonal conditions, the proliferative activity of the cells recommence under strict regulatory conditions[7].

The human prostate can be divided into three zones; the transition zone, the peripheral zone and the central zone. About 80% of the prostate cancers and prostate inflammation called prostatitis have been known to originate in the peripheral zone which lies to the rear of the prostate. The most common prostate proliferative disorder called Benign Prostate Hyperplasia (BPH) is known to originate in the transition zone which is located in the middle of the prostate and surrounds the urethra[8]. The prostatic epithelium can be divided into 3 different types of cell populations; secretory luminal cells, basal cells and the endocrine-paracrine (EP) cells. The three types of cells are known to differ markedly in their marker expression and hormonal regulation. The luminal cells are the functionally active cells responsible for synthesizing the secretory products that form part of the semen. They are highly differentiated and express androgen receptors (AR). They also synthesize prostate-specific antigen (PSA), a protein that acts as a marker for prostate cancer detection and to monitor its progress. In contrast the basal cell layer is highly undifferentiated and is known to be androgen-independent. In fact they express nuclear receptors for estrogen and progesterone but lack AR[9].

A. Prostatic Disorders

There are various problems associated with the prostate. As mentioned before, there is prostate cancer and prostitis that originate in the peripheral zone. Several studies have been performed to establish a relationship between the two. However, due to certain case study biases it has been difficult to validate this relationship. Nevertheless, an increased risk of prostate cancer has been found in men with a history of prostatis. There are four different categories of prostatitis recognized by NIH and only first three have been focused on to study the correlation between prostate cancer and prostatis[10]. Another common finding in the periphery of the prostate gland is proliferative inflammatory atrophy (PIA). These are mainly used to describe foci of inflammation with proliferative epithelial cells. PIA represents various morphologically diverging glandular structures ranging from simple atrophy, post-atrophic dysplasia to sclerotic atrophy. There have been reports suggesting the role of PIA as a cancer precursor[11]. They originate in the peripheral zone where PCa is known to originate and are also known to share some of the genetic characteristics with the PCa[12, 13, 14]. Also many groups have suggested a paradigm to explain the relationship between PCa and PIA[10, 15]. According to the proposed model, these atrophic lesion arise from normal epithelial cells due to genotoxic injury caused by inflammation (generation of reactive oxygen and nitrogen species), infection, environmental toxins (e.g. from diet) or combinations of these. The injury causes body to initiate the regenerative response in order to repair the damaged cells. These regenerative lesions have the morphological appearance of focal atrophy. If the genotoxic insult continues and if the individual PIA regions are unable to defend themselves against

genomic damage, they may progress to prostatic intraepithelial neoplasia (PIN) or even PCa. PIA may directly progress to PCa or go through the step of high grade PIN lesions formation. PIN lesions are putative precursors of PCa[16].

Other than the aforementioned abnormalities that originate in the peripheral zone, there are certain disorders that stem from transition zone, such as, benign prostatic hyperplasia (BPH) and atypical adenomatous hyperplasia (AAH). With increasing age, hormonal imbalance between estrogen and androgen action causes BPH. Studies have shown decreased dihydrotestosterone and 5 alpha-reductase activity in the epithelium and an increase in estrogen levels in the prostatic stroma. This is mainly caused by a discrepancy between cellular proliferation and apoptosis[17, 18, 19]. BPH usually manifest as small nodules at its inception, eventually proliferating and increasing the size of the gland. There is an abnormal increase in the smooth muscle tone of the prostate causing urethral obstruction. BPH is often erroneously confused with PCa. It is non malignant and is more of a differentiation abnormality rather than irregular epithelial proliferation. AAH is a hyperplastic lesion lacking significant nuclear atypia. It is localized to basal cell layer in the transition zone and like PIN lesions it may serve to act as a PCa precursor[20].

2.1.2 Prostate Cancer Cell Lines

Effort to generate suitable in vitro prostate cancer models dates back to almost half a century ago. It began with the pioneering work of Burrows *et al* leading to generation of the best studied and readily available immortalized prostate cancer cell

lines. Their use has contributed greatly to our understanding of prostate carcinogenesis and its progression[21]. Because of this better understanding, using recombinant DNA technology new cell lines have been developed in the past 2-3 years. Immortalized cells have been generated that can not only maintain expression of differentiation, but also have unlimited lifespan making them suitable to use as standardized cell models. They can help us study the anti proliferative, anti metastasis and anti invasive properties of cancers[22, 23].

The three prostate cancer lines used in this project are PC-3, DU-145 and M12. PC-3 cell line was obtained from lumbar vertebra of a 62-year old male Caucasian in 1979. PC-3 cells were initially found to not express PSA and were also stated to be AR (-). However recent studies show that they express detectable levels of AR mRNA and also show positive staining for PSA[24, 25]. PC-3 cells have shown to express high levels of TGF-α mRNA and EGF-R mRNA which probably contributes to their autonomous growth. They also show increased expression of transferrin. PC-3 cells also express high affinity for TGF-β receptors and secrete TGF-β into the culture media. Exogenous TGF-β initially inhibits the anchorage independency and growth of the cells. But prolonged exposure causes the growth to become normal again[24].

DU-145 cell line was obtained from a tumor removed from metastatic central nervous system lesion of a 69-year old Caucasian male in 1975. The doubling time of these cells is about 34 hours. As with PC-3, DU-145 has also shown mixed reports on hormone dependency and PSA expression. They express high amounts of TGF-α and

EGF receptors that are involved in the autonomous control of their proliferation. A study showed amplified TGF-α gene in these cells. Increased expression of transferrin similar to PC-3 has been reported. They also express high amounts of insulin-like growth factor receptors and secrete IGF-1 into the media that stimulates their growth. Increased production of these autocrine growth factors could explain the androgen unresponsiveness of these cells[24, 25].

M12 cell line was derived from parental P69SV40T cell line. Parental P69 cell line was created by immortalization of non-neoplastic prostate epithelial cells through transfection using an SV40 construct. Their tumorigenicity was assessed by subcutaneously injecting cells into nude mice and monitoring the tumor growth. 2 out of 18 mice showed presence of tumors after a latency period of 6 months. Cells from these mice were isolated in-vitro and re-injected three more times in athymic nude mice. All the mice injected with the sublines developed progressively growing tumors, however, none that were injected subcutaneously showed metastases. When M12 subline was injected directly into mouse prostate it produced tumors in all of the mice and showed extensive metastasis in lungs and diaphragm of these animals. These results are in direct contrast with the parental P69 cell line behavior which showed zero metastatic capability. Also the tumorigenic and metastatic capacity of M12 remained when cultured in-vitro[26, 27, 28].

	DU-145	PC-3	M12
ANDROGEN RECEPTOR	?	?	-
PSA EXPRESSION	-	?	-
EGF STIMULATION	+/-	-	+
TGF-β INHIBITION	+	+	NR
TUMORIGENECITY IN NUDE MICE	+	+	+
DERIVATIVES	BRAIN	VERTEBRAE	PROSTATE

TABLE1: Comparison between different prostate cancer cell lines. +(positive); -(negative); +/-(low response); NR(not reported)[24, 25, 26,27,28].

2.2 Inflammation and Cancer

About one and a half centuries ago Rudolph Virchow put forth a theory linking inflammation with cancer. He noticed presence of white blood cells in neoplastic tissue and made the connection, suggesting that cancer originated at sites of chronic inflammation[29]. Studies performed to explain this link proves to us that, when normal cells undergo tissue injury due to a wound, they begin cell proliferation to regenerate the damaged tissue. Once the assaulting agent is removed, proliferation and inflammation subside completing the repair. However, in tissue with damaged DNA or those suffering from mutagenic assault, the cells continue to proliferate in an environment rich in inflammatory cells and growth factors which further support their growth. Hence to put it in simple words, tumors behave as wounds that fail to completely heal[30].

Immune system of the body can be divided into innate and adaptive immune response[31, 32]. An inflammatory response could be initiated via antigen-dependent or antigen-independent stimulation. Antigen-dependent response leads to T-cells activation along with the help of T-cell receptors (TCR) which forms the adaptive immune system. Antigen-independent response involves the activation of key players of innate immune system – granulocytes, macrophages, dendritic cells, natural killer cells and mast cells. Also the inflammatory response can be divided into acute and chronic. Acute inflammation is a short lived process. Chronic inflammation on the other hand is a prolonged response due to the persistence of the causative stimuli. It could last for weeks, months or also indefinite time. This eventually causes tissue damage and is followed by healing and repair process[33].

Normal tissue has a very organized and segregated architecture compared to cancerous tissue as depicted in **Figure 1**[34]. Epithelial cells sit on a platform of basement membrane separated by dermis that has a well organized vasculature. On receiving wounds, platelets are activated leading to a series of events that helps in fibrin clot formation. Chemotactic factors are released that assist in extracellular matrix remodeling. Also epithelial cells and stromal cells participate in a reciprocal signaling to facilitate healing and once the wound is healed, this is suspended. In contrast invasive carcinomas are more chaotic in their structural design. The neoplasia-associated angiogenesis gives rise to a very poorly organized vasculature, lymphatics, and remodeled matrix to facilitate

invasion. Also many reciprocal signaling occurs simultaneously. The inflammatory cells and the cytokines released by them function to favor neoplastic spread and metastasis[34].

Chronic inflammation has the ability to directly alter the nature of the normal cells either by altering their genetic makeup (especially of the genes responsible for growth), or by providing the necessary trigger for uncontrolled growth in the cells that are already modified. Triggers that cause chronic inflammation leading to cancer include, microbial infections such as *Helicobacter Pyroli*, autoimmune diseases such as inflammatory bowel disease, and other inflammatory conditions of unknown origin like prostatitis. Inflammatory disorders such as gastritis, hepatitis, esophagitis caused by bacteria, virus, and also physical factors like heat, cold, smoke etc. are risk factors for cancer[35, 36].

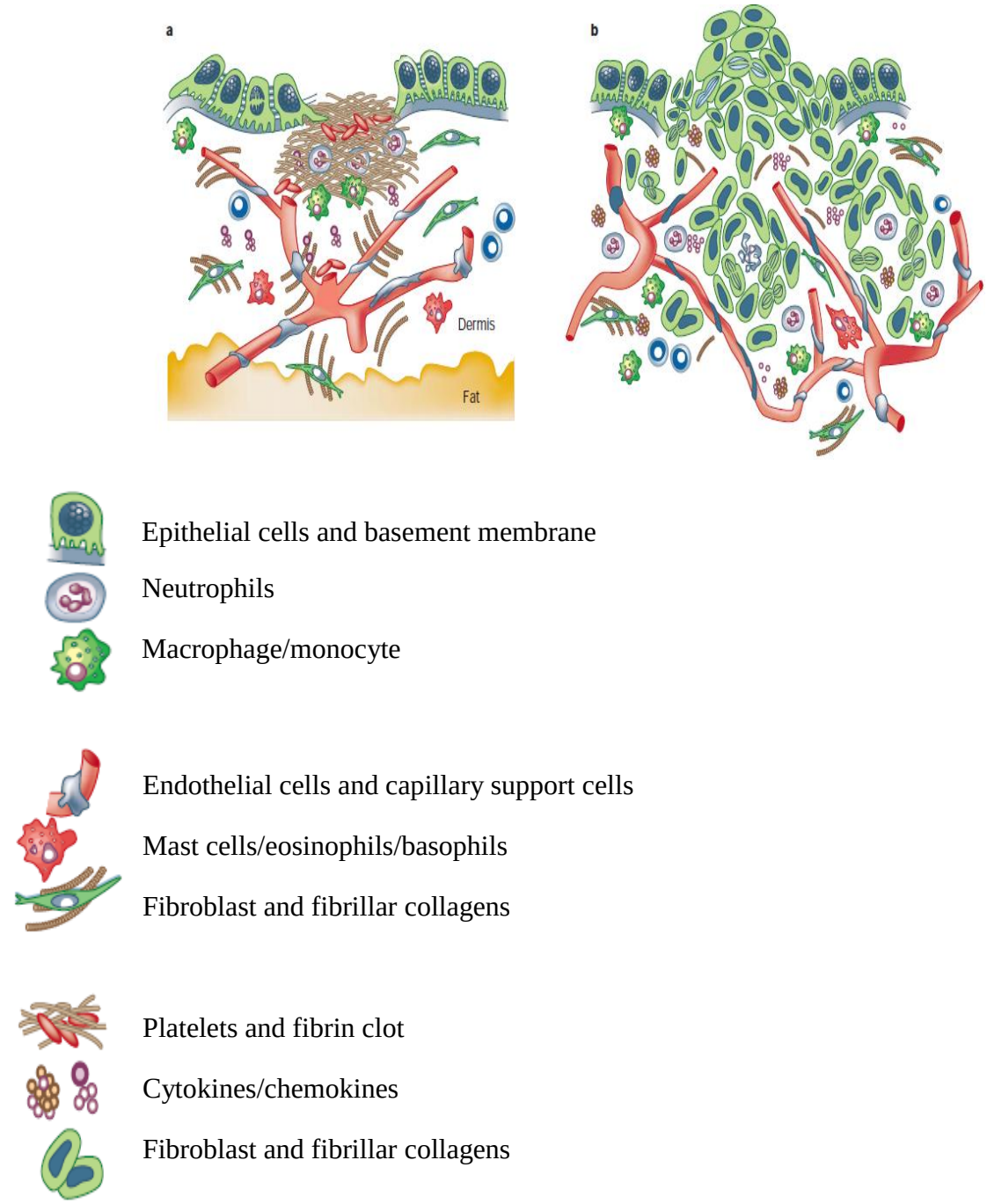

Figure 1: (a) Normal tissue wound healing versus (b) tumor growth in damaged tissue[34].

2.3 Tumor Microenvironment

Right from discovering presence of leucocytes for the first time in neoplastic tissue, to today, understanding of the link between inflammation and cancer has helped shed a lot of light on cancer prevention therapy development. Tumor cells are known to produce various cytokines that can attract leukocytes. A developing neoplasm has an environment rich in leukocyte population such as, neutrophils, dendritic cells, macrophages, eosinophils, mast cells, lymphocytes, etc. All of these cells are capable of producing various cytokines, reactive oxygen species, interferons (INF), TNF-α, interleukins, proteases, and MMPs[29, 34]. Tumor-associated macrophages (TAM) are an important component of the inflammation system of a tumor. They are derived from circulating monocyte precursors, and are lead to tumor via monocyte chemotactic protein (MCP) chemokines. TAM have two contradictory roles. When activated by IL-2, IL-12 and interferons, they kill neoplastic cells and initiate tissue destructive responses. But on the other hand, they produce potent angiogenic and lymphangiogenic growth factors and cytokines which could potentiate tumor growth. They also produce IL-10 that negates the anti-tumor response of the cytotoxic T-cells[37, 38].

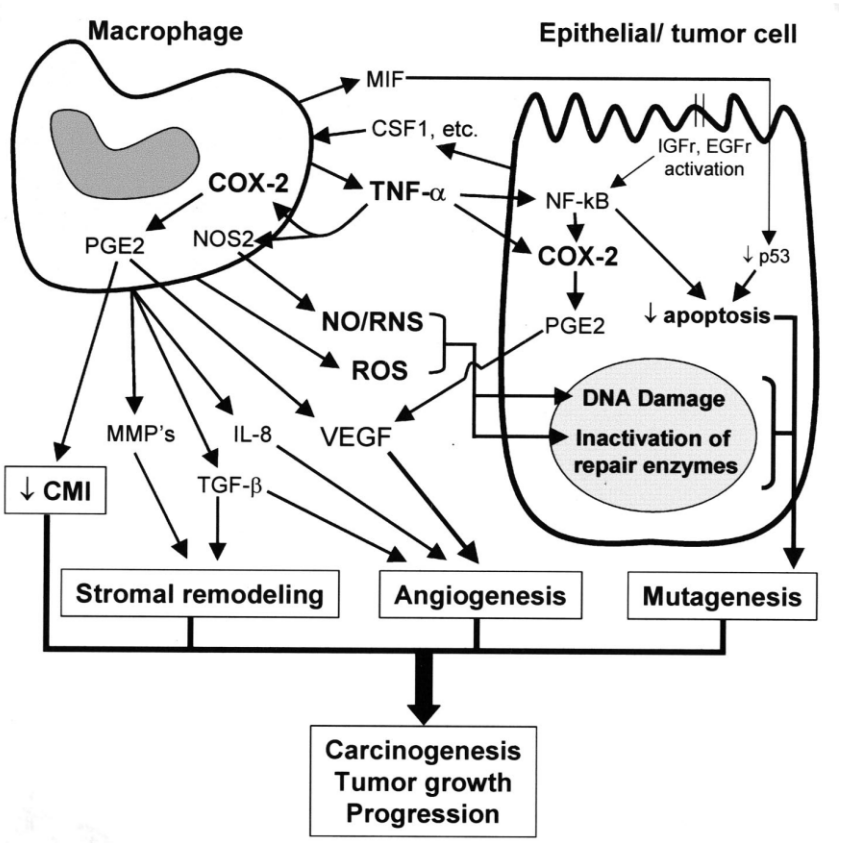

FIGURE 2: Inflammation in Cancer-Macrophages that are present in the tumor microenvironment produce factors such as MMP, TGF-β, VEGF, RNS, ROS, TNF-α, and interleukins. These factors cause stromal remodeling and angiogenesis at the tumor site. They also cause mutagenesis of the tumor epithelial cells and down-regulate apoptotic pathways, leading to mutagenesis. The end result of stromal remodeling, angiogenesis, and mutagenesis is carcinogenesis and tumor growth progression[39].

Dendritic cells (DC) play an important role in forming a link between innate and adaptive immunity. They migrate to inflamed peripheral tissue to capture antigens and and on maturation activate T-cells. Tumor associated dendritic cells (TADC) have an immature phenotype with defective ability to stimulate T-cells. They are poor inducers of effective responses to tumor antigens proved by the fact that they are found at the invasive edge of the tumor[40].

Most of the larger granular lymphocytes are natural killer cells which are rarely found in a tumor microenvironment. Out of small lymphocytes, T-cells contribute to the tumor microenvironment. Tumor infiltrating T-cells produce a repertoire of cytokines including IL-4 and IL-5. Signaling of the T-cell receptor is defective in TIL, making T-cells ineffective against tumors and viruses[34].

2.3.1 Chemokines

Cytokines are small signaling molecules that are secreted by numerous cells of the immune system and are used extensively in intercellular communication. Through cytokine receptors expressed on target cells, they can modulate function and behavior of cells at picomolar and nanomolar concentrations. They function by inducing other cytokines through cascade-like activity, transmodulating cytokine cell surface receptors or by interacting synergistically, additively or antagonistically on cell functions. They can be divided into interleukins (IL-1α, IL-1β, IL-2), the chemokines (IL-8, MCP-1), interferons (IFN-α, IFN-β, IFN-γ), cytotoxic, immunomodulatory growth factors (TNF-β,

TNF-α, TGF-β) and colony-stimulating factors (G-CSF, IL-3)[41]. Chemokines are a family of small 70-130 amino acids cytokines, or proteins secreted by cells. They have ability to induce directed chemotaxis in nearby responsive cells that is they are chemotactic cytokines. These proteins activate G-protein coupled receptors and through concentration gradient, induce the cells to accumulate at the site of chemokine production. Some chemokines are produced by cells during an infection or as an pro-inflammatory stimulus. These inflammatory chemokines cause the migration of leukocytes to the injured site, initiate an immune response and begin wound repair. Chemokines initiate the response via a two step process. In the first step it recognizes and binds specifically to the receptor. This is followed by conformational change in the chemokine in the second step. The conformational change in the chemokine is mainly due to the large flexible N terminus, and this allows the N terminus to make the necessary interactions with the receptor which leads to its activation. After the activation, bound GDP is exchanged for GTP in the α subunit of the G proteins. The G protein then dissociates from the receptor and activates several downstream effector molecules, which causes a cascade of signaling events within the cytoplasm. The result of this process is many physiological changes such as leukocyte migration and trafficking, cell differentiation, angiogenesis and leukocyte degranulation[42].

Chemokines can be sub divided into four families based on the pattern of four invariant cysteine residues that form disulfide bonds. These are found in the N terminus. Covalent bonds are formed between the first and third and also between second and

fourth residues. The four main classes are termed as CC, CXC, CX3C, C based on the number and spacing of conserved cysteine residues. Most of the chemokines are divided between CC and CXC. When there is an intervening amino acid between the first two cysteine residues it's termed as CXC or α-chemokines. If the two cysteine residues are adjacent then it's called CC or β-chemokines. CX3C or γ-chemokines has only one chemokine in its family and has three amino acid residues between the first two cysteines. CX3C chemokine is unusual in that it is part of a cell surface receptor. In C or δ-chemokines, there are only two of the four cysteines. There is a remarkable redundancy in chemokine, with multiple chemokines binding to the same receptor and multiple receptors binding the same chemokine[43]. Chemokines can also be classified as inducible or constitutive. Inducible chemokines are induced by inflammatory stimuli and hence control the leukocyte infiltration into the inflamed area. Constitutive chemokines are mainly involved in housekeeping functions in hematopoiesis in embryo and also homeostatic leukocyte movement in an immune response. Other than this, CXC chemokines can be classified as ELR+ or ELR- depending on presence or absence of 'glu-leu-arg' motif[44].

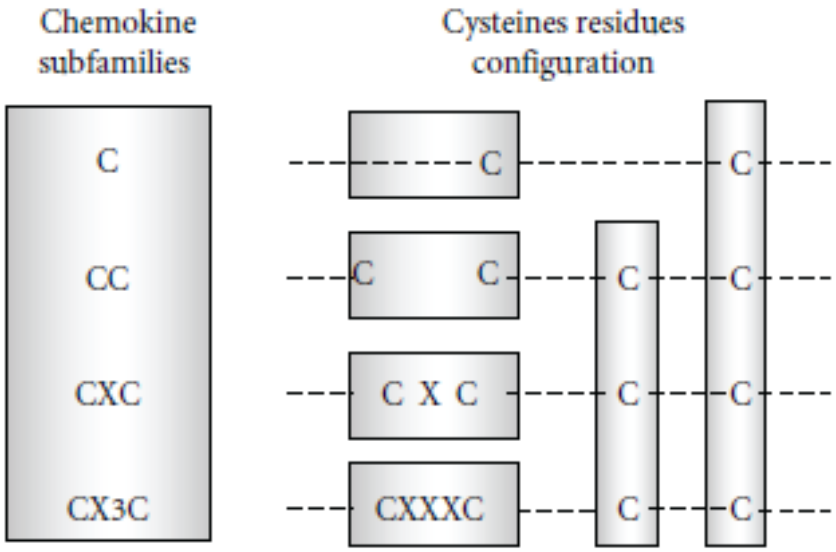

FIGURE 3: Classification of chemokines[48]

One of the earliest findings of chemokine involvement in cancer was that of endogenously produced human interleukin (IL-8), which acted as a growth factor for melanoma cells of human[45, 46]. As seen before tumors contain inflammatory cells like neutrophils, macrophages and lymphocytes. These inflammatory cells, tumor cells, and stromal cells contribute to the chemokine setting at the tumor site thereby regulating the influx of leukocytes that subsequently occurs[47]. CC chemokines are known to be the chief contributors to lymphocyte and macrophage infiltration in melanoma carcinoma of cervix, breast, ovary and also certain sarcomas[29]. Invasion and metastasis of cancer cells has been known to be associated with tumor-derived serine proteases and

metalloproteinase. Tumor cells produce and secrete lytic enzymes called proteases that have the ability to penetrate through tissues. Many chemokines are selectively cleaved by certain membrane bound soluble proteases. As a matter of fact, precursor plasma chemokines like CXCL7 and CXCL14 require proteolytic cleavage in order to attain receptor affinity. Lymphocyte migration towards CCL5 and CCL4 ligands is also brought on by cleavage. Other than this, those chemokines, like CCL2, CCL7 and CCL8, with monocyte attracting capability, have impaired capacity to attract TAM when their N-terminus is cleaved and function instead as receptor antagonist for intact CC chemokines. Proteolytic cleavage and its effect on cancer invasion and metastasis still needs to be studied more extensively in vivo[49, 50].

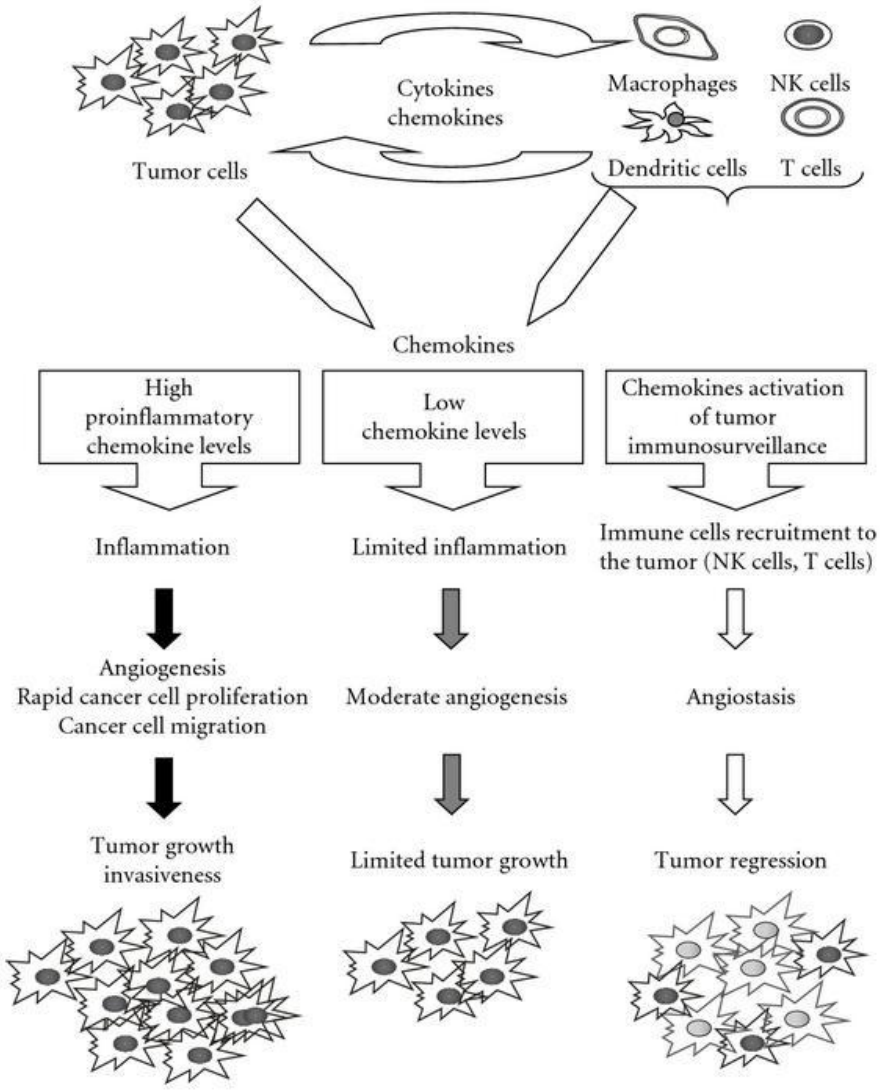

FIGURE 4: Role of chemokines in the tumor-specific immune response. The type and the amount of the chemokines secreted by tumor and inflammatory cells determine the extent and the effect of immune response leading to antitumor cytotoxic response, limited inflammatory, and vascular activation or potentiating tumor cell proliferation and neoangiogenesis[51].

Understanding role of chemokines in cancer progression and growth is a complex process. They are known to be involved in almost all steps of tumor growth, right from invasion to metastasis to distant organs. As BPH progresses to PCa, various chemokines and their receptors show alteration in their expression[51]. Murphy et. al. in 2005 revealed that CXCL8 is weakly expressed at the apical membrane of epithelial cells[52]. Studies of BPH have shown that levels of pro-angiogenic CXCL8 are higher in BPH as compared to normal prostate. This is verified by the presence of increased myofibroblasts in the stroma of BPH[53]. CXCL1 is found to be lower in BPH as compared to normal prostate but, angiostatic chemokines CXCL1 and CXCL11 are found to be more abundant in comparison[54 ,55]. Cell lines like DU-145 and PC-3 confirm high levels of CXCL1, CXCL3, CXCL5 and CXCL6[56, 57, 58]. Levels of CXCL14 are also know to increase with Gleason score[59]. A large amount of work has also been put into study of CXCL12 and its receptor. Expression levels of CXCL12 are higher in PCa tissue in comparison with BPH. It is known to be associated with perineural invasion of prostate cancer[60].

CCL5 also known as RANTES (Regulated upon Activation Normal T cell Expressed and Secreted) is a small protein of 68 amino acids. It is known to bind CCR1, CCR3, CCR4 and CCR5) and cause leukocyte migration. It regulates the movement of T cells, monocytes, basophils, eosinophils, natural killer cells, dendritic cells and mast cells. It is generated chiefly by $CD8^{+}$T cells, epithelial cells, fibroblasts and platelets. It has particularly attracted a lot of attention for its role in HIV entry into host cell. It plays

a key role in the body's immune response to viral infection. Increased RANTES expression has been associated with different kinds of inflammatory disorders like atherosclerosis, asthma, atopic dermatitis and also neurological disorders like Alzheimer's disease[61]. It has also been indicated in various types of carcinomas. When RANTES was transduced into tumor cells, it stimulated host immune response and consistently induced decreased tumorigenicity. It also activates apoptotic pathway in T cells which leads to cell death. Contradictorily, it has been known to be involved in increased chemotactic response of breast cancer cell lines[62]. Also a recent studied showed that, a chemokine receptor antagonist of the CCL5 receptors CCR5 and CCR1 was shown experimentally to inhibit breast tumor growth, further implicating CCL5[63]. Studies performed by Konig et. al. verified 67% and 89% expression of CCL5 and CCR5 mRNA respectively in PCa specimens[64]. Further studies demonstrated that chemokine CCL5 may function as an autocrine factor binding to the cell surface receptors of PCa cell lines thereby activating chain of reactions that could lead to cancer progression[65].

2.3.2 Chemokine receptors

Chemokine receptors belong to the G protein-coupled receptor (GPCR) superfamily and according to the type of chemokines with which they interact are classified as CC, CXC and CX_3C. Apart from this traditional nomenclature, they can also be classified as inducible or constitutive depending on its function. Their activation leads to formation of intracellular signaling cascade that cause the movement toward

chemokine source. They have seven trans-membrane spanning helices connected by extra membranous loops[66]. Till date twenty chemokine receptors have been identified[67]. Out of these ten are highly selective for a specific endogenous ligand. Rest of them are known to be more promiscuous and have the ability to bind to different chemokines. Unlike other types of GPCRs they tend to have overlapping specificities. For example, CCR5 has the ability to bind to CCL3, CCL4 and CCL5. Hence many chemokine-chemokine receptor-mediated signals are redundant while others are indispensable[68].

Chemokine receptors are embedded in the lipid bilayer of the cell surface. They are composed of 350 amino acids and weight approximately 40 kDa[69]. No chemokine receptor structures have been solved to date. Most of the models are based generally on bovine rhodopsin, the only 7TM receptor for which three dimensional structures are available[70, 71, 72]. The signal transduction mechanism of these receptors involve coupling to heterotrimeric G-proteins bound to the intracellular loop. The Gα subunit directly interacts with the intracellular loop of the receptor and the Gβ subunit which in turn interacts with the Gδ subunit. Gα contains a GTPase which is responsible for hydrolysis of GTP. In inactive state of the receptor Gα subunit is bound to GDP. When a ligand binds to the receptor, it causes certain conformational changes which leads to dissociation of GDP from Gα subunit and replacement with GTP instead. This Gα-GTP complex dissociates from the receptor and Gβδ heterodimer complex. The two complexes go on to activate downstream effectors that ultimately brings out the desired physiological change. Continuous stimuli lead to receptor internalization and desensitization via agonist-

dependent phosphorylation of the C-terminus of the receptor. When the receptor is phosphorylated it encourages arrestin binding, which sterically hinders further interaction with G proteins[73, 74, 75].

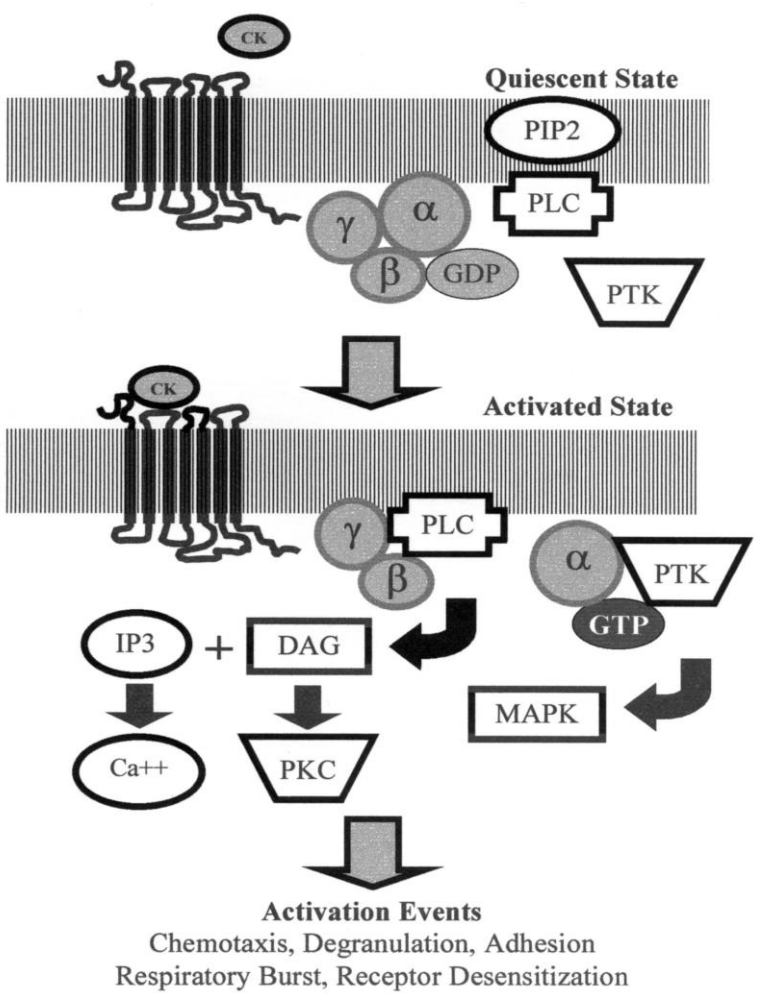

FIGURE 5: Chemokine receptor signaling pathway[65].

The steps by which tumors grow and metastasize includes, growth and survival of the primary tumor, detachment from the primary lesion, invasion into vascular and lymphatic vessels, adherence to distant target organs, and finally survival, growth and organogenesis of the metastasized cells in their new environment. These are all very complex steps. It is important for cancer cells to derive and provide signals to shape a propitious microenvironment especially because alternate environments, like bone marrow and lymph node are not naturally compatible with cells from other organs such as prostate. To assist with these processes, chemokine receptors and their corresponding chemokines provide directional prompting for migration, help with providing a suitable microenvironment and providing survival and growth signals[77, 78]. One important difference between normal cells and cancer cells is the aberrant expression of certain chemokine receptors compared to their normal counterparts. For instance, CXC4 was found to be strongly expressed in breast carcinoma when compared with normal breast epithelial cells, which do not express it at all. CXCR4 has also been implicated in 23 other cancers. Prostate cancer cells are found to express CXCR4, CXCR5, CCR9, CX3CR1 and CCR5[79, 80, 81.]

A chemokine that is generating a lot of interest among researchers, for prostate cancer treatment development is the CC chemokine receptor CCR5. It is being widely studied due to its implications in various diseases states. It is over expressed in breast as well as prostate cancer tissues. Other than that, it is also expressed on human $CD4^+$ T cells and is therefore an important requisite for human immunodeficiency virus (HIV) entry into host cell. Because this and several other implications it has been accepted as an important therapeutic target.

2.4 CCR5

2.4.1 Structure and Signaling

CCR5 was first identified in 1996[82]. CCR5 belongs to the seven transmembrane-spanning (7 TMS) receptors that signal through G proteins. Its expressed on resting T-lymphocytes, monocytes, macrophages, and immature dendritic cells[83]. It's made of 352 amino acids and weighs approximately 40.6 kDa. It also shares 71% sequence identity with CCR2, with majority of the differences located on the extracellular and cytoplasmic domains[84, 85]. Similar to other chemokine receptors, it has four cysteine residues in all four extracellular domains, a conserved DRYLAVHA sequence in the second intracellular loop which has been implicated in G protein interaction. MIP-1α (CCL3), MIP-1β (CCL4) and RANTES (CCL5) are some of the known endogenous ligands to CCR5. Other than these, monocyte chemo attractant protein-2 (CCL8) and MCP-4

(CCL13) also show reasonable activity towards CCR5. CCR5 is involved in migration, chemotaxis, cellular shape changes, metastasis, degranulation, and ROS production[23].

A model proposed to explain the mechanism of activation of the receptor describes two main steps. First step involves an initial interaction between the chemokine core and the exposed amino terminal receptor domain along with an association with the adjacent to the second extra cellular loop of CCR5. In the second step, free amino terminal domain of the chemokine interacts with the transmembrane helix bundle thereby triggering receptor activation[86].

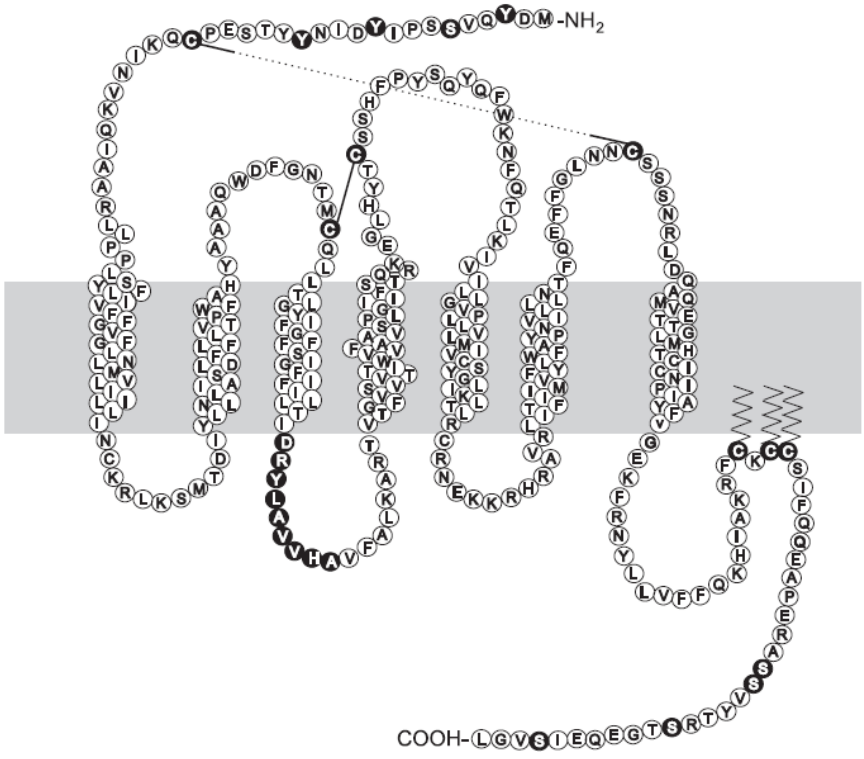

FIGURE 6: Two dimensional schematic representation of CCR5 receptor[86].

As shown in **Figure 6**, the receptor has a disulfide bond between two conserved cysteine residues on the second and third extracellular loop. There are two additional cysteine residues that form a disulfide bridge between the N-terminus and the third extracellular loop. These bridges impose a steric constraint on the receptor and hence

stabilize the conformation which is capable of ligand binding. The exact way in which chemokines interact with and activate CCR5 is not yet known. However, a study performed by Blanpain *et. al*. showed that second extracellular loop and amino terminal domain of CCR5 are essential for chemokine binding. The transmembrane helix on the other hand is involved in receptor activation. N terminus of CCR5 mediates receptor activation by interacting with the transmembrane receptor helix bundle whereas, the core domain of RANTES binds with distinct residues on extracellular loop domains of the receptor[86].

We all know that chemokine receptor activities are mediated through pertussis-sensitive heterotrimeric G proteins. The α_i subunit and $\beta\gamma$ dimers of G proteins regulate downstream effectors, such as adenylyl cyclase or phospolipase C that causes CCR5-mediated intracellular calcium mobilization and also inositol-1,4,5-triphosphate ($InsP_3$) formation[87, 88]. Activation of phospholipase C (PLC) via CCR5 leads to formation of diacyl glycerol and activation of phosphokinase C (PKC). PKC in turn causes receptor phosphorylation and helps in counter regulating the receptor activation[89]. CCR5 ligands also activate three main members of mitogen activated protein (MAP) family – ERK1/2, p38 and SAK/JNK. These are known to be important for T cell proliferation and transcriptional activation of cytokine genes[90].

CCR5 has been implicated in many diseases and conditions. It is treated as an important therapeutic target. Some of the CCR5 related diseases include breast cancer, prostate cancer, AIDS, neuropathic pain, multiple sclerosis, rheumatoid arthritis,

autoimmune diabetes, Alzheimer's disease, wound healing, chronic inflammatory disease, asthma etc. Out of all of these its role in cancer and AIDS are most highly researched.

2.4.2 CCR5 and HIV

The retrovirus HIV-1 or human immunodeficiency virus has been known to cause AIDS (Acquired immunodeficiency syndrome). It was first identified in United States almost three decades ago in 1981. It has been estimated that almost 2.7 million people get affected by this syndrome every year and almost 33 million are currently living with it. Majority of the population inflicted with this disease comprises of women[91].

Current anti-retroviral therapy (ART) comprises mainly of inhibitors targeting enzymes such as protease inhibitors and reverse transcriptase inhibitor. However, due to problems such as development of resistance, transmission of resistant virus, complication with application and toxicity of current regimen, there has been increased demand in developing better and much more effective therapy. A new promising target for the therapy that is being extensively researched is the viral mode of entry into the host cell and integration of the viral DNA into human genome. Being a novel target it shows great prospective in being active against resistant viruses as well[92].

The ingress of virus into the host cell is a complicated multi step process requiring several conformational rearrangements and extremely specific interations between the viral envelope and cellular surface receptors. Viral entry into host can be explained in

four steps – attachment, CD4 binding, co-receptor binding, and membrane fusion. Each of the four steps can be suitable targets for anti-HIV intervention. CCR5 acts mainly as an attachment inhibitor along with CXCR4. Viral envelope gp120 protein of HIV-1 interacts with CCR5, whereby CCR5 acts as co-receptor for its entry. The protein gp120 binds to the CD4 receptor on T-cells and macrophages to start the infection process. Binding with to the CD4 receptor brings about a conformational change in the gp120 protein and allows it to bind a second receptor on the host cell. Amongst these essential co-receptors are CCR5 and/or CXCR4. Binding to these receptors brings about a second conformational change in the HIV envelope of gp41 protein. This ends up revealing a peptide that fuses the HIV envelope to the host cell membrane allowing for viral transmission. Viral envelope protein gp120 therefore acts as a high affinity ligand for the CCR5 receptor and hence both CCR5 and CXCR4 can be potential targets for anti-retroviral therapy[93].

As mentioned earlier virus uses CCR5 and/or CXCR4 to interact with gp120. While all HIV-1 isolates require atleast CD4 to enter and infect, some use CCR5 and are called R5 tropic strains, others use CXCR4 and are known as X4 tropic strains. Still some can use either of the two receptors and are designated R5X4 strains[94]. The R5 strains are imperative for the person-to-person transmission of HIV and maintenance of infection, proving to us that CCR5 has a very critical role in vivo. Those individuals, that do not express CCR5 on the surface of their cells due to mutations like base pair deletions, are found to be highly resistant to HIV infection. R5X4 and X4 strains tend to then arise later

in about 30 to 50 percent of HIV infected individuals. The naturally occurring deletion mutation of 32-bp in CCR5 is known as CCR5Δ32. Those individuals that carry two alleles of this are designated as CCR5 -/-. These are the ones that are protected highly against infection by HIV-1. Those that are heterozygous for this mutant allele are represented as CCR5 +/- and are not protected against the virus. However this mutation does delay the infection progression for these individuals. This shows to us the possibility of a partial resistance if there is presence of a single copy of CCR5Δ32. Only in very rare cases individual that was homozygous for CCR5Δ32 allele showed HIV infection. Although the mechanism of infection in such cases has still not been identified, it could be hypothesized that the virus makes exclusive use of CXCR4 receptor only[95, 96].

CCL3, CCL4 and CCL5 are known to suppress infection caused by R5 tropic strain of the virus. These chemokines sterically block the site where the viral envelope interacts with the receptor. Similarly SDF-1 a CXCR4 endogenous ligand, leads to CXCR4 downregualtion thereby blocking the infection caused by X4 tropic strain[63, 97]. The anti-CCR5 monoclonal antibody PRO140 (PA14) also inhibits HIV-1 entry along with inhibiting HIV-1 replication in both peripheral blood mononuclear cells (PBMC) and primary macrophages. RANTES exhibited a limited antiviral activity in macrophage cultures[98]. Using small molecule antagonist to block the binding of gp120 to CCR5 is a prime approach for anti-HIV therapeutics. Maraviroc was the first and only CCR5 antagonist approved for public use. It acts as an allosteric and non-competitive inhibitor of the receptor. One limitation to using a CCR5 antagonist for ART therapy is that it will

be ineffective in people that are infected with X4 strain of the virus. However despite that, one major advantage of CCR5 antagonist over other therapies is that it targets the cellular rather that viral protein. Because of this there are less chances of developing viral resistance[99].

2.4.3 CCR5 and Prostate Cancer

As explained before, chronic inflammation is perpetrated to be at the root of several cancers, including prostate cancer. Progression of various cancers has been marked by increased expression of members of chemokine network. CCR5 in relation to cancer was first noticed in breast carcinoma. It was observed that CCL5 along with corresponding receptor CCR5, induced migration of breast cancer cell lines[100]. When measured, RANTES was found to be constitutively expressed by breast cancer cell lines, T47D and MCF-7, at high and physiologically relevant conditions. Its expression levels were also found to be high in tissue biopsies of advanced breast carcinoma[101]. In certain studies performed, CCR5 antagonist in presence of CCL5 was found to inhibit breast tumor growth[63, 34]. Knowing this and the possible connection between chronic inflammation and prostate cancer, genetic profiling of several genes and proteins of the inflammatory network was carried out in prostatic tissue in various disease states. Koenig et al. demonstrated by RT-PCR that, 67% of PCa specimen showed increased RANTES expression and 89% showed increased CCR5 expression[64].

In yet another set of experiments, expression of RANTES mRNA was monitored in PCa cell lines and primary cultures of prostate adenocarcinoma. Human breast carcinoma cell line MCF-7 was used as control. RANTES was also found to stimulate cell proliferation in DU-145 and LNCaP cells in a colorimetric assay using WST-1 as the colorimetric reagent[102]. It was hypothesized that endogenously synthesized CCL5 may act directly on the PCa cells by binding to CCR5. To prove this, PCa cells were cultured in vitro to check if they expressed receptors for CCL5. It was found that cell surface expression of CCR5 was significantly higher than CCR1 and CCR3 in all the cell lines that were tested. Also large intracellular pools of CCR1, CCR3, and CCR5 were observed. This was thought to be due to homologous desensitization via the binding of RANTES and receptor internalization (**Table 2**)[102].

To further explore the realm of RANTES and CCR5 involvement in PCa, studies were carried out where the cell lines were treated with TAK-779, a non-peptide CCR5 antagonist. TAK-779 was shown to inhibit RANTES induced cell proliferation, suggesting that CCR5 antagonist could possibly be an effective inhibitor of tumor growth and progression(**Figure 7**). Growth of cells exposed to TAK-779 in the absence of RANTES was not inhibited[102].

	PC-3	LNCaP	DU-145
CCR1 surface	0	22.6	16.6
CCR1 total cellular	35.2	52.4	50.2
CCR3 surface	6.1	29.5	8.0
CCR3 total cellular	95.0	88.6	77.8
CCR5 surface	28.8	48.3	38.8
CCR5 total cellular	88.3	89.5	98.6

TABLE 2: Expression of various CCL5 receptors in prostate cancer cell lines. The values are represented as percentage of positive cells determined by comparing the fluorescence emitted on staining with specific antibodies[102].

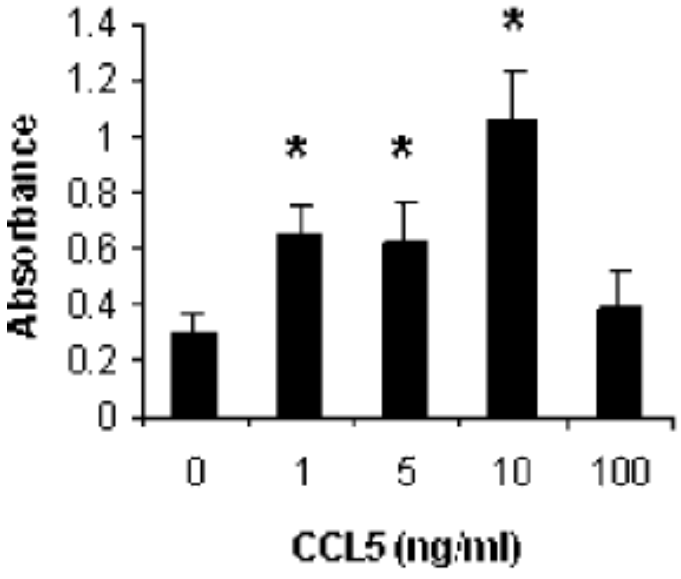

FIGURE 7: The RANTES stimulation of DU-145 prostate tumor cell proliferation. Cell proliferation was measured in response to varying concentration of RANTES (1-100 ng/ml) after 24 hours by the addition of WST-1 proliferation reagent. The absorbance was measured at 450 nm. Astericks indicate statiscally significant differences between the control cells and cells exposed to RANTES[102].

Detecting the expression of CCL5 and CCR5 in the prostate cell lines, and also the observation that TAK-779, a known CCR5 antagonist, inhibits RANTES induced cell proliferation in prostate cancer cell lines, proves to us that CCR5 could be an eligible target for PCa treatment. Lot of research is being done by industries to come up with CCR5 antagonist mainly for ART therapy to treat AIDS. However, only one has managed to clear the clinical trials till date. This makes it necessary to come up with a novel lead compound that will have the antagonistic properties of the current CCR5 antagonists being tested, without the issues that are associated with it.

2.5 Natural Product as a CCR5 antagonist

Due to the hot interest generated by discovery of CCR5 as an essential HIV entry coreceptor, a lot of pharmaceutical companies started doing high-throughput screening to

search for lead compounds that would target CCR5. The very first antagonist identified was TAK-779 published by Takeda Chemical Industries Ltd. in 1999[103]. It was obtained by optimizing compound **1**, an initial lead containing quaternary ammonium salt with an IC_{50} of 390 nM. TAK-779 however, was unable to be further developed due to its high toxicity when injected. Following that many modifications were made to come up with a successful drug but due to different drawbacks none of them made the market. Companies like Schering-Plough, Merck, Ono Pharmaceuticals, GlaxoSmithKline, came up with drugs of different structural classes from different leads but none have cleared clinical trials till date until Maraviroc. Maraviroc or UK-427,857, was capable the first CCR5 antagonist to be cleared by US Food and Drug administration advisory panel on 24th April 2007. And later, on August 6 it received full FDA approval for use in treatment of patients[104].

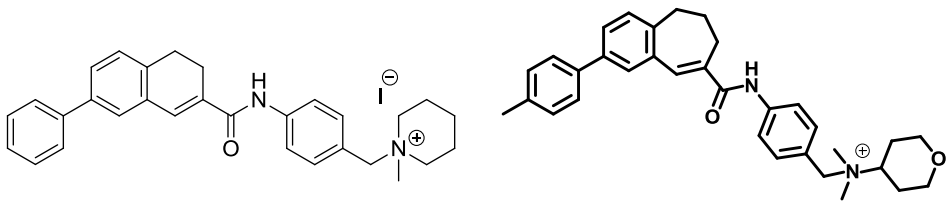

FIGURE 8: TAK 779 & lead compound used to generate TAK 779[108].

Due to lack of successful antagonists, that have been able to reach the market, it became important to explore newer realms and try discovering new leads. We know that

plants and microorganisms provide us with a wealth of unexplored molecules. Although combinatorial chemistry has become very famous due to its ability to provide new leads, it sometimes fails to provide the expected answers. In such cases, it is more fruitful to go back to nature. Natural medicine has been employed to treat maladies and illness right from the ancient times. It has especially made a huge contribution towards anti-cancer research in identifying successful drugs for cancer therapy. The importance of natural product research is emphasized by the fact that National Cancer Institute has begun screening natural products extracts against cancer cell lines producing more drug candidates. High throughput screening of natural products has come up with many successful approved anti-cancer drugs like taxol, etoposide, teniposide, vincristine, navelbine, taxotere, topetecan and irinotecan[105]. Natural products offer us many advantages over synthetic libraries. They differ from synthetic molecules in their complexity. They have more sterogenic centres, more carbon, hydrogen and oxygen, and less halogen, nitrogen and sulfur. This provides us with a unique and fresher scaffold for drug development. Not only this, but they also help us discover unique targets through novel mechanism of actions. Although it is not very often that the natural product produced directly by a given organism is the best possible drug candidate, it provides us with a suitable lead that can be optimized to be made into a successful molecule[105, 106].

Anibamine or 6,8-didec-(1Z)-enyl-5,7-dimethyl-2,3-dihydro-1H-indolizinium alkaloid was isolated first in 2004 as a TFA salt. It was obtained from *Aniba panurensis* by activity guided fractionation for its toxicity towards azole-resistant *Candida albicans*.

The sample was isolated from fungi in Guyana using methanol extraction. It was later also identified to possess CCR5 antagonistic activity and competed for binding with ^{125}I-gp120, the HIV viral envelope protein to human CCR5 with an IC_{50} of 1µM. Its log K_{ow} value was calculated to be 9.1 which suggested that it was of a lipophilic nature. Other than that it also had an undesirable hemolytic activity, hence requiring structural modifications to transform it into a more favorable drug candidate[107].

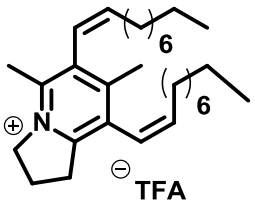

FIGURE 9: Anibamine

Anibamine was screened against the DTP 60 human tumor cell panel. This panel included prostate cancer cell lines PC-3 and DU-145, apart from other cell lines[115]. Its total synthesis was completed in our lab almost five years ago by Dr. Li by a ten step

synthesis starting with acetyl acetone and cyanoacetamide, yielding a mixture of anibamine and its isomers[108].

3. Project Objectives and Design

The chemokine receptor CCR5 has been implicated in many diseases such as AIDS, cancer, Alzheimer's, atherosclerosis etc. CCR5 and its endogenous ligand CCL5 has especially been found to be over expressed in breast and prostate cancer cells and has been proven to assist in cancer development and progression. This makes it a favorable therapeutic target to combat these diseases. Accordingly, chemokine antagonists are

being studied for their pharmacological applications[86]. CCR5 has particularly become a very hot target in anti-HIV therapy development due to its involvement as a co-receptor for viral entry into the host cell. However, this project mainly deals with development of CCR5 antagonist to treat prostate cancer.

Identification of three endogenous ligands of CCR5 – RANTES, macrophage inflammatory protein–1 α, and macrophage inflammatory protein-2 β, lead to research for developing synthetic compounds to block this receptor. Many pharmaceutical companies came up with compounds through high throughput screening. However till date only maraviroc has managed to clear the rigorous US FDA clinical trials (**TABLE 3)**. Due to adverse effects, poor bioavailabity and long term toxicity of the molecules, not many CCR5 antagonists have been successful enough to enter market[108].

TABLE 3: CCR5 antagonist in clinical trials[108]

PRODUCT	MECHANISM OF ACTION	COMPANY	STATUS
Maraviroc	Non-competitive inhibitor	Pfizer	FDA approved

Viciviroc	Non-competitive inhibitor	Schering-Plough	Phase III completed
Aplaviroc	Non-competitive inhibitor	Glaxosmithkline	Development discontinued
INCB009471	Non-competitive inhibitor	Incyte	Phase I/IIa completed
TBR 652	Non-competitive inhibitor	Tobira	Phase II completed
Pro 140	Antibody	Progenics	Phase II
HGS004	Antibody	Human Genome Sciences	Phase I completed

A few years back, screening of natural products extracts obtained from microbial fermentation, led to the discovery of anibamine. Anibamine is a pyridine quaternary ammonium alkaloid isolated from *Aniba panurensis.* Till date it is the only natural product known that has CCR5 antagonistic ability. It was found to bind CCR5 with an IC50 of 1µM[107]. Its anti-metastatic potential was proved by the fact that it interfered in the PCa cell lines growth in a growth dependent manner. To evaluate its specificity towards targeting cancer cells, hemolysis of sheep red blood cells was examined at a concentration of 1µM and below. No toxicity was noticed until the concentration was increased by 10-fold which supported the potential selectivity of the compound. Furthermore, immunohistochemical analysis of M12 cells showed that on addition of

anibamine the morphology of the cells changed. The cells that appear as a disorganized mass reflecting the metastatic ability of the cell line, turned into a more spheroid structure. This corroborated with the theory that anibamine has potential to inhibit prostate tumor metastasis. Preliminary studies also showed that anibamine has the ability to reduce the subcutaneous growth of M12 cells injected in athymic nude mice[109] (**FIGURE10**).

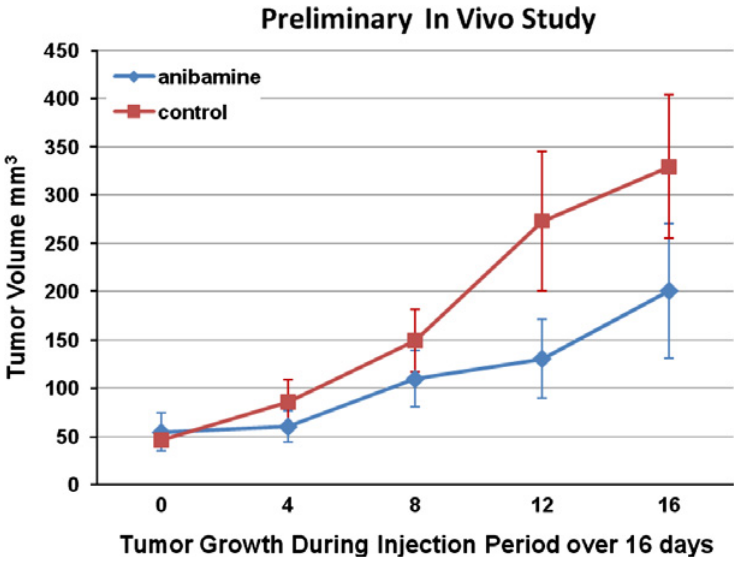

FIGURE 10: Effect on anibamine on prostate tumor growth in mice. Six nude mice were used and were injected with M12 cells. Anibamine was injected once the tumor became visible at 0.3mg/kg concentration. Tumor size versus number of days after injection was recorded[109].

Anibamine provides us with an unmatched skeleton compared to the other small CCR5 antagonists that were identified through high throughput screening targeting mainly anti-HIV therapeutics development. Molecular modeling studies showed us that there are distinct similarities and differences between binding of anibamine to the receptor when compared to other known antagonists (**FIGURE11 &12**)[110]. All in all the preclinical studies proves to us that anibamine could not only be a possible candidate for high affinity CCR5 antagonist, it also has a novel skeleton that might resolve the issues that the current antagonists are having.

Despite all this, anibamine also had certain shortcomings that did not make it an ideal drug candidate. Its calculated log K_{ow} was found to be 9.2 which did not conform to the 'Lipinski's Rule of Five' for drug like compounds. Also compared to other known CCR5 antagonist it had very simple undecorated aliphatic side chains. Hence, there was scope for improvement. In spite of these drawbacks, anibamine still serves as an indispensable lead compound from which different analogues can be designed and synthesized to use in metastatic cancer therapy. Its unique structure and promising in

vitro as well as in vivo experimental data, provides us with the much needed platform to design more ideal drugs[109].

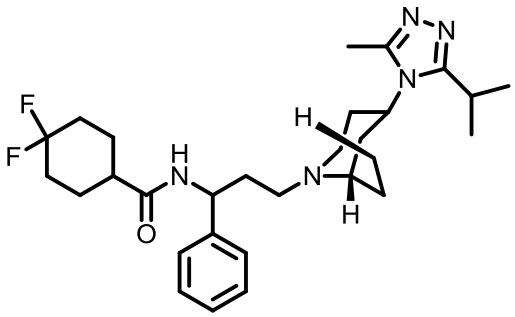

Maraviroc

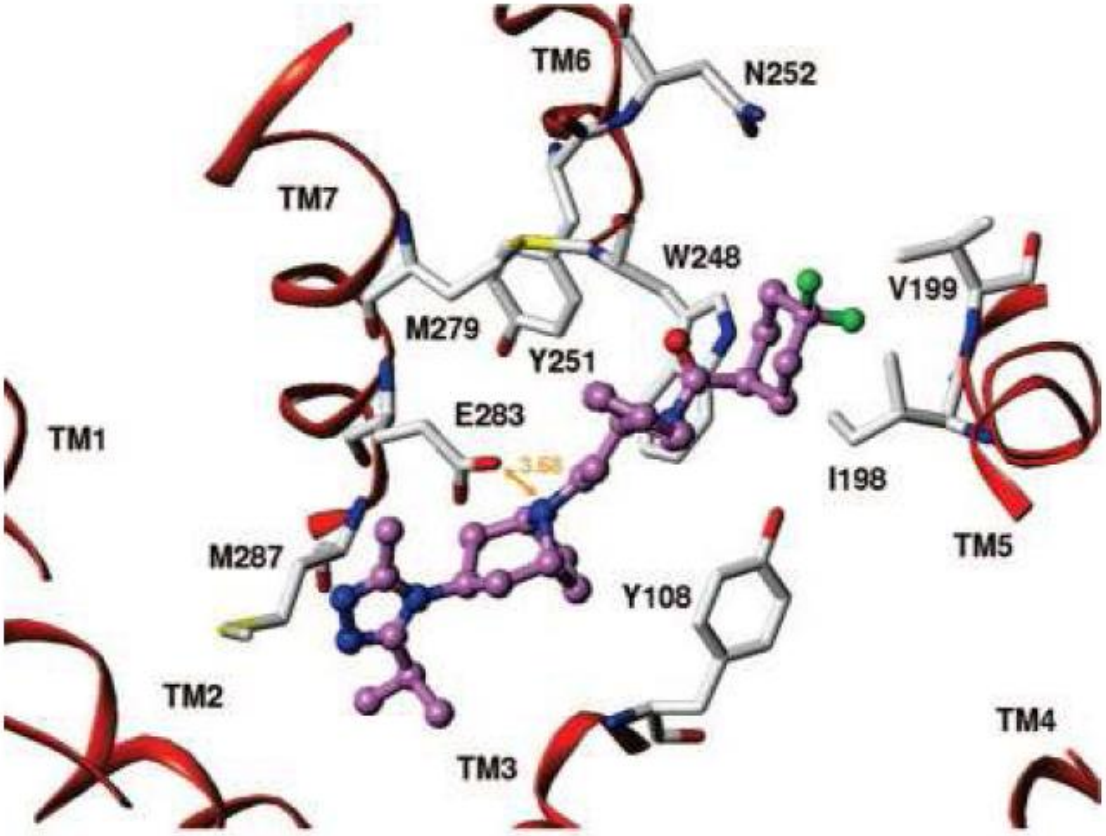

FIGURE 11: Binding mode of Maraviroc (purple) in homology model of CCR5[110].

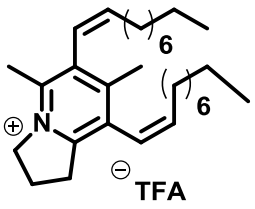

Anibamine

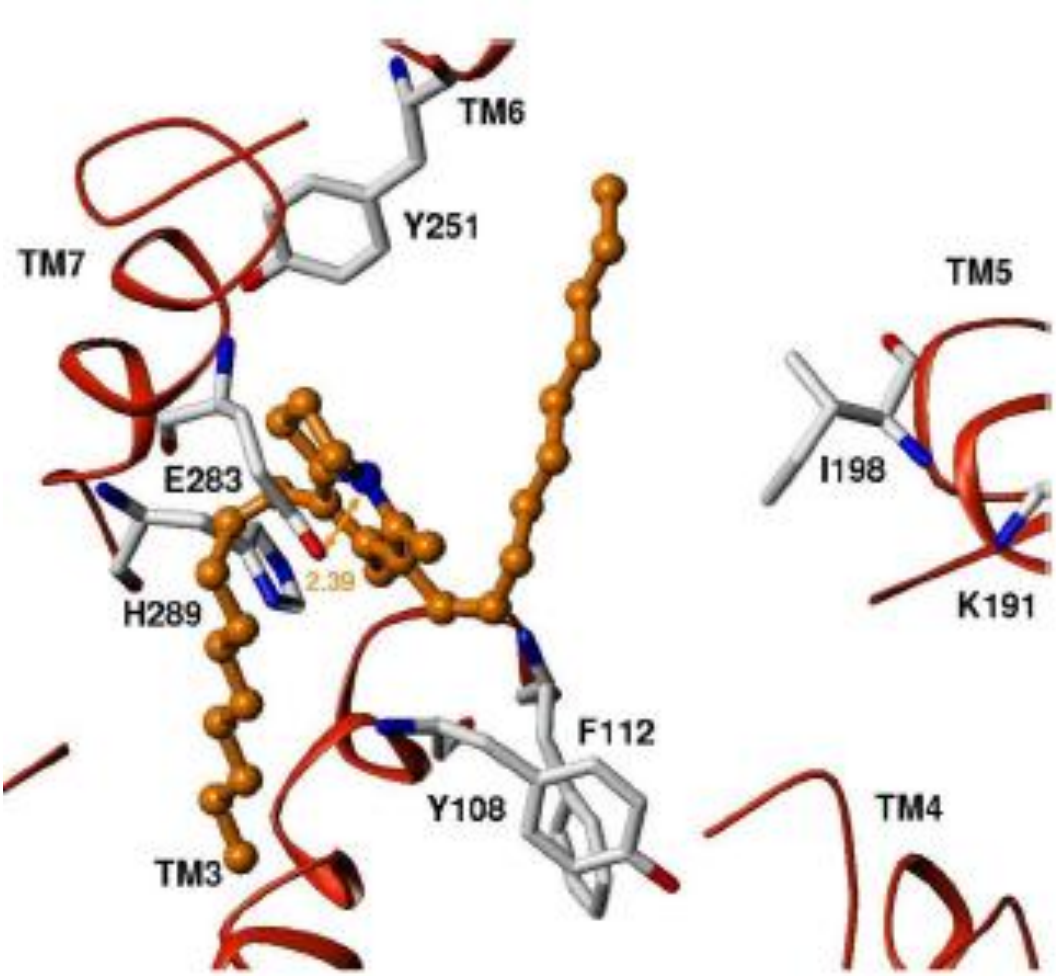

FIGURE 12: Binding mode of anibamine (orange) in homology model of CCR5[110].

3.1 PROJECT DESIGN

Anibamine was first totally synthesized in our lab in 2007 (**FIGURE 3**)[111]. Its synthetic route was figured out with the help of retrosynthetic analysis. Two synthetic routes were explored to prepare intermediate 6. From there anibamine (**13**) was synthesized in seven more steps.

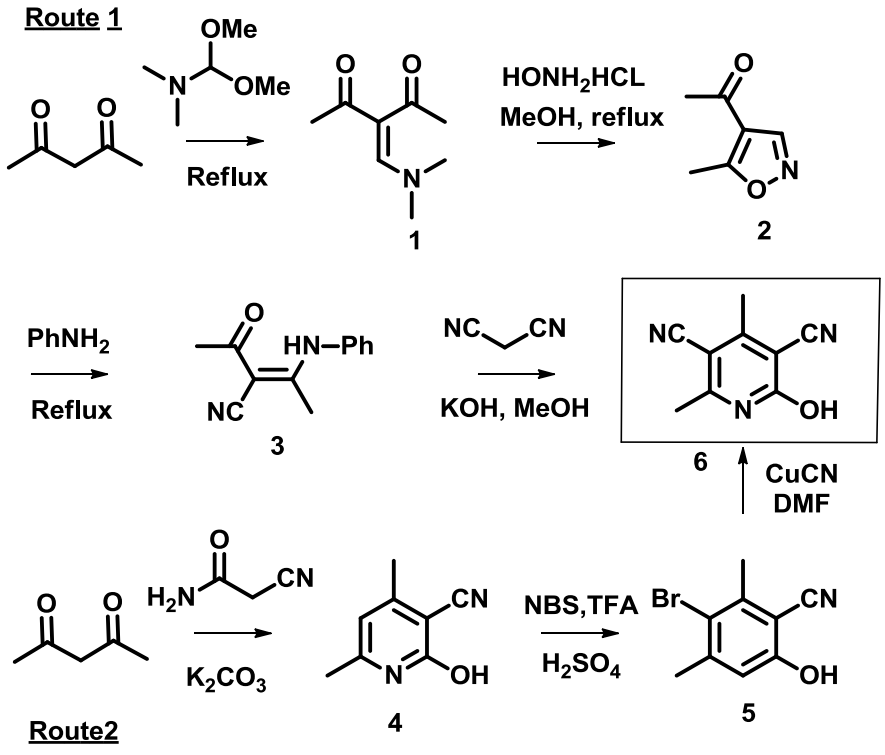

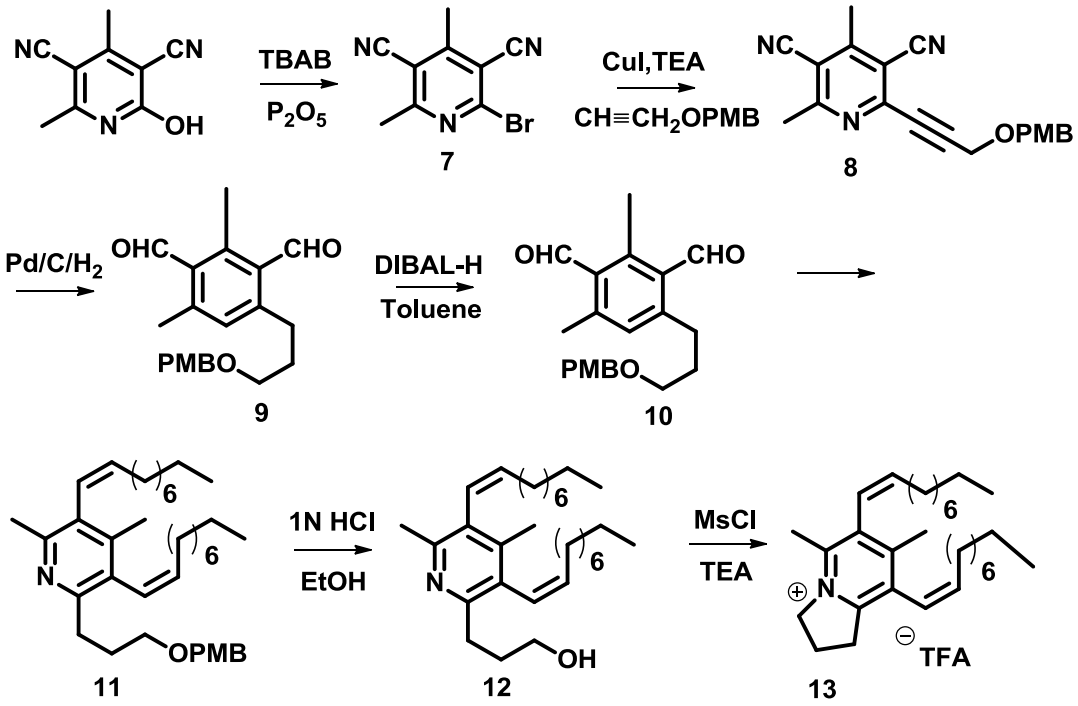

FIGURE 13: The complete synthetic route of anibamine[111].

To further improve its characteristics and develop newer and better analogs, it became essential to establish a structure-activity relationship for this compound. This task was approached by using 'Deconstruction-Reconstruction-Elaboration' strategy (**FIGURE 14**). By doing this different analogues were designed and synthesized in our lab. This approach helped us to determine the influence of various substituent groups of anibamine on its potency, receptor affinity, receptor selectivity, toxicity, functional activity etc.

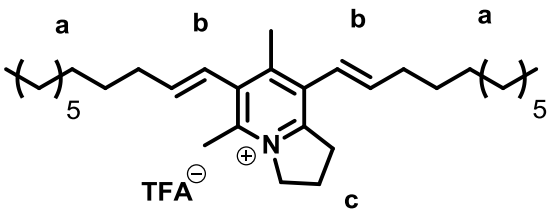

FIGURE 14: Anibamine as lead compound

a) Deconstruction of side chains was done to test its influence on the anti-cancer activity.

b) Elaboration of the side chains by changing the configuration of the double bond or completely removing it was done.

c) Deconstruction and elaboration of the ring was done by removing it or changing its size to test its importance.

Primary structural modifications were focused on fused ring size of the compound. Different analogues with five, six and seven membered ring were synthesized and tested. It appeared that seven membered ring was not favorable for binding and most of the other analogues did not show a marked improvement of the activity profile over that of the lead compound. Apart from this, isomerization and saturation of the double bond was also performed to test its affect on the anti-prostate activity. For a single cell line the different analogues showed more or less similar activity[112]. This validated the need for a more comprehensive structural change in the lead compound to establish a more accurate structure activity relationship spectrum.

Other than these ongoing modifications to the structure, it was noted that the two side chains were completely undecorated and simple. Significant modifications done on these side chains could give revealing results that could go a far way in establishing an important aspect of the structure-activity relationship and also generate next generation lead compound. Also, since the molecule was determined to be highly lipophilic, modifying the plain aliphatic side chains could also help in solving this issue.

Keeping this in mind, an amide bond was introduced as a linkage for the side chain so as to introduce hydrogen bonding and also to make use of its partial double bond character. Also the position of the amide bond on the chain was shifted as compared to the original structure, increasing its distance from the ring. To the amide bond, an aromatic moiety was attached to simulate the aliphatic carbon length. An amide bond acts as an isostere for a double bond and hence is a suitable candidate to replace it without causing too drastic a change in the possible activity. For further optimization, certain substitutions were introduced at the para position of the phenyl ring, to give the compound different characteristics and also to obtain the best possible combination **(TABLE 4).** These substituents were chosen on the basis of Craig's plot so as to get all possible blends with respect to electronic characteristics, lipophilicity, bulkiness and hydrogen bonding.

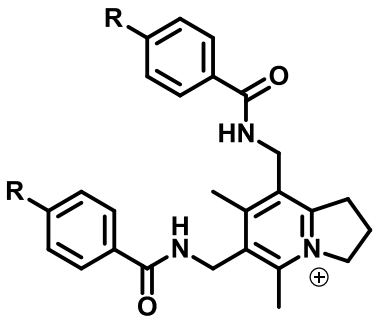

TABLE 4: Different substituents for R.

BULKY GROUPS	ELECTRON WITHDRAWING		ELECTRON DONATING	
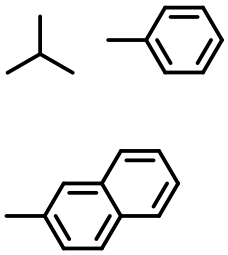	$—NO_2$ $—NH_2$	—Br —Cl	$—OCH_3$	$—CH_3$ $—C_2H_5$

3.2 Project Objectives

The primary objective of this project is to prepare different analogues of anibamine and help structure an SAR for our lead compound. We also wish to test our hypothesis that by embellishing the two simple aliphatic side chains we can decrease the lipophilicity of anibamine to acceptable levels. By doing so we would also establish the significance of these two side chains in the SAR. Ten analogues were prepared, each with a different type of substituent to give different electronic properties to the compound. The synthetic route of anibamine preparation was altered to accommodate these changes.

Following this, biological profiling of the synthesized compounds was carried out. Three assays were performed – anti-proliferation assay, cytotoxicity assay and calcium mobilization assay. Anti-proliferation assay was done on PC-3, DU-145, and M12 cell lines. All of these cell lines express CCR5 receptor on their surface. WST-1 was colorimetric agent that was used. These anti proliferative studies were performed to test the ability of the CCR5 antagonist to inhibit the proliferation of prostate tumor cells. Cytotoxicity assay was performed on NIH-3T3 cell line. It's performed to measure the therapeutic index of the drug. Finally the calcium assay was done to identify compounds that will inhibit the intracellular calcium release stimulated by endogenous ligand

RANTES. Only the compounds with high affinity for the receptor will be able to inhibit the binding of RANTES to the receptor. This is a functional assay.

These biological assays will help in validating our hypothesis and also confirm the structure-activity relationship of the lead compound.

4. Results and Discussion

4.1 Chemical synthesis of Second Generation Anibamine Analogues

The total synthesis of anibamine was completed in our lab in 2007[111]. In order to accommodate the changes made in the anibamine structure to generate second generation anibamine analogues, the synthetic route for total synthesis of anibamine was modified. The complete route involved synthesis of two key intermediates **6, 14.** Synthesis of **6** was accomplished by using two alternate routes.

4.1.1 Synthesis of key intermediate 6

SCHEME 1: Two routes for synthesis of intermediate **6.**

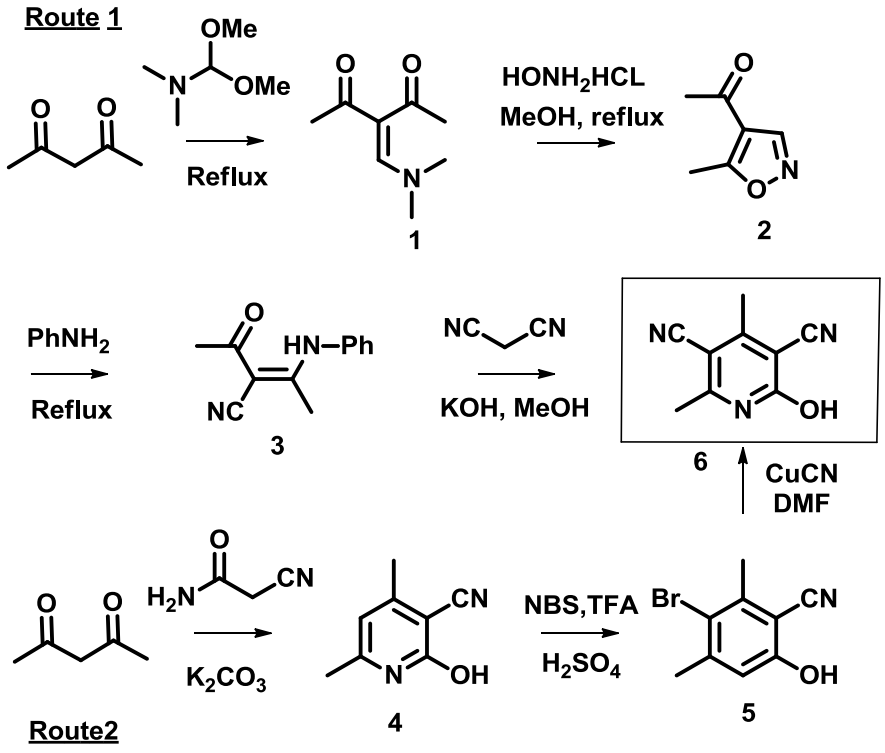

SCHEME 2 : Route 1 for synthesis of intermediate **6**

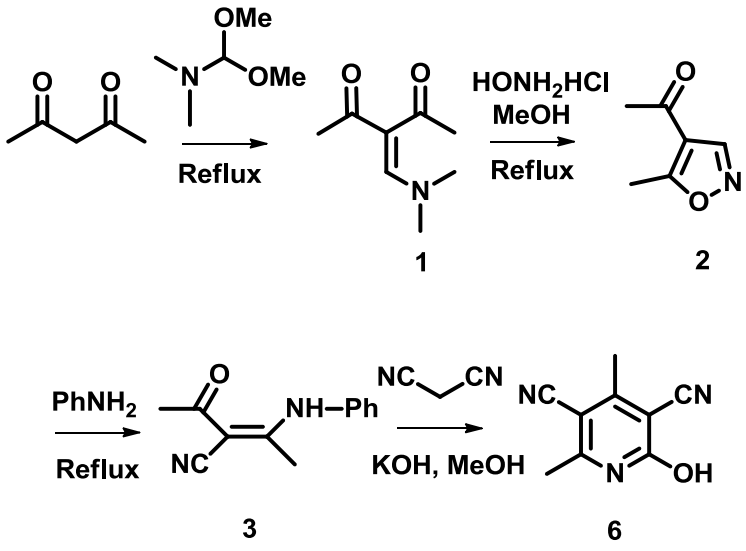

Scheme 1 involved four steps in all. Although it was longer than scheme 1, it proved to be much easier to carry out. Starting material used in this scheme was acetyl acetone. It was refluxed with N,N-dimethylformamide dimethyl acetal for about three hours[113]. The condensation between the two reagents gave product **1**. It was then purified by recrystallizing from EtOAc giving 85% yield in light yellow crystals. Compound**1** was refluxed with hydroxylamine hydrochloride in MeOH under acidic conditions to give product **2**[114]. This product was purified by distillation under reduced pressure conditions furnishing 65% yield. Following that compound **2** was yet again refluxed with aniline to give a β-enaminonitrile product **3** in 62% yield[115]. Compound **3** was purified by recrystallization in EtOH. Refluxing malononitrile with compound **3** under basic conditions yielded the key intermediate **6**. Purification of this compound proved to be a little difficult. Glacial acetic acid was used to recrystallize pure light yellow crystals, however care was taken to ensure complete removal of the acid from the crystals which otherwise proved harmful for the next reaction[116]. To ensure this, the crystals were washed thoroughly with cold MeOH. Product yield of this reaction was 89%.

SCHEME 3 : Route 2 for synthesis of intermediate **6**

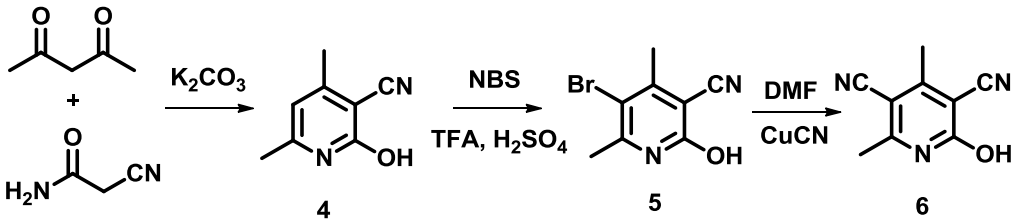

Route is shorter, comprising only three steps, proved to be more cumbersome than the other. This was mainly due to the last, key intermediate synthesizing step. The starting material of this route was also acetylacetone. This was condensed with cyanoacetamide at room temperature in a basic potassium carbonate solution to give product **4**[117]. This product required no purification and was obtained at a good yield of 94%. Compound **4** was then brominated at 5th position of the pyridine ring using NBS as the brominating agent[118]. It was purified by recrystallization in acetone and water mixture in 73% yield. The next and last reaction of this scheme was an 80 year old Rosenmond-von Braun reaction. This reaction utilizes cuprous cyanide as the nitrile source and DMF as the high boiling solvent. The reaction was carried out at a very high temperature of greater than 150°C. This reaction proceeds by nucleophilc substitution of the bromide with the nucleophile[119].

SCHEME 4 : Mechanism of Rosenmund-von Braun reation.

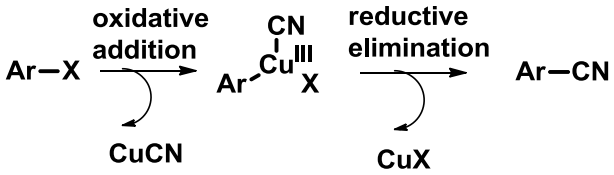

Over the period of time as the reaction proceeded, its color changed from yellow to a very dark brown. Also it had a very thick consistency which made it difficult to work with. The reaction was quenched using acidic $FeCl_3$ solution. The mechanism of this

reaction involves oxidative addition of the nitrile to the starting material forming a copper^{III} complex. This complex is reduced via reductive elimination to yield the corresponding aryl nitrile and copper halide as the side product. Isolation of the product from the reaction mixture proved to be a very time consuming and difficult step. Neutralizing the reaction mixture caused formation of a thick viscous mass which trapped the product. It was very tricky to remove copper halide from the reaction mixture. Extraction using EtOAc and dichloromethane was performed that extracted the product from above and below the reaction mixture. The obtained product **6** was then purified by crystallization using glacial acetic acid again taking care to completely get rid of the acid.

4.1.2 Synthesis of key intermediate 14

SCHEME 5 : Synthesis of intermediate **14**

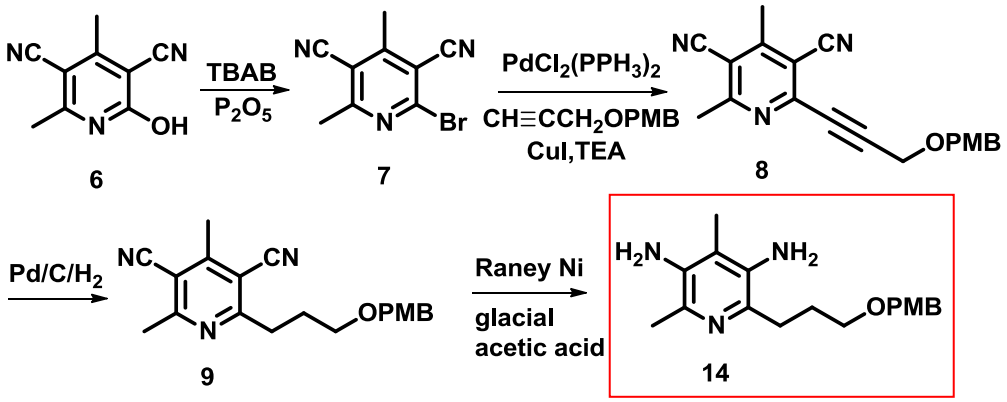

The first step of synthesis of **14** was a bromination step. The hydroxyl group at 2nd position was brominated using tetrabutylammonium bromide as the brominating reagent to give **7**. The reaction was carried out at about 90-100°C for 6 hours[120]. Although presence of electron withdrawing group at 3rd position should aid reaction, the reason why it still took such a long time was due to the presence of hygroscopic phosphorus pentaoxide. P_2O_5 was added to provide the phosphate leaving group. However, at the reaction temperature it melted and formed a black viscous mass at the bottom of the flask trapping the starting material. This also explained the reason why this reaction did not give higher yields. Using higher amount of solvent and increasing the equivalents of the brominating agent increased the yield considerably. Also to ensure maximum stirring efficiency, mechanical stirrer was used for the reaction. Using mechanical stirrer helped displacing the trapped starting material from the melted P_2O_5 mass. Purification was done via column chromatography on Al_2O_3 column.

From here the introduced bromide group at 2 position was coupled with PMB protected propargyl alcohol through Sonogashira coupling. Before the coupling reaction the **16** was prepared (**SCHEME 6**).

SCHEME 6: Synthesis of **16**

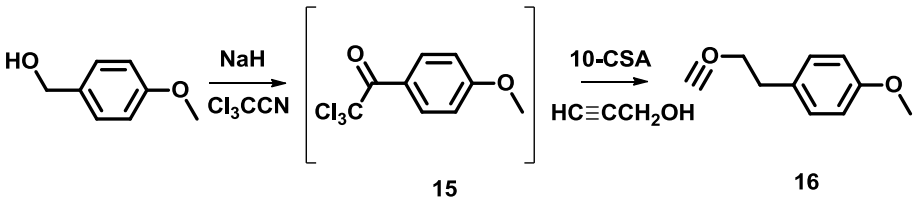

In this two step reaction, a solution of sodium hydride was added to 4-methoxy benzyl alcohol under nitrogen protection. This caused deprotonation of the starting material at which point tricholoroacetonitrile was added at 0°C to form 4-methoxybenzyl trichloroacetimidate. On concentrating the mixture, a yellow crude oil was obtained which was then dissolved in CH_2Cl_2. To this solution propargyl alcohol was added dropwise and cooled to 0°C. A catalytic amount of 10-camphorsulfonic acid was added till the pH of the solution was around 3 - 4. The reaction was allowed to come to room temperature overnight[121]. This protecting group was purified through column chromatography giving colorless oil in 83% yield.

For Sonogashira reaction, compound **7** was dissolved in diethyl ether and to this CuI, $Pd(PPh_3)_2Cl_2$, and TEA was added. Once everything dissolved, the PMB protected propargyl alcohol solution in ether was added to the reaction slowly under N_2 protection. The reaction was allowed to go on for 24 hours over the course of which brown precipitate formed in the ether layer[122]. The precipitate was extracted using EtOAc and purified using column chromatography. Care was taken during purification as it was difficult to get rid of the catalyst used during the reaction and further crystallization was required in MeOH to finally get the pure product in a 66% yield. Another method for removing the residual catalyst of the reaction was to pass the reaction mixture first

through an Al_2O_3 column and then performing the usual purification protocol. It was observed that if the product was not pure, it poisoned the catalyst used in the next reaction giving low yields.

Following the coupling reaction, the triple bond was reduced by hydrogenation using Pd/C catalyst. The starting material **8** was dissolved in methanol and catalytic amount of catalyst added. The reaction was carried out on Barr hydrogenator at H_2 pressure of 56-58 psi. This was a clean reaction requiring no further purification and furnished high yields of 96%.

After reducing the triple bond, the synthetic route was deviated from original anibamine synthetic route in order to reduce the cyano groups to amine instead of aldehyde. This reaction initially posed lots of problems. It was difficult to achieve the reducing conditions strong enough to reduce the two cyano groups yet at the same time not too strong so as to cleave the PMB protected group. Several, chemical methods were tried such as using $NaHPO_2$ as the reducing agent. But at the end of the reaction when the TLC was examined, it showed degradation of the PMB protecting group. Varying the reaction conditions proved to have no effect on the outcome. Following that hydrogenation was attempted using 10% w/w Pd/C catalyst. However, even after prolonged reaction time, no change was noticed in the starting material. Finally after researching some more literature a different approach was tried. The catalyst was changed to 50% w/w Raney Nickel and glacial acetic acid was used as the solvent. On doing so, the reaction was completed in 48 hours and an examination of the TLC showed

formation of primary amine. This was further confirmed by doing ninhydrin test for primary amines. The product was concentrated thoroughly to completely get rid of the acid and then purified by column chromatography to give intermediate **14**.

4.1.3 Synthesis of final compounds.

The last stage in the final compound synthesis was introducing different side chains at 3 and 5 position of the pyridine ring. The two amino methyl groups were coupled with acid to form amide bond. Each acid had a different sustitution at the *para* position. The different acids used are listed below.

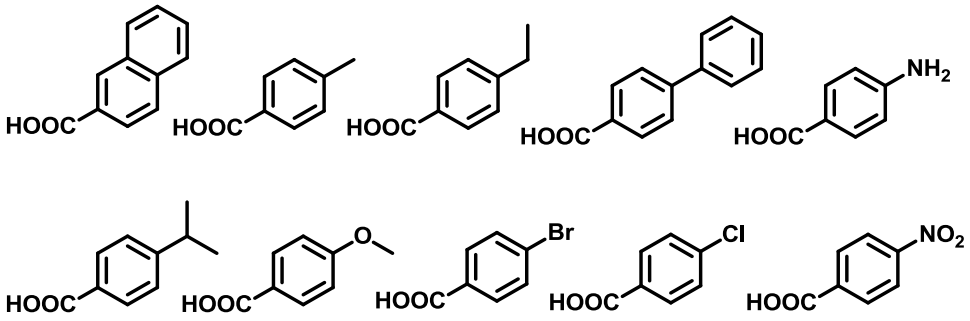

FIGURE15: List of acids used in coupling reaction.

SCHEME 7: Amide coupling reaction

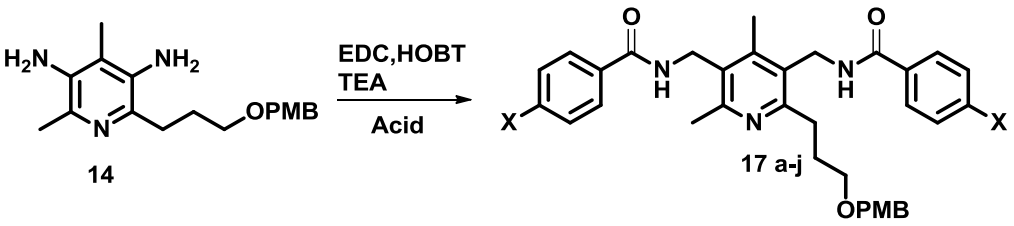

This acid-base coupling reaction was carried out by using EDC or 1-ethyl-3-(3-dimethylaminopropyl) carbodiimide hydrochloride as the coupling reagent. The carbodiimide acts as a carboxyl activating agent for the coupling of primary amines to yield amide bonds. It reacts with acid to form an O-acylisourea. This then reacts with amine to give the corresponding amide. However, there are also some side reactions that take place. The O-acylisourea can rearrange to form a stable N-acylurea which would stop the reaction. To avoid this dichloromethane was used as the solvent since it had low dielectric constant.

SCHEME 8: Side reactions of the coupling reaction.

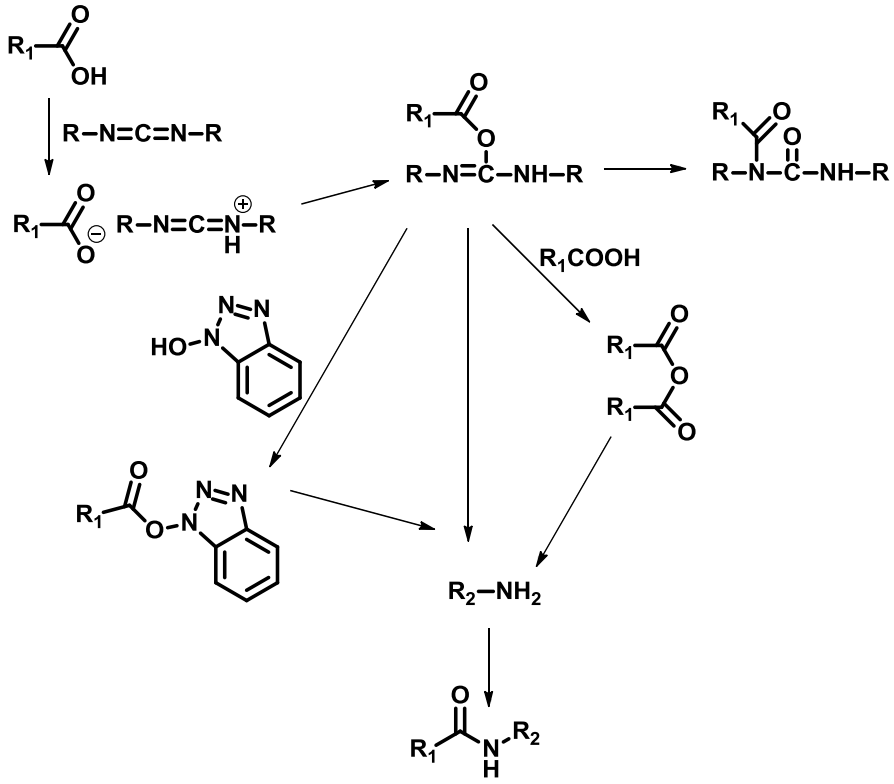

For this reaction it is very important to maintain anhydrous conditions. Molecular sieves were used and also the reaction was carried out under N_2 atmosphere. Also the reagents were added in the right sequence to avoid side reactions. First 2.1 equivalents of acid were stirred with EDC, HOBT, TEA and solvent for 15 mins in ice bath. To this a solution of amine in DCM was added slowly. The reaction was allowed to carry out at room temperature overnight. To ensure that both the groups were allowed to form the amide bond with acid, 1 equivalent acid along with EDC, HOBT and TEA were added next day. The reaction was allowed to proceed for another 24 hours or till all of the

starting material was used up. The product was extracted using DCM from the mixture and purified using column chromatography. The yield of this reaction varied with different types of acids.

After the side chains were coupled, the PMB protecting group was cleaved to expose the alcohol which was cyclized to give the final product.

SCHEME 9: Deprotection reaction

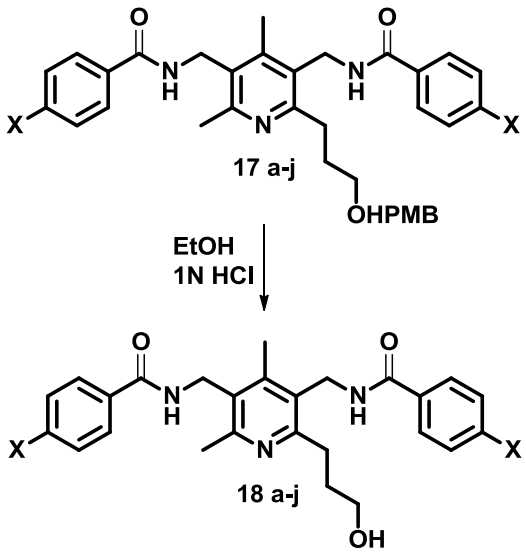

1N hydrochloric acid in ethanol was used to carry out the deprotection reaction. The reaction was allowed to reflux for 5-6 hours depending on the side chain. The acid was neutralized using ammonium hydroxide and the entire mixture was filtered. This is done instead of direct extraction due to the high water solubility of the product. After concentrating and removing all traces of water, the crude product was purified on silica gel column to give compounds **18 a-j**.

The last step of the synthesis was the cyclization step. Methane sulfonyl chloride in presence of TEA was used as the cyclizing agent giving the final indolizinium ion salt. The reaction was carried out at 0°C in anhydrous dichloromethane and allowed to come to room temperature over 1 hour.

SCHEME 10: Cyclization reaction

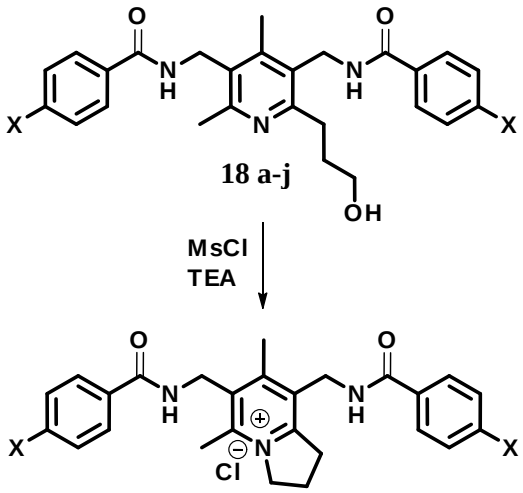

18 a-j

19 a-j

Due to lack of difference in polarity between the final compound in salt form and TEA.HCL salt formed during the reaction, it became difficult to extract the former. Various methods were tried to separate the two salts. Even after passing through silica gel column traces of triethylamine salt still remained. So to extract the salt completely, consecutive washings with 1N HCl were performed. This effectively removed the TEA salt and the final compound was purified by column chromatography in CH_2Cl_2: MeOH solvent system. The purity of the final compound was also tested by performing HPLC.

Finally ten new second generation analogues of anibamine (**19 a-j**) with variable side chains were prepared by modifying the original route. All the final compounds were in their chloride salt form. The compounds were all characterized using H^1 NMR, C13 NMR, IR, mass spectrometry and HPLC. Following their synthesis, they were screened for biological activity.

4.2 Biological screening of Second Generation Anibamine Analogues

The ten final compounds were screened for three biological assays. These were anti-proliferation assay and cytotoxicity assay, calcium mobilization assay.

4.2.1 Anti-proliferation assay.

Anti-proliferation assay is performed to observe the proliferation inhibition effects of the synthesized ligands on PCa cells. The cell lines used for this assay included PC-3, DU-145 and M12. The assay was miniaturized by culturing the cells in a 96-well plate in order to test higher number of drugs together. The media used for PC-3 and DU-145 cells was RPMI, 1% L-glutamine, 0.1% ITS (insulin, 5 μg/mL; transferring, 5 μg/mL; and selenium, 5 μg/mL) and 0.1% gentamicin. The media for M12 was slightly different from that of PC-3 and DU-145. It contained 5% fetal bovine serum instead of the 10% used for PC-3 and DU-145. About thousand cells were plated per well in 100 μL of media. On the second day, various concentrations of the drugs were added to make up the volume to 150 μL. The cells were incubated for 72 hours following which the media was dumped out and anti-proliferative reagent WST-1 was added. The cells were

incubated for three more hours at the end of which absorbance of each well was measured at 450 nm.

The anti-proliferative reagent used for this assay is a tetrazolium salt that acts as a colorimetric agent. The advantage of using this salt was that it required no prior solubilization step before enzymatic cleavage as needed by previously used salts. WST-1 is cleaved by enzyme mitochondrial reductase into a water soluble formazan dye that is dark red in color. The tetrazole ring of the dye opens up when the enzyme system introduces hydrogen into the structure. The energy for the reaction is obtained by reducing NADH into NAD^+ by electron chain transport system. Only the viable cells have the ability to cleave the salt and form formazan. So higher the number of viable cells, greater the amount of formazan formed. The color change form can be measured using an ELISA instrument. The incubation time with WST-1 has been optimized to three hours and has produced the best proliferative results.

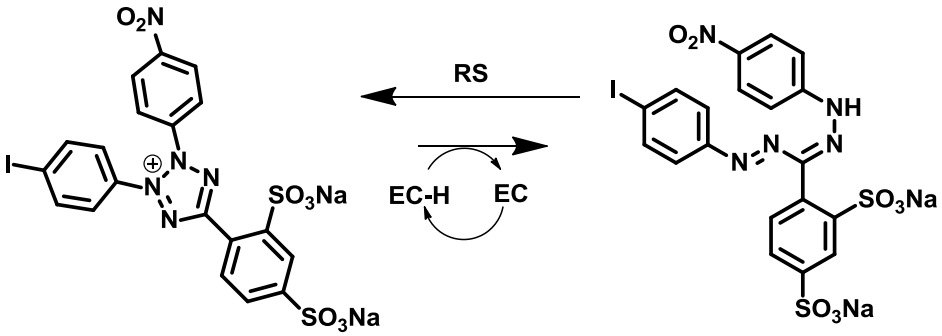

FIGURE 16: Metabolically driven WST-1 cleavage to form water soluble formazan dye. RS – mitochondrial cleavage, EC – electron coupling reagent[127].

	PC3		**M12**		**DU145**	
	IC50	**SEM**	**IC50**	**SEM**	**IC50**	**SEM**
19a	192.1	17.6	101.4	11.4	72.7	16.2
19b	184.8	4.9	243.5	2.5	149.9	13.1
19c	169.3	13.6	161.9	8.3	107.9	9.5
19d	49.1	1.2	47.1	8.4	43.4	1.1
19e	98.6	0.1	107.4	1.6	100.8	4.6
19f	120.2	6.6	167.9	43.0	139.3	13.8
19g	127.0	13.1	153.9	5.3	123.8	3.7

19h	92.0	25.0	147.3	5.0	107.3	3.1
19i	134.7	23.1	178.6	18.0	120.4	26.2
19j	160.9	26.5	>300	NA	181.8	13.1

TABLE 5: Anti-proliferation data of the ten final compounds in three different PCa cell lines.

Discussion:

According to the data obtained, compound **19d** shows the best anti-proliferative activity in all the cell lines, persistently. It displayed the lowest IC_{50} of 43.4µM for DU-145 cell line while the highest value of 49.1 µM for PC-3 cell line. Majority of the compounds displayed better activity for DU-145 cell line as compared to the other two cell lines. Apart from **19d** that had an IC_{50} of 43.4 µM, **19a** was another compound that showed a lower IC_{50} of 72.7 µM compared to other compounds. It was also noticed that some of the compounds like **19g**, **19h** and **19e** showed better activity profile in PC-3 cells.

This difference in the values among the cell lines probably was due to the fact that all the cell lines do not exhibit same level of CCR5 receptor expression. PC-3 shows the lowest CCR5 expression as compared to M12 and DU145. The varied level of receptor

expression in the cell lines may affect the function of the drugs. Apart from that, the downstream signaling pathways of the receptor may counterbalance differently the antagonism of CCR5 among different cancer cell lines. This also probably explains the reason why some of the other compounds like **19h** and **19j** did not show consistent results among the three different cell lines.

By examining the trend in the IC_{50} values it can be deduced that maintaining the hydrophobicity in the side chain is essential for the activity. For DU-145 cell line, bulkier groups showed better inhibition of the proliferation. **19d** that displayed the best activity had a phenyl subsitiution, and **19a** having an IC_{50} of 72.7 had a naphthalene substitution supporting our conclusion.

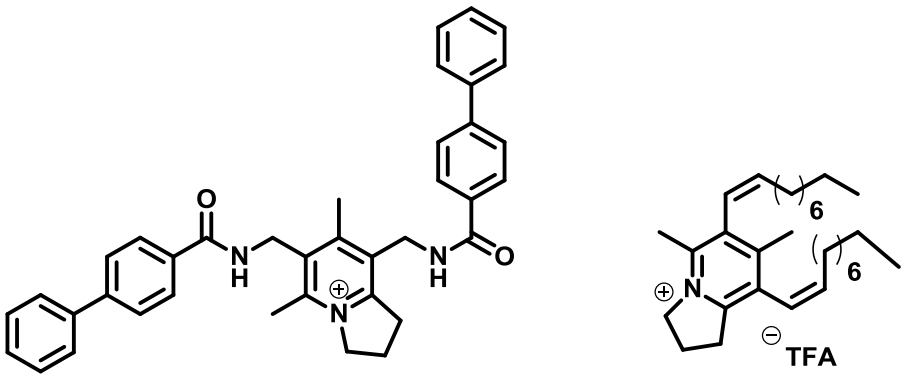

FIGURE 17: Structure of **19d** and lead compound anibamine.

More polar substitutions hampered the activity which is proved by **19h, 19f** and **19i** with IC_{50} of 181.8 µM, 139.3 µM and 120.4 µM respectively. Also **19d** had the

longest side chain length out of all the analogues proving to us that maybe keeping the chain length conserved is also imperative for the activity.

4.2.2 Cytotoxicity assay.

Cytotoxicity is the harmful effect induced by a compound in a cell culture system *in vitro*. It acts as a measure of the potency of the drug and also its effect on normal cells. It can be performed by both qualitative and quantitative methods. For this project we used a method that measures the metabolic integrity of the cells. The cell line used was NIH3T3 cell line. It's a primary mouse fibroblast cell line. Like anti-proliferation assay the agent used to detect the cell viability was WST-1. If the membrane of the cell is not ruptured by the drug and it is still viable, the mitochondrial reductase enzyme will break down WST-1 to form a water soluble formazan dye that imparts red color. Color intensity is measured in terms of absorbance and TC_{50} is calculated.

3T3(WST-1)	IC50±SEM (µM)
19a	165.6±4.7
19b	229.0±2.3
19c	254.7±10.6
19d	227.8±13.6

19e	171.2±18.4
19f	269.5±3.9
19g	>300uM
19h	181.8±5.5
19i	263.4±27.6
19j	226.4±13.2

TABLE 6: Cytotoxicity results of the final compounds.

Discussion:

Measuring TC_{50} gives us a measure of the effect of the drug on normal cells. It's the ability of the drugs to induce death in 50% of the cells as compared to control. If the drug is cytotoxic, it causes necrosis and the cell membrane ruptures. The cell ruptures as a result of cell lysis. Looking at the cytotoxicity results it is apparent that except for **19a** most of the compounds have a very low cytotoxic profile and that they require higher concentrations to induce toxicity in 3T3 as compared to prostate cancer cell lines. Compound **19d** which showed the highest activity shows a high LD_{50} of 227.8 µM. **19a**

appeared to be cytotoxic for cells and hence not suitable. Also compared to the lead compound anibamine that had a TC_{50} of 23.47 µM, all the compounds displayed low cytotoxicity in the cells. Compound **19g** was the least toxic with TC_{50} of >300 µM.

4.2.1 Calcium mobilization assay.

This assay is performed for in-cell measurement of agonist-stimulated and antagonist-inhibited calcium signaling through CCR5 receptor. It is performed on MOLT-4 cell line expressing surface CCR5 receptors. This cell line was obtained from acute lymphoblastic leukemia cells of a human. Fluo-4 is used as the indicator dye. It has an affinity for Ca^{2+} ions, exhibiting a K_D of 345 nM (ref). When at rest it displays low emission intensity, however, when bound to calcium it emits very high intensity fluorescence. When the receptor binds to agonist RANTES, the level of intracellular calcium ion increases which can be detected by the Flou-4 dye. However, in presence of an antagonist the receptor binding with agonist is blocked and the calcium ion release thereby obstructed. This is revealed by decrease in emission intensity of the dye. The assay data for the first five compounds is displayed below.

	IC_{50} (µM)	**SEM**

19a	12.7	0.9
19b	18.7	1.2
19c	23.9	0.9
19d	17.3	1.8
19e	38.5	13.1

TABLE 7: Inhibitory effects on CCL5 induced Ca2+mobilization in MOLT-4/CCR5 cells.

Discussion:

From the assay results of the first five compounds that were tested, it is apparent that all of them show antagonistic ability towards CCR5 receptor. Lowest IC_{50} was displayed by 18a. This can be interpreted as; **19a** has the ability to inhibit binding of 50% of the RANTES to the receptor at a concentration of 12.7 µM. **19b** that showed greatest

anti-proliferation activity, displayed an IC_{50} of 17.3 µM. These results are consistent with the anti-proliferation assay obtained. Both **19a** and **19d** that had showed the lowest IC_{50} for the anti-proliferation assay also displayed the lowest IC_{50} in the calcium mobilization assay. This also further supports our theory that having a bulky and hydrophobic group in the side chain is important for the activity of the compound.

Compound **19d** while showed the best anti proliferative activity, yet did not show the best antagonistic activity. This can be explained by the fact that antagonism of the drug may not correlate to its activity. This can be explained by the phenomenon of functional selectivity. A GPCR has the ability to attain several multiple active isoforms. These sites can be stabilized by ligands so that only a certain part of the complete signaling pathways are selectively activated. The ligand can bind to one of the isoforms of the receptor and still cause differential changes depending on the cellular localization of the receptor-G protein complex. One of the mechanisms to explain this is probably the atypical conformational changes induced as compared to endogenous ligand.

5. EXPERIMENTAL

5.1 Chemical Synthesis

Melting points were determined on a Fisher-Scientific melting point apparatus. ^{1}H-NMR and ^{13}C-NMR spectra were obtained on a Brucker 400 MHz spectrometer and tetramethylsilane was used as an internal standard. Infrared spectra were obtained on a Nicolet 5ZDX FT-IR spectrometer. Column chromatography was performed on silica gel (grade 60 mesh; Bodman Industries, Aston, PA). Routine thin-layer chromatography (TLC) was performed on silica gel GHIF plates (250 μm, 2.5 x 10 cm; Analtech Inc., Newark, DE).

Scheme 1:

3-((Dimethylamino)methylene)pentate-2,4-dione

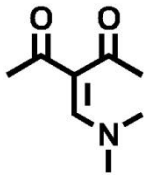

A solution of *N*,*N*-dimethylformamide dimethyl acetal (35.7 g, 0.3 mol) and acetylacetone (15 g, 0.15 mol) was refluxed for 3 hours. The mixture was then concentrated to remove excess acetal to give a dark red oil. The crude product was

recrystallized in ethyl acetate to give light yellow crystals of 3-((dimethylamino)methylene)pentate-2,4-dione (19.75 g, 85% yield). M.p. 55-57°C ^{1}HNMR (400 MHz, $CDCl_3$) 7.45 (s, 1H), 3.1 (s, 6 H), 2.34 (s, 6H).

1-(5-Methylisoxazol-4-yl)ethanone

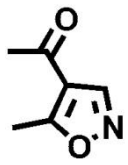

3-((dimethylamino)methylene)pentate-2,4-dione (19g, 0.122 mol) was added into a solution of hydroxylamine hydrochloride (8.47g, 0.122 mol) in 60 mL methanol. This solution was refluxed for 2 hours. The mixture was concentrated to remove methanol and then partitioned between 100 mL water and 200 mL dichloromethane. The dichloromethane layer was dried over Na_2SO_4, filtered and concentrated to give a crude red residue. The residue was purified by reduced pressure distillation (95°C, 10 torr) to give a colorless oil of 1-(5-methylisoxazol-4-yl)ethanone (9.95 g, 65% yield). ^{1}HNMR (400 MHz, CDCl3) 8.49 (s, 1H), 2.74 (s, 3 H), 2.45 (s, 3H).

(*E*)-2-Methyl-4-oxo-3-(phenylamino)pent-2-enenitrile

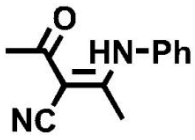

A mixture of aniline (20.38 g, 0.218 mol) and 1-(5-methylisoxazol-4-yl)ethanone (9.1 g, 72.8 mmol) was refluxed for 30 minutes. After cooling, the mixture was poured into ice cold 100 ml 2N HCl and stirred while a precipitate formed. The precipitate was recrystallized in ethanol to give (*E*)-2-methyl-4-oxo-3-(phenylamino)pent-2-enenitrile (9.28 g, 62% yield) as clear plate crystals. M.p.: 132-133°C ^{1}HNMR (400 MHz, CDCl3) 7.46 (m, 3H), 7.14 (m, 2H), 2.41 (s, 3H), 2.27 (s, 3H).

Scheme 2:

2-hydroxy-4,6-dimethylnicotinonitrile

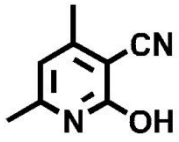

To a solution of K_2CO_3 in water (20 ml), cyanoacetamide (0.84 g, 10 mmol) and acetylacetone (1.00 g, 10 mmol) was added. The reaction mixture was stirred overnight at room temperature. The precipitate was filtered and washed with hexane to give 2-

hydroxy-4,6-dimethylnicotinonitrile (1.385 g, 94% yield) as a white powder. M.p.: 188-189°C ^{1}HNMR (400 MHz, CDCl3) 12.38 (br, 1H), 6.12 (s, 1H), 2.3 (s, 3H), 2.23 (s, 3H).

5-bromo-2-hydroxy-4,6-dimethylnicotinonitrile

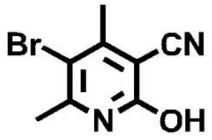

A solution of 2-Hydroxy-4,6-dimethylnicotinonitrile (1.2 g, 8 mmol) in trifluoroacetic acid (1.28 mL) was cooled to 0˚C. To this mixture concentrated H_2SO_4 (1.7 mL) was added followed by slow addition of NBS (2.88 g, 16 mmol). The reaction was kept at 0˚C and stirred for 1.5 hours then poured into crushed ice. The resulting precipitate was filtered and recrystallized in a 4:1 mixture of acetone and water yielding 5-bromo-2-hydroxy-4,6-dimethylnicotinonitrile (1.34 g, 73% yield) as clear white crystals. M.p.: 256-257˚C ^{1}HNMR (400 MHz, CDCl3) 12.83 (br, 1H), 2.43 (s, 3H), 2.37 (s, 3H).

2-hydroxy-4,6-dimethylpyridine-3,5-dicarbonitrile

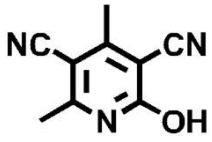

Method 1: (*E*)-2-methyl-4-oxo-3-(phenylamino)pent-2-enenitrile (9.1 g, 44.3 mmol) was added to a solution of malononitrile (2.92 g, 44.3 mmol), and KOH (2.48 g, 44.3 mmol) in 150 mL methanol. The mixture was refluxed for 5 hours. After cooled down, it was concentrated to remove methanol. The dark brown residue obtained was recrystallized in glacial acetic acid to give white crystals of 2-hydroxy-4,6-dimethylpyridine-3,5-dicarbonitrile (6.82 g, 89% yield).

Method 2 : Cuprous cyanide (284.13 mg, 3.17 mmol) was dissolved in DMF (5 mL). To this, 5-bromo-2-hydroxy-4,6-dimethylnicotinonitrile (600 mg, 2.6mmol) was added. The reaction was heated and refluxed under N_2 protection for 48 hours. On cooling, the reaction mixture was poured into an $FeCl_3$ solution (4 g FeCl3, 4 mL H2O, 1 ml HCl) and stirred at 60°C for 15 minutes. Then the mixture was poured over crushed ice and dilued with 50 ml water. The water solution was neutralized with 1M NaOH and then filtered. The aqueous solution so obtained was extracted with ethyl acetate (80 x 3 ml) and dichloromethane (50 x 2 ml). The combined organic layers were washed with brine, dried over Na_2SO_4, filtered and concentrated to give 720 mg crude product. The crude products were recrystallized in glacial acetic acid to give 2-hydroxy-4,6-dimethylpyridine-3,5-dicarbonitrile (278mg, 61% yield) as a white powder.

^{1}HNMR (400 MHz, DMSO) 3.32 (br, 1H), 2.5 (s, 3H), 2.22 (s, 3H).

After convergence of the two schemes:

2-Bromo-4,6-dimethylpyridine-3,5-dicarbonitrile

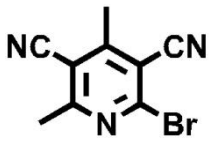

A solution of 2-hydroxy-4,6-dimethylpyridine-3,5-dicarbonitrile (5 g, 28.7 mmol), tetrabutyl ammonium bromide (13.97 g, 43.3 mmol) and phosphorous pentaoxide (12.3 g, 86.7 mmol) was heated in toluene (130 mL) at 100°C under N_2 protection for 5 hours. After cooled down, the mixture was partitioned with brine(50ml) and EtOAc(100ml). The aqueous layer was then extracted with EtOAc (80 x 3 ml). The combined organic layers were dried over Na_2SO_4, filtered and concentrated to give 6.1 g crude brown solid. The crude product was purified by column chromatography on neutral aluminum oxide with a Hexane:EtOAc solvent system (6:1 v/v) as eluent to give 2-bromo-4,6-dimethylpyridine-3,5-dicarbonitrile (4.26 mg, 67% yield) as a white powder. M.p.: 127-129°C ^{1}HNMR (400 MHz, $CDCl_3$) 2.83 (s, 3H), 2.78 (s, 3H).

1-Methoxy-4-((prop-2-ynyloxy)methyl)benzene (10)

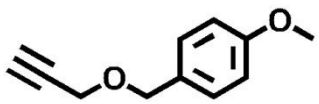

A solution of 4-methoxybenzylalcohol (3.32g, 24 mmol) in anhydrous Et_2O (24 mL) was added to a suspension of NaH (58 mg, 2.4 mmol) at room temperature and stirred under N_2 protection. After stirring for 30 minutes, the mixture was cooled to 0°C and trichloroacetonitrile (3.46 g, 24 mmol) was added. The reaction mixture was allowed to warm up slowly to room temperature over 4 hours. The solution was concentrated to remove ether and the residue so obtained was dissolved in anhydrous hexane (28 mL) and anhydrous methanol (0.12 mL) and filtered through celite. It was then concentrated again to give yellow oil (6.7 g). The crude intermediate was dissolved in 40 ml dichloromethane. Propargyl alcohol (896 mg, 16 mmol) was added to the reaction. The solution was cooled to 0°C and 10-camphorsulfonic acid was added until the pH turned to 3-4. The reaction was stirred overnight under N_2 protection while a white precipitate formed. The solution was filtered through celite, washed with saturated sodium bicarbonate solution, dried over Na_2SO_4, filtered and concentrated to give 3.4 g crude product. The crude product was purified on silica gel with Hexane:EtOAc (20:1 v/v) to give 1-methoxy-4-((prop-2-ynyloxy)methyl)benzene (2.4 g, 83% yield)as a colorless oil. ^{1}HNMR (400 MHz, CDCl3) 7.29 (m, 2H), 6.89 (m, 2H), 4.53 (s, 2H), 4.13 (d, *J=2.4 Hz*, 2H), 379 (s, 3H), 2.45 (t, *J=2.4 Hz*, 1H).

2-(3-((4-Methoxybenzyloxy)prop-1-ynyl)-4,6-dimethylpyridine-3,5-dicarbonitrile (11a)

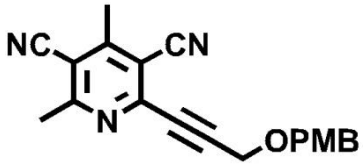

To a solution of 2-bromo-4,6-dimethylpyridine-3,5-dicarbonitrile (620 mg, 2.6 mmol) in anhydrous diethyl ether (60 mL), CuI (24 mg, 0.26 mmol), $PdCl_2(PPh_3)_2$ (91 mg, 0.13 mmol), and triethylamine (18 mL) was added. After stirring for 15 minutes, 1-methoxy-4-((prop-2-ynyloxy)methyl)benzene (554 mg, 3.15 mmol) in diethyl ether (2 mL) was added slowly drop wise under N_2 protection. The reaction was allowed to stir under N_2 protection overnight while a precipitate formed. Then water (25 mL) was added. The organic layer was separated and the water layer was extracted with EtOAc (50 x 2 ml). The combined organic layers were washed with brine, dried over Na_2SO_4 and concentrated. Purification by chromatography on silica gel with a Hexane/EtOAc (5:1) solvent system as eluent gave 2-(3-((4-Methoxybenzyloxy)prop-1-ynyl)-4,6-dimethylpyridine-3,5-dicarbonitrile (565 mg, 66% yield) as white crystals. ^{1}HNMR (400 MHz, $CDCl_3$): 7.34 (d, 2H), 6.90 (d, 2H), 4.68 (s, 2H), 4.47 (s, 2H), 3.8 (s, 3H), 2.82 (s, 3H), 2.76 (s, 3H).

2-(3-((4-Methoxybenzyloxy)propyl)-4,6-dimethylpyridine-3,5-dicarbonitrile (12a):

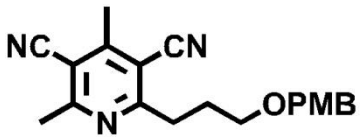

A mixture of 2-(3-((4-methoxybenzyloxy)prop-1-ynyl)-4,6-dimethylpyridine-3,5-dicarbonitrile (500 mg, 1.4mmol) and Pd/C (47 mg, 10% by weight) in MeOH (40 mL) was hydrogenated under 57 psi H_2 for 12 hours. The mixture was filtered through celite to remove Pd/C and concentrated to remove MeOH to give 2-(3-((4-methoxybenzyloxy)propyl)-4,6-dimethylpyridine-3,5-dicarbonitrile (485 mg, 95% yield) as a white solid without further purification. ^{1}HNMR (400 MHz, $CDCl_3$) 7.16 (d, 2H), 6.88 (d, 2H), 4.32 (s, 2H), 3.74 (s, 3H), 3.48 (t, *J=6.0 Hz*, 2H), 3.05 (m, 2H), 2.68 (s, 3H), 2.58 (s, 3H), 2.03 (m, 2H).

(2-(3-(4-Methoxybenzyloxy)propyl)-4,6-dimethylpyridine-3,5-diyl)dimethanamine

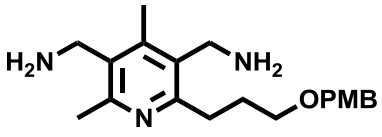

Hydrogenation was conducted on a mixture of 2-(3-((4-methoxybenzyloxy)propyl)-4,6-dimethylpyridine-3,5-dicarbonitrile (350 mg, 1.04 mmol) and wet Raney Nickel slurry

(700 mg) in glacial acetic acid (15 mL) under 58 psi H_2 for 24 hours. The mixture was filtered through celite to remove the catalyst and concentrated to remove AcOH. The crude product was purified by flash column chromatography on silica gel with Dichloromethane/Methanol (15:1) to give 2-(3-((4-methoxybenzyloxy)propyl)-4,6-dimethylpyridine-3,5-dicarbonitrile (210 mg, 57% yield) as a brown semi-solid. ^{1}HNMR (400 MHz, $CDCl_3$) 7.16 (m, 2H), 6.88 (m, 2H), 4.32 (s, 2H), 3.74 (s, 3H), 3.48 (t, *J=6.0 Hz*, 2H), 3.05 (m, 2H), 2.68 (s, 3H), 2.58 (s, 3H), 2.11 (m, 2H). ^{13}C NMR (100MHz, MeOD) 159.12, 157.33, 154.37, 144.32, 132.32-129.21, 113.75, 72.47, 69.56, 55.29, 40.1, 39.56, 31.7, 30.33, 22.42, 14.53.

6.1.2 Synthesis of final products :

***N,N*-(2-(3-(4-methoxybenzyloxy)propyl)-4,6-dimethylpyridine-3,5-diyl)bis(methylene)di-2-napthamide**

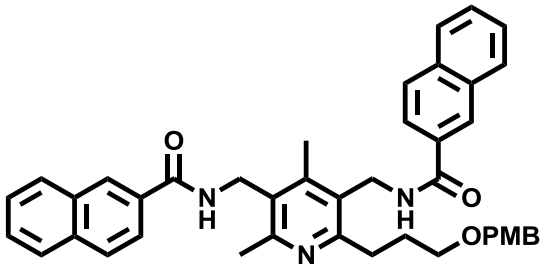

On an ice water bath a solution of napthoic acid (0.311 g , 1.8 mmol) in DMF (3ml), 1-(3-Dimethylaminopropyl)-3-ethylcarbodiimide hydrochloride (0.485 g, 2.5 mmol),

hydroxybenzotriaoxazole (0.342 g, 2.5 mmol), molecular sieve and TEA (0.549g , 5.4 mmol) with N_2 protection. After 20 minutes a solution of (2-(3-(4-Methoxybenzyloxy)propyl)-4,6-dimethylpyridine-3,5-diyl)dimethanamine (0.2 g, 0.6 mmol) in DMF was added drop wise. After stirring at room temperature overnight the resulting mixture was filtered through celite. The filtrate was concentrated in vacuum. The residue was dissolved in 50 ml DCM and washed with brine, dried and concentrated to give 0.240 g crude. Purification by chromatography on silica gel with a DCM/MeOH (15:1) as eluent gave 0.140 g product as a white solid in % yield. ^{1}HNMR (400 MHz, $CDCl_3$) 8.2 (s, 2H), 8.07 (s, 1H), 7.77 (d, , *J*=8Hz, 2H), 7.68 (d, *J*=8Hz, 2H), 6.8 (d, 2H), 4.64 (d, d, *J*=4.68Hz, *J*=10.04Hz 4H), 4.26 (t, 2H), 3.73 (s, 3H), 3.51 (t, 2H), 3.1 (t, 2H), 2.59 (s, 3H), 2.54 (s, 3H), 2.0 (m, 2H).

***N,N*-(2-(3-hydroxypropyl)-4,6-dimethylpyridine-3,5-diyl)bis(methylene)di-2-naphthamide**

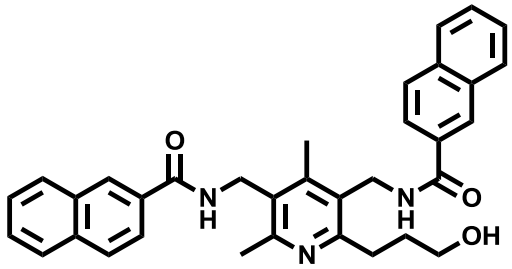

The solution of *N*,*N*-(2-(3-(4-methoxybenzyloxy)propyl)-4,6-dimethylpyridine-3,5-diyl)bis(methylene)di-2-napthamide (120 mg, 0.2 mmol) in 6 ml EtOH and 3 ml 1N HCl was refluxed for 3 hours. After cooled down, the mixture was concentrated to remove EtOH. The combined organic layers were washed with brine, dried over anhydrous Na_2SO_4, filtered and concentrated to give 150 mg crude. Purification on silica gel column with a DCM / MeOH (10:1) solvent system as eluent to give 80 mg white solid in 82% yield. ^{1}HNMR (400 MHz, $CDCl_3$) 8.38 (d, 2H), 7.8 (m, 8H), 7.54 (m, 4H), 4.76 (m, 4H), 3.67 (t, 2H), 3.1 (t, 2H), 2.69 (s, 3H), 2.57 (s, 3H), 2.04 (m, 2H).

6,8-(bis(methylene)di-napthylcarboxamide)5,7-dimethyl-2,3-dihydro-1*H*-indolizinium

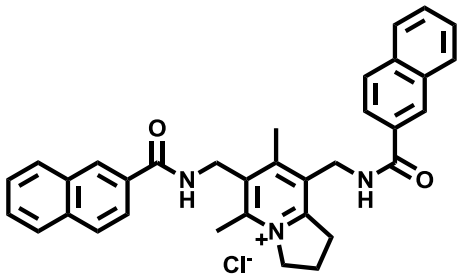

Methanesulfonyle chloride (46 mg, 0.4 mmol) was added into the solution of *N*,*N*-(2-(3-hydroxypropyl)-4,6-dimethylpyridine-3,5-diyl)bis(methylene)di-2-naphthamide (75 mg, 0.14 mmol) in 5 ml CH_2Cl_2 and triethylamine (60 mg, 0.6mmol) at 0°C. The resulting mixture was allowed to warm to room temperature over 1 hour. The mixture was diluted with 20 ml CH_2Cl_2. The CH_2Cl_2 layer was washed with 1N HCl twice followed by brine ,

dried over Na_2SO_4, filtered and concentrated. Purification with chromatography on silica gel with a CH_2Cl_2/MeOH (10:1) solvent system as the eluent to give 40 mg pure white solid in 51% yield. ^{1}HNMR (400 MHz, MeOD) 8.34 (d, 2H), 7.88 (m, 8H), 7.52 (m, 4H), 4.82 (m, 4H), 4.75 (s, 2H), 3.85 (t, 2H), 2.9 (s, 3H), 2.87 (s, 3H), 2.54 (m, 2H). ^{13}C NMR (400MHz, MeOD) 170.36 (2 carbons), 158.7, 158.15, 152.32-124.78, 59.19, 39.95, 39.14, 33.107, 21.42, 17.92, 17.62. MS m/z: 514.25

***N,N*-(2-(3-(4-methoxybezyloxy)propyl)-4,6-dimethylpyridine-3,5-diyl)bis(methylene)bis(4-methylbenzamide)**

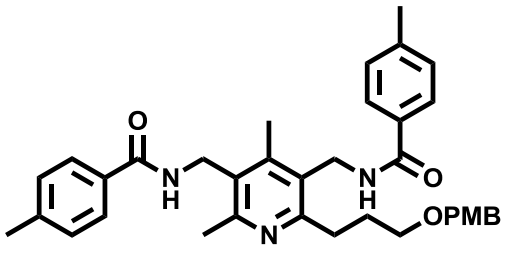

On an ice water bath, a solution of benzoic acid (0.291 g , 1.8 mmol) in DMF (3ml), 1-(3-Dimethylaminopropyl)-3-ethylcarbodiimide hydrochloride (0.485 g, 2.5 mmol), hydroxybenzotriaoxazole (0.342 g, 2.5 mmol), molecular sieve and TEA (0.549g , 5.4 mmol) with N_2 protection. After 20 minutes a solution of (2-(3-(4-Methoxybenzyloxy)propyl)-4,6-dimethylpyridine-3,5-diyl)dimethanamine (0.22 g, 0.6

mmol) in DMF was added drop wise. After stirring at room temperature overnight the resulting mixture was filtered through celite. The filtrate was concentrated in vacuum. The residue was dissolved in 50 ml DCM and washed with brine, dried and concentrated to give 0.240 g crude. Purification by chromatography on silica gel with a DCM/MeOH (15:1) as eluent gave 0.15 g product as a white solid in 40% yield. ^{1}HNMR (400 MHz, $CDCl_3$) 8.2 (s, 1H), 7.77 (d, *J*= 7.76 *Hz*, 2H), 7.62 (d, 2H), 7.59 (d, *J*= 1.96 *Hz*, 2H), 7.53 (d, 2H), 7.07 (m, 4H) 7.00 (d, 2H), 6.70 (d, 2H), 4.66 (d,d, *J*= 1.84 *Hz*, *J*= 8.40 *Hz*, 4H), 4.22 (t, 2H), 3.73 (s, 3H), 3.51 (t, 2H), 3.1 (t, 2H), 2.59 (s, 3H), 2.54 (s, 3H), 2.35 (s, 3H), 2.0 (m, 2H).

***N,N*-(2-(3-hydroxypropyl)-4,6-dimethylpyridine-3,5-diyl)bis(methylene)bis(4-methylbenzamide)**

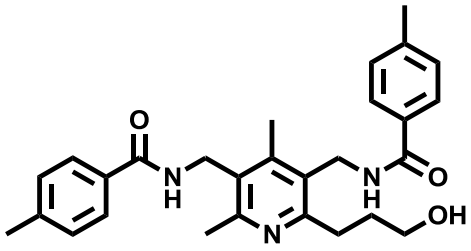

The solution of *N*,*N*-(2-(3-(4-methoxybezyloxy)propyl)-4,6-dimethylpyridine-3,5-diyl)bis(methylene)bis(4-methylbenzamide) (120 mg, 0.2 mmol) in 6 ml EtOH and 3 ml

1N HCl was refluxed for 3 hours. After cooled down, the mixture was concentrated to remove EtOH. The combined organic layers were washed with brine, dried over anhydrous Na_2SO_4, filtered and concentrated to give 1650 mg crude. Purification on silica gel column with a DCM / MeOH (10:1) solvent system as eluent to give 88 mg white solid in 64% yield. ^{1}HNMR (400 MHz, $CDCl_3$) 7.83 (m, 4H), 7.24 (m, 5H), 4.76 (m, 4H), 3.67 (t, 2H), 3.1 (t, 2H), 2.69 (s, 3H), 2.57 (s, 3H), 2.35 (s, 3H), 2.04 (m, 2H).

5,7-dimethyl-6,8-bis((4-methylbenzamido)methyl)-2,3-dihydro-1H-indolizin-4-ium chloride

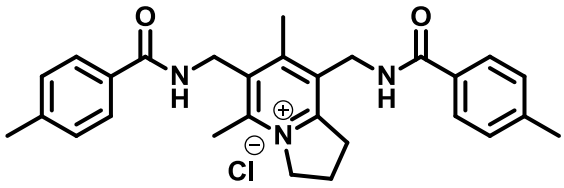

Methanesulfonyle chloride (46 mg, 0.4 mmol) was added into the solution of *N*,*N*-(2-(3-hydroxypropyl)-4,6-dimethylpyridine-3,5-diyl)bis(methylene)di-2-naphthamide (75 mg, 0.14 mmol) in 5 ml CH_2Cl_2 and triethylamine (60 mg, 0.6mmol) at 0°C. The resulting mixture was allowed to warm to room temperature over 1 hour. The mixture was diluted with 20 ml CH_2Cl_2. The CH_2Cl_2 layer was washed with 1N HCl twice followed by brine , dried over Na_2SO_4, filtered and concentrated. Purification with chromatography on silica

gel with a CH_2Cl_2/MeOH (10:1) solvent system as the eluent to give 40 mg pure white solid in 51% yield. ^{1}HNMR (400 MHz, MeOD) 8.82 (s, 1H), 8.69 (s, 1H), 7.91 (d, *J*= 7.92 *Hz*, 4H), 7.10 (t, 4H), 4.82 (d,d, *J*= 2.68 *Hz*, *J*= 2.96 *Hz* 4H), 3.71 (m, 2H), 2.79 (s, 3H), 2.69 (s, 3H), 2.48 (m, 2H). ^{13}C NMR (400MHz, MeOD) 167.36 (2 carbons), 158.7, 156.15, 150.34, 152.32-124.78, 57.72, 39.02, 38.33, 32.16, 21.42, 17.92, 17.62. MS m/z: 442.

***N,N'*-((2-(3-((4-methoxybenzyl)oxy)propyl)-4,6-dimethylpyridine-3,5-diyl)bis(methylene))bis(4-ethylbenzamide)**

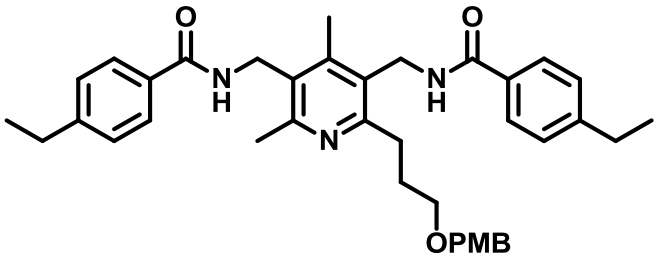

On an ice water bath, a solution of p-ethylbenzoic acid (0.291 g , 1.93 mmol) in DMF (3ml), 1-(3-Dimethylaminopropyl)-3-ethylcarbodiimide hydrochloride (0.520 g, 2.7 mmol), hydroxybenzotriaoxazole (0.366 g, 2.7 mmol), molecular sieve and TEA (0.589g , 5.8 mmol) with N_2 protection. After 20 minutes a solution of (2-(3-(4-Methoxybenzyloxy)propyl)-4,6-dimethylpyridine-3,5-diyl)dimethanamine (0.22 g, 0.6

mmol) in DMF was added drop wise. After stirring at room temperature overnight the resulting mixture was filtered through celite. The filtrate was concentrated in vacuum. The residue was dissolved in 50 ml DCM and washed with brine, dried and concentrated to give 0.521 g crude. Purification by chromatography on silica gel with a DCM/MeOH (15:1) as eluent gave 0.338 g product as a white solid in 86% yield. ^{1}HNMR (400 MHz, $CDCl_3$) 8.00 (S, 2H), 7.65 (d, *J*= 8.40 *Hz*, 2H), 7.63 (d, *J*= 7.9 *Hz*, 2H), 7.22 (d, *J*= 2.2 *Hz*, 2H), 7.16 (d, *J*= 3.1 *Hz*, 2H), 4.68 (d,d, *J*= 5.28 *Hz*, *J*= 1.6 *Hz*, 4H), 4.2 (s, 2H), 3.57 (m, 2H), 3.01 (t, 2H), 2.68 (s, 3H), 2.66 (s, 3H), 2.62 (s, 3H), 2.54 (s, 3H), 2.39 (s, 4H), 2.09 (m, 2H). ^{13}C NMR (400MHz, CDCl3): δ 169.93, 167.40, 167.21, 159.22, 150.21, 148.43, 148.12, 131.36, 130.24, 130.07, 129.46, 129.31, 128.11, 127.74, 127.16, 127.05, 113.83, 113.72, 72.17, 69.45, 55.29, 55.22, 38.75-15.20.

***N,N'*-((2-(3-hydroxypropyl)-4,6-dimethylpyridine-3,5-diyl)bis(methylene))bis(4-ethylbenzamide)**

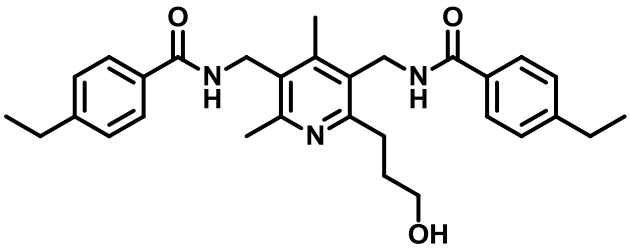

The solution of *N,N'*-((2-(3-((4-methoxybenzyl)oxy)propyl)-4,6-dimethylpyridine-3,5-diyl)bis(methylene))bis(4-ethylbenzamide) (338 mg, 0.5 mmol) in 12 ml EtOH and 6 ml 1N HCl was refluxed for 3 hours. After cooled down, the mixture was concentrated to remove EtOH. The combined organic layers were washed with brine, dried over anhydrous Na_2SO_4, filtered and concentrated to give 0.468 g crude. Purification on silica gel column with a DCM / MeOH (10:1) solvent system as eluent to give 103 mg white solid in 40% yield. ^{1}HNMR (400 MHz, $CDCl_3$) 8.2 (br, 1H), 7.98 (d, *J*= 7.84 *Hz*, 2H), 7.83 (d, *J*= 7.84 *Hz*, 2H), 7.21 (m, 4H), 4.72 (m, 4H), 3.60 (t, 2H), 3.2 (t, 2H), 2.86 (s, 3H), 2.67 (m, 4H), 2.58 (s, 3H), 2.04 (m, 2H). ^{13}C NMR (400MHz, CDCl3): δ 167.71, 167.56, 155.11, 148.42, 130.70, 130.41, 127.87, 127.60, 60.94, 37.55, 31.94, 28.74, 28.06, 18.00, 16.84, 15.17.

6,8-bis((4-ethylbenzamido)methyl)-5,7-dimethyl-2,3-dihydro-1H-indolizin-4-ium chloride

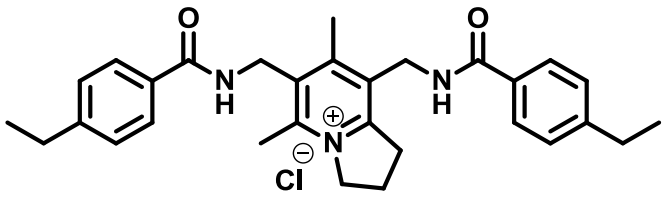

Methanesulfonyle chloride (51.3 mg, 0.44 mmol) was added into the solution of *N,N'*-((2-(3-hydroxypropyl)-4,6-dimethylpyridine-3,5-diyl)bis(methylene))bis(4-ethylbenzamide) (103 mg, 0.21 mmol) in 5 ml CH_2Cl_2 and triethylamine (68 mg, 0.6mmol) at 0°C. The resulting mixture was allowed to warm to room temperature over 1 hour. The mixture was diluted with 5 ml CH_2Cl_2. The CH_2Cl_2 layer was washed with 1N HCl twice followed by brine , dried over Na_2SO_4, filtered and concentrated. Purification with chromatography on silica gel with a CH_2Cl_2/MeOH (10:1) solvent system as the eluent to give 45 mg pure white solid in 45% yield. ^{1}HNMR (400 MHz, MeOD) 8.8 (s, 1H), 8.6 (s, 1H), 7.98 (d, *J*= 6.20 *Hz*, 2H), 7.96 (d, *J*= 7.1 *Hz*, 2H), 7.1 (m, 4H), 4.62 (d,d, *J*= 5.3 *Hz*, *J*= 1.40 *Hz*, 2H), 3.7 (t, 2H), 2.7 (s, 3H), 2.72 (s, 3H), 2.49 (m, 4H), 2.45 (m, 2H). ^{13}C NMR (400MHz, MeOD) 167.36 (2 carbons), 158.7, 158.15, 156.20, 150.32-127.78, 59.19, 39.95, 39.14, 33.107, 21.42, 17.92, 17.62. MS m/z: 470.28

***N,N'*-((2-(3-((4-methoxybenzyl)oxy)propyl)-4,6-dimethylpyridine-3,5-diyl)bis(methylene))bis(([1,1'-biphenyl]-4-carboxamide))**

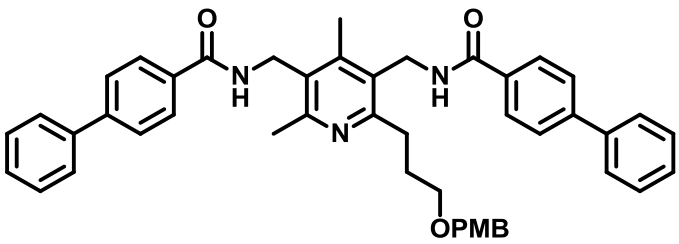

On an ice water bath, a solution of p-phenylbenzoic acid (0.433 g , 1.8 mmol) in DMF (6ml), 1-(3-Dimethylaminopropyl)-3-ethylcarbodiimide hydrochloride (0.586 g, 3 mmol), hydroxybenzotriaoxazole (0.413 g, 3 mmol), molecular sieve and TEA (0.549 g , 5.4 mmol) with N_2 protection. After 20 minutes a solution of (2-(3-(4-Methoxybenzyloxy)propyl)-4,6-dimethylpyridine-3,5-diyl)dimethanamine (0.25 g, 0.7 mmol) in DMF was added drop wise. After stirring at room temperature overnight the resulting mixture was filtered through celite. The filtrate was concentrated in vacuum. The residue was dissolved in 50 ml DCM and washed with brine, dried and concentrated to give 0.630 g crude. Purification by chromatography on silica gel with a DCM/MeOH (15:1) as eluent gave 0.24 g product as a white solid in 40% yield. ^{1}HNMR (400 MHz, $CDCl_3$) 7.89 (d, *J*= 8.6 *Hz*, 2H), 7.79 (d, *J*= 8.12 *Hz*, 2H), 7.4 (m, 8H), 7.04 (d, *J*= 2.1 *Hz*, 2H), 6.70 (d, *J*= 8.52 *Hz*, 2H), 4.72 (d,d, *J*= 5.9 *Hz*, *J*= 2.2 *Hz*, 4H), 4.2 (s, 2H), 3.7 (s, 3H), 3.52 (t, 2H), 2.01 (m, 2H), 2.61 (s, 3H), 2.56 (s, 3H), 2.02 (m, 2H). ^{13}C NMR (400MHz, CDCl3): δ 167.62, 167.40, 159.33, 153.54, 144.43, 144.32, 142.18, 139.95, 132.28, 130.72, 129.60-124.95, 117.85, 113.76, 110.78, 55.21, 38.19, 37.71, 29.96, 29.36, 19.58, 16.52.

***N,N'*-((2-(3-hydroxypropyl)-4,6-dimethylpyridine-3,5-diyl)bis(methylene))bis(([1,1'-biphenyl]-4-carboxamide))**

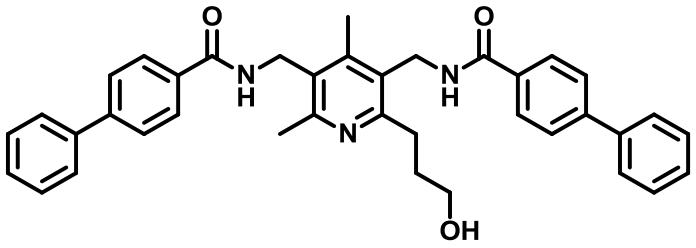

The solution of *N*,*N'*-((2-(3-((4-methoxybenzyl)oxy)propyl)-4,6-dimethylpyridine-3,5-diyl)bis(methylene))bis(([1,1'-biphenyl]-4-carboxamide)) (240 mg, 0.3 mmol) in 12 ml EtOH and 6 ml 1N HCl was refluxed for 5 hours. After cooled down, the mixture was concentrated to remove EtOH. The combined organic layers were washed with brine, dried over anhydrous Na_2SO_4, filtered and concentrated to give 680 mg crude. Purification was done on silica gel column with a DCM / MeOH (10:1) solvent system as eluent to give 88 mg white solid in 44% yield. ^{1}HNMR (400 MHz, $CDCl_3$) 7.85 (d, *J*= 7.80 *Hz*, 2H), 7.83 (d, *J*= 7.37 *Hz*, 2H), 7.69 (d, *J*= 6.40 *Hz* 2H), 7.6 (d, *J*= 1.90 *Hz* 2H), 7.4 (m, 6H), 4.77 (d,d, *J*= 3.88 *Hz*, *J*= 7.04 *Hz*, 4H), 3.7 (t, 2H), 2.94 (s, 3H), 2.81 (s, 3H), 2.00 (m, 2H). ^{13}C NMR (400MHz, CDCl3): δ 167.8, 167.92, 155.5, 15535, 144.5, 143.5, 130.2-127.54, 62.45, 39.4, 38.35, 33.85, 18.6, 16.9.

6,8-bis([1,1'-biphenyl]-4-ylcarboxamidomethyl)-5,7-dimethyl-2,3-dihydro-1H-indolizin-4-ium chloride

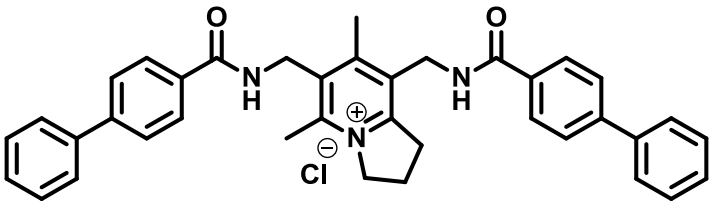

Methanesulfonyle chloride (46 mg, 0.4 mmol) was added into the solution of *N*,*N'*-((2-(3-hydroxypropyl)-4,6-dimethylpyridine-3,5-diyl)bis(methylene))bis(([1,1'-biphenyl]-4-carboxamide)) (88 mg, 0.15 mmol) in 6 ml CH_2Cl_2 and triethylamine (60 mg, 0.45mmol) at 0°C. The resulting mixture was allowed to warm to room temperature over 1 hour. The mixture was diluted with 20 ml CH2Cl2. The CH_2Cl_2 layer was washed with 1N HCl twice followed by brine , dried over Na_2SO_4, filtered and concentrated. Purification was performede with chromatography on silica gel with a CH_2Cl_2/MeOH (10:1) solvent system as the eluent to give 42 mg pure white solid in 46% yield. ^{1}HNMR (400 MHz, MeOD) 9.04 (s, 1H), 8.9 (s, 1H), 8.17 (d, *J*= 8.04 *Hz*, 2H), 7.5 (m, 8H), 7.38 (m, 6H), 4.7 (d,d, *J*=3.96 *Hz*, *J*= 2.35 *Hz*, 4H), 3.7 (t, 2H), 2.82 (s, 3H), 2.77 (s, 3H), 2.50 (m, 2H). ^{13}C NMR (400MHz, MeOD) 167.36 (2 carbons), 158.7, 158.15, 152.32-124.78, 59.19, 39.95, 39.14, 33.107, 21.42, 17.92, 17.62. MS m/z: 566.

***N,N'*-((2-(3-((4-methoxybenzyl)oxy)propyl)-4,6-dimethylpyridine-3,5-diyl)bis(methylene))bis(4-isopropylbenzamide)**

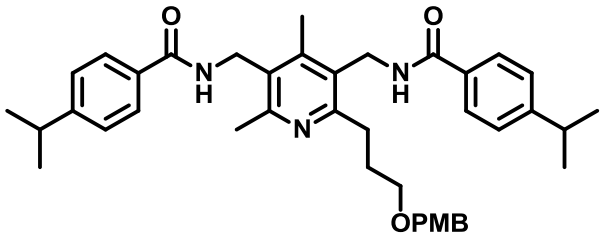

On an ice water bath, a solution of p-isopropylbenzoic acid (0.358 g , 2.1 mmol) in DMF (4ml), 1-(3-Dimethylaminopropyl)-3-ethylcarbodiimide hydrochloride (0.586 g, 3 mmol), hydroxybenzotriaoxazole (0.413 g, 3 mmol), molecular sieve and TEA (0.662g , 6.3 mmol) with N_2 protection. After 20 minutes a solution of (2-(3-(4-Methoxybenzyloxy)propyl)-4,6-dimethylpyridine-3,5-diyl)dimethanamine (0.2 g, 0.58 mmol) in DMF was added drop wise. After stirring at room temperature overnight the resulting mixture was filtered through celite. The filtrate was concentrated in vacuum. The residue was dissolved in 50 ml DCM and washed with brine, dried and concentrated to give 0.400 g crude. Purification by chromatography on silica gel with a DCM/MeOH (15:1) as eluent gave 0.15 g product as a white solid in 86% yield. ^{1}HNMR (400 MHz, $CDCl_3$) 7.84 (d, *J*= 8.84 *Hz*, 2H), 7.74 (d, *J*= 8.28 *Hz*, 2H), 7.22 (m, 4H), 7.18 (d, *J*=

8.56 *Hz*, 2H), 6.7 (d, *J*= 8.6 *Hz*, 2H), 4.67 (d,d, *J*= 4.76 *Hz*, *J*= 9.2 *Hz*, 4H), 4.26 (s, 2H), 3.7 (s, 3H), 3.51 (m, 3H), 3.07 (t, 2H), 2.903 (m, 2H), 2.62 (s, 3H), 2.48 (s, 2H), 2.01 (m, 2H). ^{13}C NMR (400MHz, CDCl3): δ 167.55, 167.33, 159.2727, 153.11, 152.82, 131.211-214.67, 118.13, 113.71, 110.68, 72.39, 69.25, 55.22, 38.26, 37.73, 34.06, 30.54, 29.45, 23.73, 23.72, 20.50, 16.10.

_N,N'_-((2-(3-hydroxypropyl)-4,6-dimethylpyridine-3,5-diyl)bis(methylene))bis(4-isopropylbenzamide)

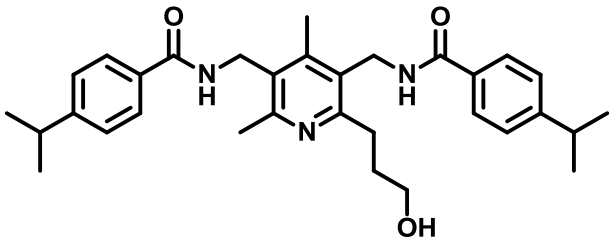

The solution of *N*,*N'*-((2-(3-((4-methoxybenzyl)oxy)propyl)-4,6-dimethylpyridine-3,5-diyl)bis(methylene))bis(4-isopropylbenzamide) (400 mg, 0.62 mmol) in 16 ml EtOH and 8 ml 1N HCl was refluxed for 6 hours. After cooled down, the mixture was concentrated to remove EtOH. The combined organic layers were washed with brine, dried over anhydrous Na_2SO_4, filtered and concentrated to give 340 mg crude. Purification was done on silica gel column with a DCM / MeOH (10:1) solvent system as eluent to give 160 mg white solid in 51% yield. ^{1}HNMR (400 MHz, $CDCl_3$) 7.79 (d, *J*= 7.64 *Hz*, 2H), 7.75 (d,

J= 8.28 *Hz*, 2H), 7.13 (d, *J*= 3.5 *Hz* 2H), 7.09 (d, *J*= 1.60 *Hz* 2H), 4.69 (d, *J*= 8.64 *Hz*, 4H), 3.65 (t, 2H), 3.1 (t, 2H), 2.9 (m, 2H), 2.67 (s, 3H), 2.49 (s, 3H), 2.00 (m, 2H). ^{13}C NMR (400MHz, CDCl3): δ 167.57, 167.22, 153.04, 129.82, 127.4, 127.31, 126.62, 61.85, 38.25, 37.82, 34.07, 31.29, 23.73, 16.06.

6,8-bis((4-isopropylbenzamido)methyl)-5,7-dimethyl-2,3-dihydro-1H-indolizin-4-ium chloride

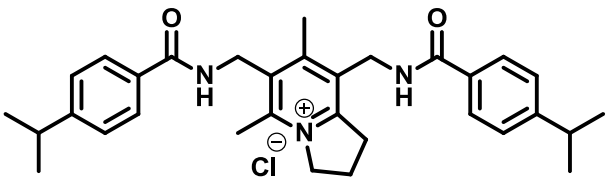

Methanesulfonyle chloride (73 mg, 0.6 mmol) was added into the solution of *N*,*N*'-((2-(3-hydroxypropyl)-4,6-dimethylpyridine-3,5-diyl)bis(methylene))bis(4-isopropylbenzamide) (160 mg, 0.3 mmol) in 5 ml CH_2Cl_2 and triethylamine (94 mg, 0.6mmol) at 0°C. The resulting mixture was allowed to warm to room temperature over 1 hour. The mixture was diluted with 20 ml CH2Cl2. The CH_2Cl_2 layer was washed with 1N HCl twice followed by brine, dried over Na_2SO_4, filtered and concentrated. Purification was done by chromatography on silica gel with a CH_2Cl_2/MeOH (12:1) solvent system as the eluent to give 52 mg pure white solid in 41% yield. ^{1}HNMR (400 MHz, MeOD) 8.7 (s, 1H), 8.64 (s, 1H), 7.79 (d, *J*= 8.1 *Hz* ,2H), 7.95 (d, *J*= 8.5 *Hz*, 2H),

7.21 (m, 4H), 4.74 (d,d, *J*= 6.2 *Hz*, *J*= 5.8 *Hz* 4H), 4.65 (m, 2H), 3.66 (t, 2H), 2.76 (m, 2H), 2.76 (s, 3H), 2.67 (s, 3H), 2.59 (s, 3H), 2.48 (m, 2H). ^{13}C NMR (400MHz, MeOD) 167.36 (2 carbons), 158.7, 156.15, 152.32-124.78, 57.19, 39.95, 38.14, 38.39, 33.107, 23.72, 21.42, 17.92, 17.62. MS m/z: 499.

_N,N'_-((2-(3-((4-methoxybenzyl)oxy)propyl)-4,6-dimethylpyridine-3,5-diyl)bis(methylene))bis(4-methoxybenzamide)

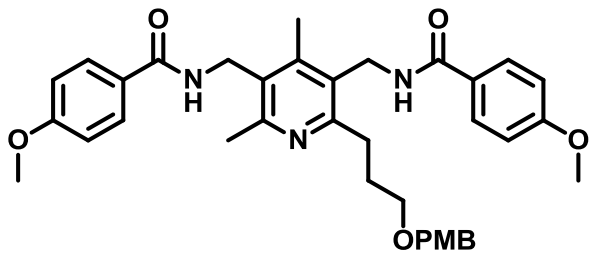

On an ice water bath, a solution of p-methoxybenzoic acid (0.339 g , 2.2 mmol) in DMF (6ml), 1-(3-Dimethylaminopropyl)-3-ethylcarbodiimide hydrochloride (0.513 g, 2.6 mmol), hydroxybenzotriaoxazole (0.361 g, 2.6 mmol), molecular sieve and TEA (0.676g , 6.6 mmol) with N_2 protection. After 20 minutes a solution of (2-(3-(4-Methoxybenzyloxy)propyl)-4,6-dimethylpyridine-3,5-diyl)dimethanamine (0.255 g, 0.7 mmol) in DMF was added drop wise. After stirring at room temperature overnight the resulting mixture was filtered through celite. The filtrate was concentrated in vacuum.

The residue was dissolved in 50 ml DCM and washed with brine, dried and concentrated to give 0.4 g crude. Purification by chromatography on silica gel with a DCM/MeOH (15:1) as eluent gave 0.15 g product as a white solid in 90% yield. ^{1}HNMR (400 MHz, $CDCl_3$) 8.2 (s, 1H), 8.18 (s, 1H), 7.78 (d, *J*= 7.79 *Hz*, 2H), 7.69 (d, *J*= 7.80 *Hz*, 2H), 7.59 (d, *J*= 2.96 *Hz*, 2H), 7.53 (d, 2H), 7.12 (m, 4H), 7.05 (d, 2H), 6.70 (d, 2H), 4.72 (d,d, *J*= 2.84 *Hz*, *J*= 6.40 *Hz*, 4H), 4.22 (t, 2H), 3.73 (s, 3H), 3.41 (t, 2H), 3.1 (t, 2H), 2.56 (s, 3H), 2.55 (s, 3H), 2.39 (s, 3H), 2.02 (m, 2H). ^{13}C NMR (400MHz, CDCl3): δ 169.93, 167.40, 167.21, 159.22, 150.21, 148.43, 148.12, 131.36, 130.24, 130.07, 129.46, 129.31, 128.11, 127.74, 127.16, 127.05, 113.83, 113.72, 72.17, 69.45, 55.29, 55.22, 38.75-15.20.

***N,N'*-((2-(3-hydroxypropyl)-4,6-dimethylpyridine-3,5-diyl)bis(methylene))bis(4-methoxybenzamide)**

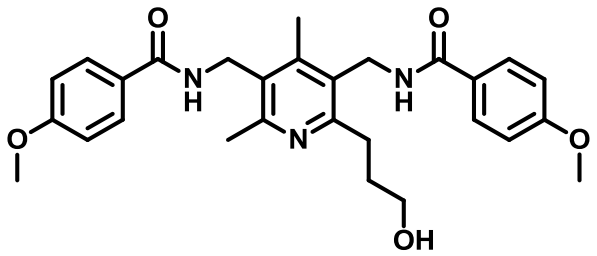

The solution of *N,N'*-((2-(3-((4-methoxybenzyl)oxy)propyl)-4,6-dimethylpyridine-3,5-diyl)bis(methylene))bis(4-methoxybenzamide) (400 mg, 0.6 mmol) in 16 ml EtOH and 8 ml 1N HCl was refluxed for 6 hours. After cooled down, the mixture was concentrated to remove EtOH. The combined organic layers were washed with brine, dried over anhydrous Na_2SO_4, filtered and concentrated to give 491.58 mg crude. Purification was done on silica gel column with a DCM / MeOH (10:1) solvent system as eluent to give 120 mg white solid in 40% yield. ^{1}HNMR (400 MHz, $CDCl_3$) 7.93 (m, 4H), 7.44 (m, 5H), 4.76 (m, 4H), 3.67 (t, 2H), 3.23 (t, 2H), 2.68 (s, 3H), 2.57 (s, 3H), 2.35 (s, 3H), 2.04 (m, 2H). ^{13}C NMR (400MHz, CDCl3): δ 167.61, 167.56, 154.11, 147.42, 133.50, 133.42, 128.87, 127.60, 60.94, 37.55, 31.94, 28.74, 28.06, 18.00, 16.84, 15.17.

6,8-bis((4-methoxybenzamido)methyl)-5,7-dimethyl-2,3-dihydro-1H-indolizin-4-ium chloride

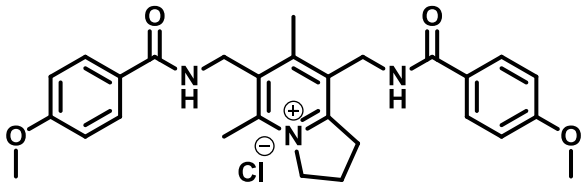

Methanesulfonyle chloride (54 mg, 0.4 mmol) was added into the solution of *N,N'*-((2-(3-hydroxypropyl)-4,6-dimethylpyridine-3,5-diyl)bis(methylene))bis(4-methoxybenzamide) (120 mg, 0.2 mmol) in 5 ml CH_2Cl_2 and triethylamine (74 mg, 0.7mmol) at 0°C. The resulting mixture was allowed to warm to room temperature over 1 hour. The mixture was diluted with 20 ml CH_2Cl_2. The CH_2Cl_2 layer was washed with 1N HCl twice followed by brine, dried over Na_2SO_4, filtered and concentrated. Purification was done using chromatography on silica gel with a CH_2Cl_2/MeOH (10:1) solvent system as the eluent to give 53 mg pure white solid in 80% yield. ^{1}HNMR (400 MHz, MeOD) 7.78 (d, , *J*= 3.56 *Hz*, 2H), 7.75 (d, , *J*= 3.56 *Hz*, 2H), 6.96 (d, , *J*= 4.52 *Hz*, 2H), 6.94 (d, , *J*= 4.7 *Hz*, 2H), 4.87 (d,d, *J*= 4.84 *Hz*,, *J*= 6.4 *Hz*, 2H), 4.66 (s, 2H), 3.82 (s,63H), 3.77 (t, 2H), 2.85 (s, 3H), 2.69 (s, 3H), 2.49 (m, 2H). ^{13}C NMR (400MHz, MeOD) 167.6 (2 carbons), 158.7, 158.15, 152.32-124.78, 58.19, 37.95, 37.14, 33.107, 21.42, 17.92, 16.62. MS m/z: 474.24. MS m/z: 482.14

***N,N'*-((2-(3-((4-methoxybenzyl)oxy)propyl)-4,6-dimethylpyridine-3,5-diyl)bis(methylene))bis(4-bromobenzamide)**

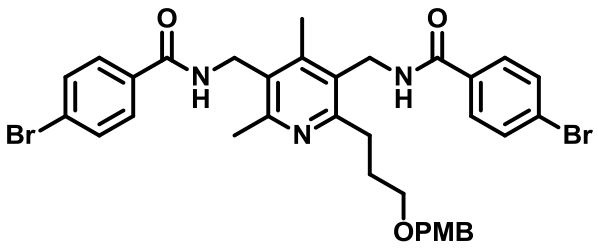

On an ice water bath, a solution of p-bromobenzoic acid (0.439 g , 2.1 mmol) in DMF (8ml), 1-(3-Dimethylaminopropyl)-3-ethylcarbodiimide hydrochloride (0..502 g, 2.6 mmol), hydroxybenzotriaoxazole (0.354 g, 2.6 mmol), molecular sieve and TEA (0.662 g , 6.5 mmol) with N_2 protection. After 20 minutes a solution of (2-(3-(4-Methoxybenzyloxy)propyl)-4,6-dimethylpyridine-3,5-diyl)dimethanamine (0.25 g, 0.7 mmol) in DMF was added drop wise. After stirring at room temperature overnight the resulting mixture was filtered through celite. The filtrate was concentrated in vacuum. The residue was dissolved in 50 ml DCM and washed with brine, dried and concentrated to give 0.68 g crude. Purification by chromatography on silica gel with a DCM/MeOH (15:1) as eluent gave 0.438 g product as a white solid in 85% yield. ^{1}HNMR (400 MHz, $CDCl_3$) 7.92 (d, *J*= 8.84 *Hz*, 2H), 7.90 (d, *J*= 8.28 *Hz*, 2H), 7.75 (m, 4H), 7.72 (d, *J*= 8.56 *Hz*, 2H), 6.99 (d, *J*= 8.6 *Hz*, 2H), 6.91 (d, 2H), 4.47 (d,d, *J*= 4.76 *Hz*, *J*= 9.2 *Hz*, 4H), 4.38 (s, 2H), 3.83 (s, 3H), 3.01 (t, 2H), 2.95 (m, 2H), 2.52 (s, 3H), 2.38 (s, 2H), 2.01 (m, 2H). ^{13}C NMR (400MHz, CDCl3): δ 167.8, 167.33, 155.27, 153.11, 152.82, 131.7,

214.67, 118.13, 113.71, 110.68, 72.39, 69.25, 55.22, 38.26, 37.73, 34.06, 30.54, 29.45, 23.73, 23.72, 20.50, 16.10.

_N,N'_-((2-(3-hydroxypropyl)-4,6-dimethylpyridine-3,5-diyl)bis(methylene))bis(4-bromobenzamide)

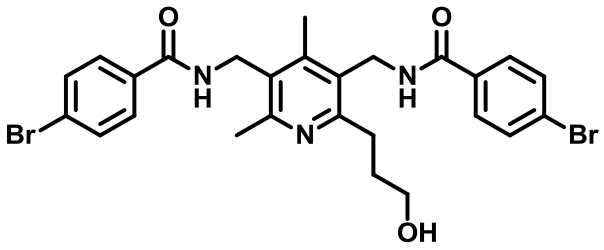

The solution of *N,N'*-((2-(3-((4-methoxybenzyl)oxy)propyl)-4,6-dimethylpyridine-3,5-diyl)bis(methylene))bis(4-bromobenzamide) (420 mg, 0.6 mmol) in 18 ml EtOH and 9 ml 1N HCl was refluxed for 5 hours. After cooled down, the mixture was concentrated to remove EtOH. The combined organic layers were washed with brine, dried over anhydrous Na_2SO_4, filtered and concentrated to give 545 mg crude. Purification was done on silica gel column with a DCM / MeOH (10:1) solvent system as eluent to give 155 mg white solid in 52% yield. ^{1}HNMR (400 MHz, $CDCl_3$) 7.92 (d, *J*= 7.94 *Hz*, 2H), 7.82 (d, *J*= 8.24 *Hz*, 2H), 7.56 (d, *J*= 2.5 *Hz* 2H), 7.55 (d, *J*= 1.60 *Hz* 2H), 4.71 (d, *J*= 8.64 *Hz*, 4H), 3.3 (t, 2H), 3.12 (m, 2H), 2.77 (s, 3H), 2.69 (s, 3H), 2.09 (m, 2H). ^{13}C NMR (400MHz, CDCl3): δ 167.87, 167.72, 154.04, 153.89 129.82, 125.4, 125.31, 124.62, 60.85, 38.5, 37.82, 34.07, 31.29, 23.73, 16.05.

6,8-bis((4-bromobenzamido)methyl)-5,7-dimethyl-2,3-dihydro-1H-indolizin-4-ium chloride

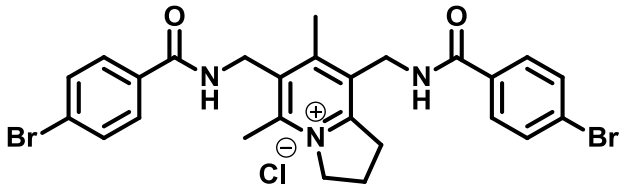

Methanesulfonyle chloride (60.1mg, 0.52 mmol) was added into the solution of *N,N'*-((2-(3-hydroxypropyl)-4,6-dimethylpyridine-3,5-diyl)bis(methylene))bis(4-bromobenzamide) (0.155 mg, 0.26 mmol) in 6 ml CH_2Cl_2 and triethylamine (79.1 mg, 0.78mmol) at 0°C. The resulting mixture was allowed to warm to room temperature over 1 hour. The mixture was diluted with 25 ml CH_2Cl_2. The CH_2Cl_2 layer was washed with 1N HCl twice followed by brine , dried over Na_2SO_4, filtered and concentrated. Purification was performed on chromatography on silica gel with a CH_2Cl_2/MeOH (10:1) solvent system as the eluent to give 46 mg pure white solid in 30% yield. ^{1}HNMR (400 MHz, MeOD) 7.82 (d, , *J*= 8.4 *Hz*, 2H), 7.79 (d, *J*= 7.94 *Hz* 2H), 7.36 (d, 2H), 7.33 (d, *J*= 2.04 *Hz* 2H), 4.73 (d,d, *J*= 2.3 *Hz*, *J*= 6.2 *Hz* 4H), 3.75 (t, 2H), 3.48 (s, 2H), 3.16 (m, 2H), 2.62 (s, 3H), 2.5 (s, 3H), 2.03 (m, 2H). ^{13}C NMR (400MHz, MeOD) 167.36 (2 carbons), 158.7, 156.15, 152.32-124.78, 60.19, 39.8, 39.14, 34.107, 21.56, 17.89, 16.2. MS m/z: 570.04.

***N,N'*-((2-(3-((4-methoxybenzyl)oxy)propyl)-4,6-dimethylpyridine-3,5-diyl)bis(methylene))bis(4-chlorobenzamide)**

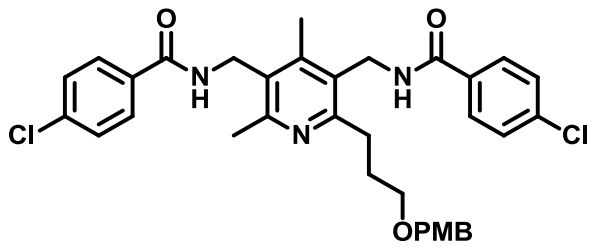

On an ice water bath, a solution of p-chlorobenzoic acid (0.342 g , 2.1 mmol) in DMF (6ml), 1-(3-Dimethylaminopropyl)-3-ethylcarbodiimide hydrochloride (0.502 g, 2.6 mmol), hydroxybenzotriaoxazole (0.354 g, 2.6 mmol), molecular sieve and TEA (0.66g , 6.5 mmol) with N_2 protection. After 20 minutes a solution of (2-(3-(4-Methoxybenzyloxy)propyl)-4,6-dimethylpyridine-3,5-diyl)dimethanamine (0.22 g, 0.6 mmol) in DMF was added drop wise. After stirring at room temperature overnight the resulting mixture was filtered through celite. The filtrate was concentrated in vacuum. The residue was dissolved in 50 ml DCM and washed with brine, dried and concentrated to give 0.648 g crude. Purification by chromatography on silica gel with a DCM/MeOH

(15:1) as eluent gave 0.306 g product as a white solid in 68% yield. ^{1}HNMR (400 MHz, $CDCl_3$) 7.97 (d, *J*= 7.84 *Hz*, 2H), 7.96 (d, *J*= 7.28 *Hz*, 2H), 7.76 (m, 4H), 7.75 (d, *J*= 8.1 *Hz*, 2H), 6.98 (d, *J*= 8.6 *Hz*, 2H), 6.86 (d, 2H), 4.78 (d,d, *J*= 2.7 *Hz*, *J*= 6.5 *Hz*, 4H), 4.68 (s, 2H), 3.97 (s, 3H), 3.33 (t, 2H), 2.85 (m, 2H), 2.72 (s, 3H), 2.38 (s, 2H), 2.01 (m, 2H). ^{13}C NMR (400MHz, CDCl3): δ 167.8, 167.33, 155.27, 153.11, 152.82, 131.7, 214.67, 118.13, 113.71, 110.68, 72.39, 69.25, 55.22, 38.26, 37.73, 34.06, 30.54, 29.45, 23.73, 23.72, 20.50, 16.10.

***N,N'*-((2-(3-hydroxypropyl)-4,6-dimethylpyridine-3,5-diyl)bis(methylene))bis(4-chlorobenzamide)**

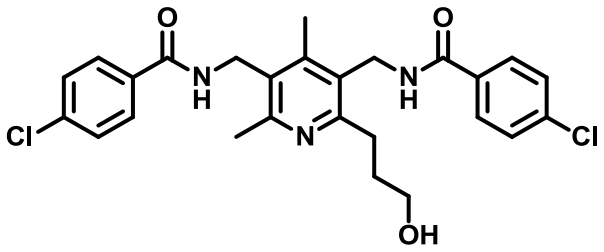

The solution of *N,N'*-((2-(3-((4-methoxybenzyl)oxy)propyl)-4,6-dimethylpyridine-3,5-diyl)bis(methylene))bis(4-chlorobenzamide) (306 mg, 0.2 mmol) in 12 ml EtOH and 6 ml 1N HCl was refluxed for 5 hours. After cooled down, the mixture was concentrated to remove EtOH. The combined organic layers were washed with brine, dried over

anhydrous Na_2SO_4, filtered and concentrated to give 423 mg crude. Purification was done on silica gel column with a DCM / MeOH (10:1) solvent system as eluent to give 125 mg white solid in 51% yield. ^{1}HNMR (400 MHz, $CDCl_3$) 7.83 (m, 4H), 7.24 (m, 5H), 4.76 (m, 4H), 3.67 (t, 2H), 3.1 (t, 2H), 2.69 (s, 3H), 2.57 (s, 3H), 2.35 (s, 3H), 2.04 (m, 2H).

6,8-bis((4-chlorobenzamido)methyl)-5,7-dimethyl-2,3-dihydro-1H-indolizin-4-ium chloride

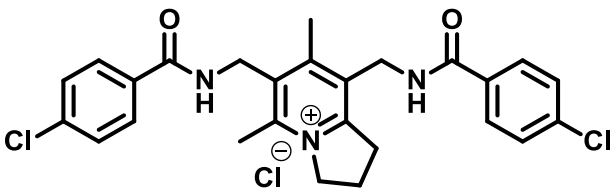

Methanesulfonyle chloride (56 mg, 0.48 mmol) was added into the solution of *N*,*N*′-((2-(3-hydroxypropyl)-4,6-dimethylpyridine-3,5-diyl)bis(methylene))bis(4-chlorobenzamide) (125 mg, 0.2 mmol) in 5 ml CH_2Cl_2 and triethylamine (75 mg, 0.75mmol) at 0°C. The resulting mixture was allowed to warm to room temperature over 1 hour. The mixture was diluted with 25 ml CH_2Cl_2. The CH_2Cl_2 layer was washed with 1N HCl twice followed by brine , dried over Na_2SO_4, filtered and concentrated. Purification was performed with chromatography on silica gel with a CH_2Cl_2/MeOH (10:1) solvent system as the eluent to give 48 mg pure white solid in 40% yield. ^{1}HNMR (400 MHz, MeOD)

7.8 (d, *J*= 8.04 *Hz*, 2H), 7.78 (d, *J*= 8.64 *Hz*, 2H), 7.46 (d, *J*= 3.04 *Hz*, 2H), 7.43 (d, 2H), 4.82 (d,d, *J*= 3.65 *Hz*, *J*= 6.04 *Hz*, 4H), 4.68 (s, 2H), 3.78 (t, sH), 2.86 (s, 3H), 2.78 (s, 3H), 2.5 (m, 2H). ^{13}C NMR (400MHz, MeOD) 167.82, 167.75, 158.3, 158.1, 152.2, 150.51, 134.36, 131.13, 130.70, 130.67, 127.94, 126, 126, 126.36, 124.8, 59.9, 39.5, 39.4, 33.1, 21.2, 17.2, 17.2. MS m/z: 482.14.

***N,N'*-((2-(3-((4-methoxybenzyl)oxy)propyl)-4,6-dimethylpyridine-3,5-diyl)bis(methylene))bis(4-nitrobenzamide)**

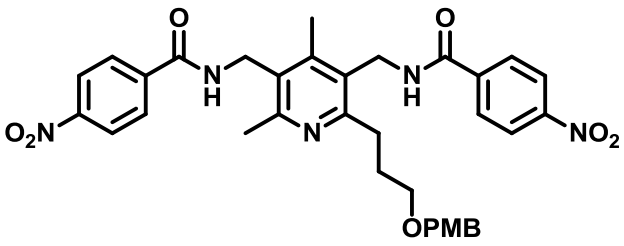

On an ice water bath, a solution of p-nitrobenzoic acid (0.876 g , 5.2 mmol) in DMF (4ml), 1-(3-Dimethylaminopropyl)-3-ethylcarbodiimide hydrochloride (1.206 g, 6.2 mmol), hydroxybenzotriaoxazole (0.495 g, 6.2 mmol), molecular sieve and TEA (1.59g , 15.7 mmol) with N_2 protection. After 20 minutes a solution of (2-(3-(4-Methoxybenzyloxy)propyl)-4,6-dimethylpyridine-3,5-diyl)dimethanamine (0.600 g, 1.7 mmol) in DMF was added drop wise. After stirring at room temperature overnight the resulting mixture was filtered through celite. The filtrate was concentrated in vacuum. The residue was dissolved in 50 ml DCM and washed with brine, dried and concentrated

to give 1.5 g crude. Purification by chromatography on silica gel with a DCM/MeOH (15:1) as eluent gave 645 mg product as a white solid in 85% yield. ^{1}HNMR (400 MHz, $CDCl_3$) 7.8 (d, *J*= 8.6 *Hz*, 2H), 7.78 (d, *J*= 8.12 *Hz*, 2H), 7.65 (d, 4H), 7.03 (d, *J*= 2.1 *Hz*, 2H), 6.70 (d, *J*= 8.52 *Hz*, 2H), 4.72 (d,d, *J*= 5.9 *Hz*, *J*= 2.2 *Hz*, 4H), 4.2 (s, 2H), 3.7 (s, 3H), 3.52 (t, 2H), 2.01 (m, 2H), 2.61 (s, 3H), 2.56 (s, 3H), 2.02 (m, 2H). ^{13}C NMR (400MHz, CDCl3): δ 167.62, 167.40, 159.33, 153.54, 144.43, 139.95, 132.28, 129.60-124.95, 117.85, 113.76, 110.78, 55.21, 38.19, 37.71, 29.96, 29.36, 19.58, 16.52.

***N,N'*-((2-(3-hydroxypropyl)-4,6-dimethylpyridine-3,5-diyl)bis(methylene))bis(4-nitrobenzamide)**

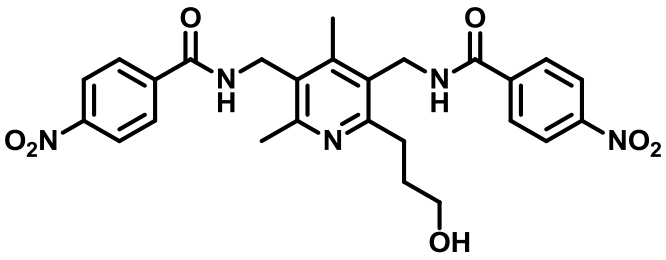

The solution of *N,N'*-((2-(3-((4-methoxybenzyl)oxy)propyl)-4,6-dimethylpyridine-3,5-diyl)bis(methylene))bis(4-nitrobenzamide) (1.1 mg, 1.7 mmol) in 60 ml EtOH and 30 ml 1N HCl was refluxed for 6 hours. After cooled down, the mixture was concentrated to remove EtOH. The combined organic layers were washed with brine, dried over anhydrous Na_2SO_4, filtered and concentrated to give 1.5g crude. Purification was done on

silica gel column with a DCM / MeOH (10:1) solvent system as eluent to give 659 mg white solid in 73% yield ^{1}HNMR (400 MHz, $CDCl_3$) 7.85 (d, *J*= 7.80 *Hz*, 2H), 7.83 (d, *J*= 7.37 *Hz*, 2H), 7.68 (d, *J*= 6.40 *Hz*, 2H), 7.63 (d, *J*= 1.90 *Hz*, 2H), 4.75 (d,d, *J*= 3.88 *Hz*, *J*= 7.04 *Hz*, 4H), 3.72 (t, 2H), 2.96 (s, 3H), 2.83 (s, 3H), 2.05 (m, 2H). ^{13}C NMR (400MHz, CDCl3): δ 167.8, 167.92, 155.5, 155.35, 144.5-127.54, 62.45, 39.4, 38.35, 33.85, 18.6, 16.9.

5,7-dimethyl-6,8-bis((4-nitrobenzamido)methyl)-2,3-dihydro-1H-indolizin-4-ium chloride

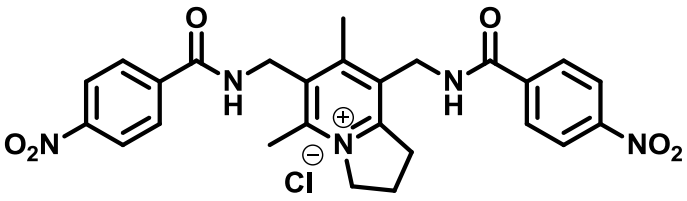

Methanesulfonyle chloride (288 mg, 2.5 mmol) was added into the solution of *N*,*N*'-((2-(3-hydroxypropyl)-4,6-dimethylpyridine-3,5-diyl)bis(methylene))bis(4-nitrobenzamide)

(657 mg, 1.2 mmol) in 38 ml CH_2Cl_2 and triethylamine (382 mg, 3.7mmol) at 0°C. The resulting mixture was allowed to warm to room temperature over 1 hour. The mixture was diluted with 50 ml CH_2Cl_2. The CH_2Cl_2 layer was washed with 1N HCl twice followed by brine , dried over Na_2SO_4, filtered and concentrated. Purification was done by chromatography on silica gel with a CH_2Cl_2/MeOH (10:1) solvent system as the

eluent to give 421 mg pure white solid in 6.2% yield. ^{1}HNMR (400 MHz, MeOD) 7.70 (d, *J*= 8.2 *Hz*, 2H), 7.69 (d, *J*= 8.04 *Hz*, 2H), 7.61 (d, *J*= 2.05 *Hz*, 2H), 7.59 (d, *J*= 2.12 *Hz*, 2H), 4.82 (m, 4H), 4.79 (t, 4H), 4.67 (s, 2H), 3.7 (t, 2H), 2.87 (s, 3H), 2.79 (s, 3H), 2.5 (m, 2H). ^{13}C NMR (400MHz, MeOD) 170.36 (2 carbons), 158.7, 158.15, 152.32-124.78, 59.19, 39.95, 39.14, 33.107, 21.42, 17.92, 17.62. ^{13}C NMR (400MHz, MeOD) 1670.3 (2 carbons), 158.7, 152.32-124.78, 59.19, 39.95, 39.14, 33.107, 21.42, 17.92, 17.62. MS m/z: 570.04

6,8-bis((4-aminobenzamido)methyl)-5,7-dimethyl-2,3-dihydro-1H-indolizin-4-ium chloride

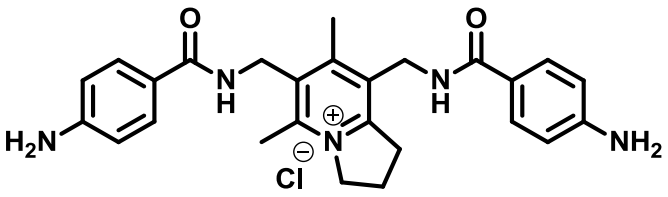

A mixture of 5,7-dimethyl-6,8-bis((4-nitrobenzamido)methyl)-2,3-dihydro-1H-indolizin-4-ium chloride (81 mg, 0.15 mmol), Pd/C (10 mg, 10% by weight) and conc. HCl in MeOH (10 mL) was hydrogenated under 57 psi H_2 for 6 hours. The mixture was filtered through celite to remove Pd/C and concentrated to remove MeOH. Purification was done by performing chromatography in DCM/MeOH (5:1) system to give 6,8-bis((4-aminobenzamido)methyl)-5,7-dimethyl-2,3-dihydro-1H-indolizin-4-ium chloride

(65 mg, 85% yield) as a white solid. ^{1}HNMR (400 MHz, MeOD) 8.29 (d, *J*= 8.8 *Hz*, 2H), 8.27 (d, *J*= 3.3 *Hz*, 2H), 8.02 (d, *J*= 3.3 *Hz*, 2H), 7.59 (d, *J*= 8.7 *Hz*, 2H), 4.80 (m, 4H), 4.72 (t, 4H), 3.81 (s, 2H), 2.89 (s, 3H), 2.82 (s, 3H), 2.54 (m, 2H). ^{13}C NMR (400MHz, MeOD) 170.36 (2 carbons), 158.7, 158.15, 152.32-124.78, 59.19, 39.95, 39.14, 33.107, 21.42, 17.92, 17.62. ^{13}C NMR (400MHz, MeOD) 167.8, 167.78, 153.56, 153.01, 150.9, 150.3, 143.4, 143.2-124.78, 57.19, 40.95, 39.14, 34.107, 22.42, 16.92, 16.62. MS m/z: 444.

5.2 Biological Screening

5.2.1 Anti-proliferation assay

A. Cell culturing:

The CCR5 antagonists were tested on three prostate cancer cell lines – PC-3, DU-145 and M12. All the cell lines were incubated at 37^{0}C and 5% CO_2. The media used to grow the cells was made of RPMI1640 (500 mL), 1% L-glutamine, 0.1% ITS (5 µg/mL insulin, 5 µg/mL transferin, 5 µg/mL selenium), 0.1% gentamycin and 10% fetal bovine serum (FBS). The media used for M12 cell lines contained only 5% FBS and 0.1% geneticin. After 24 hours of incubation of the M12 cells, the media was replaced with

serum free media containing 0.1% epidermal growth factor (EGF). PC-3 and DU-145 had the same media composition containing 0.1% gentamicin.

B. Anti-Proliferation Assay protocol:

On the first day, all the three cell lines were plated in 96 well plates. The number of cells plated in each well was a fixed number of 1000. The cells were plated in a 100µl of total media. All the cells were incubated for 24 hours at 37°C and 5% CO_2. On the second day, after 24 hours, the drug solutions of different concentrations were aliquoted out into each well. The drug dilutions were prepared in phosphate buffer solution (PBS). PBS and DMSO solution was used as a negative control. The percentage of DMSO used was the amount that was present in the highest concentration of drug tested. 50 µL of drug solution was added to each well. The cells were incubated with the drug solution for 72 hours. On the fifth day, the media, PBS and drug solutions were dumped out from the plate. This was followed by the addition of 100 µL of serum free media with 10% of anti-proliferative reagent WST-1. The plates were incubated for 3 hours. The absorbance was then measured at 450 nM on Flex station 3.The software Prism was used to obtain the IC_{50} values of the drugs.

5.2.2 Cytotoxicity assay

A. Cell culturing:

NIH3T3 cells were used to perform the cytotoxicity assay. They were cultured in in DMEM (Invitrogen 11995065) media which contains 4,500 mg/L D-glucose, L-

glutamine, and 110 mg/L sodium pyruvate. 10% New Born Calf Serum was used along with penicillin and streptomycin as antibiotics. They were grown in 8% CO_2 and 37°C.

B. Assay protocol:

NIH3T3 cells are plated into 96-well plate in a 100 µl cell solution volume. An equal amount of 2,000,000 are plated into each well. The control wells do not get any cells. After 24 hours, the culture media is dumped out and immediately 50 µl of 10% fresh and warm media is added into each well. To the drug wells, 50 µl of 2x concentrated drug solutions is added. The negative wells get 50 µl of just media. After 72 hours, WST-1 dye is prepared and old media is dumped out again. Each well is carefully rinsed with 200 µl HBSS. After rinsing, 200 µl of the WST-1 media is added and incubated for 3 hours. After the incubation period, WST-1 media is removed from the wells and another round of rinsing is carried out. After 5 mins, reading is taken at 540 nm wavelength using blank as the reference.

5.2.2 Calcium mobilization assay

MOLT-4 cell line was used to perform this assay. The assay buffer which comprised of 25 mL HBBS and 0.5 mL HEPES was used to prepare the drug dilutions of various concentrations. 50 µL of drug solutions was added to each well. This was followed by the addition of MOLT-4 cells which were plated in a concentration of 80 µL per well. The cells along with the drug were incubated for 60 minutes at 37^0C. The

reaction buffer which comprised of 5 mL of assay buffer, 100 µL probenecid, and 40 µL Fluo-4 dye was prepared. 50 µL of the reaction buffer was added to the wells followed by incubation for 60 minutes at 37^0C.

The stock solution of the agonist RANTES was prepared by adding 25 µL of the RANTES stock solution and 2.475 mL assay buffer. The RANTES solution was added to all wells except the blank cells, to which only assay buffer was added. The Flex station was used to add RANTES and assay buffer to the wells. The fluorescence emission signal was recorded by the Flex station. The software Prism was used to obtain the IC_{50} values of the antagonists.

6. CONCLUSION

Due to increasing number of cases of prostate cancer every year, and few options for treatment of the advanced stage of disease, it has become imperative to develop new anti-prostate cancer therapeutics. By investigating the role of inflammation and its network in cancer cells, research groups managed to identify overexpression of CCR5 in PCa cell lines. Due to its implication in many other diseases apart from cancer, this receptor became an important target to develop drugs against. Many compounds were identified through high throughput screening. However only a few managed to reach clinical trials and only one– Maraviroc, managed to clear them to reach market. This necessitated the discovery of a novel lead compound that would provide with a fresh perspective on designing an effective antagonist.

Anibamine, a natural CCR5 antagonist that was isolated in 2004 for its anti-microbial properties was found to have the required novel skeleton to develop a new line of drugs. It competed for binding with ^{125}I-gp120, the HIV viral envelope protein to human CCR5 with an IC_{50} of 1μM. The main objective of this project was to use the correlation between CCR5 and prostate cancer to develop new line of drugs based on anibamine. Using this compound as the lead, ten analogues were designed and synthesized. From the total synthesis of anibamine, a new route was designed to accommodate the changes required in the structure.

Intermediate **6** was synthesized using two different schemes. Following that intermediate **14** was prepared at which point the original route deviated to give ten different analogues with a modified side chain as compared to the original lead. Their biological screening was performed to test their ability to inhibit proliferation of PCa cell lines, their cytoxicity and their binding to the receptor.

Anti-proliferation data showed to us that these compounds were more sensitive to DU-145 cell line as compared to PC-3 and M12. Compound **18d** was found to inhibit the proliferation maximum in all the three cell lines. Apart from that among all the compounds **18a** was another compound to cause relatively better inhibition of proliferation. Compounds having a more electronic substitution did not show good inhibition. This proved to us that increasing the polarity in the side chain seemed to decrease the activity of the compound, whereas having a more lipophilic and bulky group was necessary for a better activity. Also since the compound that showed maximum

activity had a chain length closest to the length of the original compound, it was important to maintain the chain length for the activity. Majority of the compounds, save for a few, displayed low toxicity towards normal cells. Out of the compounds that were tested for their inhibition of calcium mobilization, all of them exhibited good antagonistic ability in presence of RANTES with **18a** displaying the best results.

Although a new lead could not be generated due to limited number of analogues, these studies formed a benchmark to further carry on a thorough exploration into the structure activity profile of anibamine. These data along with future modeling studies will help us in designing the third generation of anibamine analogues that will be successful in generating a new lead with a higher potency and a better therapeutic profile.

7. REFERENCES

1. http://www.cancer.gov/cancertopics/treatment/types-of-treatment (accessed 06/26, 2010).
2. Siegel, R.; Ward, E.; Brawley, O.; Jemal, A. Cancer statistics, 2011: the impact of eliminating socioeconomic and racial disparities on premature cancer deaths. *C. A. Cancer J. Clin.* **2011**, *61*, 212-236.
3. Hart, C.A.; Brown, M.; Bagley, S.; Sharrard, M.; Clarke, N.W. Invasive characteristics of human prostatic epithelial cells: understanding the metastatic process. *Br. J. Cancer*,**2005** *92*, 503-512.

4. Foster, S. C.; Bostwick, G. D. *Pathology of the Prostate;* W.B. Saunders Company: Pensylvania, 1998; Vol. 34, pp 443.

5. Nelson, W. G. and De Marzo, A. M.; Isaacs, W.B. Mechanisms of disease: prostate cancer. *N.Engl. J. Med.* **2003**, *349*, 366-381.

6. Silverthorn, D.U.; Ober, W.C.; Garrison, C.W.; Silverthorn, A.C.; Johnson, B.R. Human Physiology: An Integrated Approach, 3rd Ed.; Berriman, L.; Eds.; Pearson Education, Inc., Benjamin Cummings: San Fransico, **2004**; pp 805-810.

7. Algaba, F.; Trias, I.; Arce, Y. Natural History of Prostatic Carcinoma: The Pathologist's Perspective. In *Prostate Cancer*; Ramon, J., Denis, L.J.; Springer-Verlag Berlin Heidelberg: New York, 2001, 9-24.

8. Renshaw, A.A.; Corless, C.L. Prognostic Features in the Pathology of Prostatic Carcinoma. In Prostate Cancer A Multidisciplinary Guide, Kantoff, P.W., Wishnow, K.I., Loughlin, K.R.; Blackwell Science: Massachusetts, 1997, 11-40.

9. Feldman, B.J.; Feldman, D. The development of androgen-independent prostate cancer. *Nature Reviews Cancer* **2001**,*1*,34-45.

10. Ganesh S. Palapattu, Siobhan Sutcliffe, Patrick J. Bastian, Elizabeth A. Platz, Angelo M.De Marzo, William B. Isaacs, William G. Nelson Prostate carcinogenesis and inflammation: emerging insights. *Carcinogenesis* **2004**, *7*, 1170-1181.

11. Reznik, G.; Hamlin, M. H.; Ward, J. M. Prostatic hyperplasia and neoplasia in aging F344 rats. *Prostate* **1981**, *2*, 261-268.

12. Nakayama, M.; Bennette, C. J.; Hicks, J. L.; Epstein, J. I.; Platz, E. A.; Nelson, W. G.; DeMarzo, A. M. Hypermethylation of the human glutathione S-transferase-pi gene (GSTP1) CpG island is present in a subset of proliferative inflammatory atrophy lesions but not in normal or hyperplastic epithelium of the prostate: a detailed study using laser-capture microdissection. *American journal of pathology* **2003**, *163*, 923-933.

13. Shah, R.; Mucci, N. R.; Amin, A.; Macoska, J. A.; Rubin, M. A. Postatrophic hyperplasia of the prostate gland: neoplastic precursor or innocent bystander? *American journal of pathology* **2001**, *158*, 1767-1773.

14. Macoska, J. A.; Trybus, T. M.; Wojno, K. J. *Urology* **2000**, *55*, 776-782.

15. Nelson, W.G.; De Marzo, M.A.; DeWeese, L.T.; Isaacs, B. W. The role of inflammation in the pathogenesis of prostate cancer. *The Journal of Urology* **2004**, *172*, S6-S12.

16. Hart, C.A.; Brown, M.; Bagley, S.; Sharrard, M.; Clarke, N.W. Invasive characteristics of human prostatic epithelial cells: understanding the metastatic process. *Br J Cancer* **2005**,*92*,503-512.

17. Ventura, S.; Oliver, V. L.; White, C. W.; Xie, J. H.; Haynes, J. M.; Exintaris, B. Novel drug targets for the pharmacotherapy of benign prostatic hyperplasia (BPH). *British Journal of Pharmacology* **2011**, *163*, 891-907.

18. Tumm, S.; Hochstrate, H.; St. Grunwald, H. Effect of aging on kinetic parameters of 5-alpha reductase in epethelium and stroma of normal and hyperplastic human prostate. *J. Clin. Endocrinol. Metab.* **1988**, *67*, 979-985.

19. Kreig, M.; Nass, R.; Tumm, S. Effect of aging on endogenous level of 5 alpha-dihydrotestorene, testosterone, estradiol, and estrone in epethelium and stroma of normal and hyperplastic human prostate (BPH). *J. Clin. Endocrinol. Metab.* **1993**, *77*, (in press).

20. Bonkhoff, H.; Remberger, K. Differentiation pathways and histogenetic aspects of normal and abnormal prostatic growth: A stem cell model. *The Prostate* **1996**, *28*, 98-106.

21. Burrows, M. T. *et al*. In Vitro Cultivation of Epithelial Cells Derived from Tumors of the Human Urinary Tract1. *J. Urol.* **1997**, *1*, 3-15.

22. Rhim, J. S. *In vitro* human cell culture models for the study of prostate cancer. *Prostate Cancer and Prostatic Diseases* **2000**, *3*, 229-235.

23. Webber, M. M.; Bello, D.; Quadar, S. Immortalized and tumorigenic adult human prostatic epithelial cell lines: characteristics and applications. Part 1. Cell markers and immortalized nontumorigenic. *The Prostate* **1996**, *29*, 386-394.

24. Webber, M. M.; Bello, D.; Quadar, S. Immortalized and tumorigenic adult human prostatic epithelial cell lines: characteristics and applications. Part 2. Tumorigenic cell lines. *The Prostate* **1997**, *30*, 58-64.

25. Alimirah, F.; Chen, J.; Basrawala, Z.; Xin, H.; Chobey, D. DU-145 and PC-3 human prostate cancer cell lines express androgen receptor: Implications for the androgen receptor functions and regulation. *FEBS Letters* **2006**, *580,* 2294-2300.

26. Jackson-Cook, C.; Bae, V.; Edelman, W.; Brothman, A.; Ware, J. Cytogenetic Characterization of the Human Prostate Cancer Cell Line P69SV40T and its Novel Tumorigenic Sublines M2182 and M15. *Cancer Genet. Cytogenet.* **1996**, *87,* 14-23.

27. Bae, V.; Jackson-Cook, C. K.; Maygarden, S. J.; Plymate, S. R.; Chen, J.; Ware, J. L. Metastatic Sublines of an SV40 Large T Antigent Immortalized Human Prostate Epithelial Cell Line. *The Prostate* **1998**, *34,* 275-282.

28. Bae, V. L.; Jackson-Cook, C. K.; Brothman, A. R.; Maygarden, S. J.; Ware, J. L. Tumorgenicity of SV40 T Antigen Immortalized Human Prostate Epithelial Cells: Association with Decreased Epidermal Growth Factor Receptor (EGFR) Expression. *Int. J. Cancer* **1994**, *58,* 721-729.

29. Balkwill, F.; Mantovani, A. Inflamation and cancer: back to Virchow? *The* **2001**, *357,* 539-545.

30. Dvorak, H. F. Tumors: wounds that do not heal. Similarities between tumor stroma generation and wound healing. *N. Engl. J. Med.* **1986**, *315,* 1650-1659.

31. deVisser, K. E.; Cossens, L. M. The interplay between innate and adaptive immunity regulates cancer development. *Cancer Immunol. Immunother.* **2005**, *54,* 1143-1152.

32. Baniyash, M. TCR zeta-chain down-regulation: curtailing an excessive inflammatory immune response. *Nat. Rev. Immunol.* **2004**, *4,* 675-87.

33. Baniyash, M. Chronic inflammation, immunosuppression and cancer: New insights and outlook. *Seminars in Cancer Biology* **2006**, *16,* 80-88.

34. Coussens, L. M.; Werb, Z. Inflamation and cancer. *Nature* **2002**, *420,* 860-867.

35. Ohshima, H.; Tazawa, H.; Sylla, B. S.; Sawa, T. Prevention of human cancer by modulation of chronic inflammatory processes. *Mutation Research* **2005**, *591*, 110-122.

36. Mantovani, A. Cancer-related inflammation: The seventh hallmark of cancer. *American Society of Clinical Oncology* **2009**, 723-726.

37. Mantovani, A.; Bottazzi, B.; Colotta, F.; Sozzani, S.; Ruco, L. The origin and function of tumor-associated macrophages. *Immunol. Today* **1992**, *13,* 265-270.

38. Mantovani, A.; Bussolino, B.; Dejana, E. Cytokine regulation of endothelial cell function. *FASEB J.* **1992**, *6,* 2591-2599.

39. Lucia, M. S.; Torkko, K. C. Inflammation as a target for prostate cancer chemoprevention: pathological and laboratory rationale. *J. Urol.* **2004**, *171*, S30-S35.

40. Allavena, P.; Sica, A.; Vecchi, A.; Locati, M.; Sozzani, S.; Mantovani, A. The chemokine receptor switch paradigm and dendritic cell migration: it's significance in tumor tissues. *Immunol. Rev.* **2000**, *177,* 141-149.

41. Rahir, G.; Moser, M. Tumor microenvironment and lymphocyte infiltration. *Cancer Immunol. Immunother.* **2012**.

42. O'Hayre, M.; Salanga, C. L.; Handel, T. M.; Allen, S. J. Chemokines and cancer: migration, intracellular signalling and intercellular communication in the microenvironment. *Biochem. J.* **2008**, *409*, 635-649.

43. Fernandez, E.; Lolis, E. Structure, Function, and Inhibition of Chemokines. *Annu. Rev. Pharmacol. Toxicol.* **2002**, *42*, 469-499.

44. Jin, T.; Xu, X.; Hereld, D. Chemotaxis, chemokine receptors and human disease. *Cytokine* **2008**, *44*, 1-8.

45. Schadendorf, D.; Moller, A.; Algermissen, B.; Worm, M.; Sticherling, M.; Czarnetzki, B. M. IL-8 Produced by Human Malignant Melanoma Cells in Vitro Is an Essential Autocrine Growth Factor. *J. Immunol.* **1993**, *151*, 2667-2675.

46. Miyamoto, M.; Shimizu, Y.; Okada, K.; Kashii, Y.; Higuchi, K.; Watanabe, A. Effect of interleukin-8 on production of tumor-associated substances and autocrine growth of human liver and pancreatic cancer cells. *Cancer Immunol. Immunother.* **1998**, *47*, 47-57.

47. Kakinuma, T.; Hwang, S. T. Chemokines, chemokine receptors, and cancer metastasis. *Journal of Leukocyte Biology* **2006**, *79*, 639-651.

48. Barbieri, F.; Bajetto, A.; Florio, T. Role of chemokines network in the development and progression of ovarian cancer: A potential novel pharmacologicl target. *Journal of Oncology* **2009**, *2010*, 1-15.

49. Opdenakker, G.; Van Damme, J. Cytokines and Proteases in Invasive Processes: Molecular Similarities Between Inflammation and Cancer. *Cytokine* **1992**, *4*, 251-258.

50. VanDamme, J.; Struyf, S.; Opdenakker, G. Chemokine-protease interactions in cancer. *Semin. Cancer Biol.* **2004**, *14*, 201-208.

51. Vindrieux, D.; Escobar, P.; Lazennec, G. Emerging roles of chemokines in prostate cancer. *Endocr. Relat. Cancer* **2009**, *16*, 663-673.

52. Murphy, C.; McGurk, M.; Pettigrew, J.; Santinelli, A.; Mazzucchelli, R.; Johnston, P. G.; Montironi, R.; Waugh, D. J. Nonapical and cytoplasmicexpression of interleukin-8, CXCR1, and CXCR2 correlates with cell proliferation and microvessel density in prostate cancer. *Clin Cancer Res.* **2005**, *11*, 4117-4127.

53. Schauer, I. G.; Ressler, S. J.; Tuxhorn, J. A.; Dang, T. D.; Rowley, D. R. Elevated epithelial expression of interleukin-8 correlates with myofibroblast reactive stroma in benign prostatic hyperplasia. *Urology* **2008**, *72*, 205-213.

54. Nagpal, M. L.; Davis, J.; Lin, T. Overexpression of CXCL10 in human prostate LNCaP cells activates its receptor (CXCR3) expression and inhibits cell proliferation**.**. *Biochim. Biophys. Acta.* **2006**, *1762*, 811-818.

55. Ferrer, F. A.; Miller, L. J.; Andrawis, R. I.; Kurtzman, S. H.; Albertsen, P. C.; Laudone, V. P.; Kreutzer, D. L. Angiogenesis and prostate cancer: in vivo and in

vitro expression of angiogenesis factors by prostate cancer cells. *Urology* **1998**, *51,* 161-167.

56. Engl, T.; Relja, B.; Blumenberg, C.; Müller, I.; Ringel, E. M.; Beecken, W. D.; Jonas, D.; Blaheta, R. A. Prostate tumor CXC-chemokine profile correlates with cell adhesion to endothelium and extracellular matrix. *Life Sci.* **2006**, *78(16),* 1784-1793.

57. Aalinkeel, R.; Nair, M. P.; Sufrin, G.; Mahajan, S. D.; Chadha, K. C.; Chawda, R. P.; Schwartz, S. A. Gene expression of angiogenic factors correlates with metastatic potential of prostate cancer cells. *Cancer Res.* **2004**, *64,* 5311-5321.

58. Lu, Y.; Cai, Z.; Xiao, G.; Liu, Y.; Keller, E. T.; Yao, Z.; Zhang, J. CCR2expressioncorrelates with prostate cancerprogression. *J. Cell. Biochem.* **2007**, *101,* 676-685.

59. Schwarze, S. R.; Luo, J.; Isaacs, W. B.; Jarrard, D. F. Modulation of CXCL14 (BRAK) expression in prostate cancer. *Prostate* **2005**, *64,* 67-74.

60. Zhang, S.; Qi, L.; Li, M.; Zhang, D.; Xu, S.; Wang, N.; Sun, B. Chemokine CXCL12 and its receptorCXCR4expression are associated with perineural invasion of prostate cancer. *J. Exp. Clin. Cancer Res.* **2008**, *27,* 62.

61. Appay, V.; Rowland-Jones, S. L. RANTES: a versatile and controversial chemokine. *Trends Immunol.* **2001**, *22,* 83-87.

62. Wang, J. M.; Deng, X.; Gong, W.; Su, S. Chemokines and their role in tumor growth and metastatis. *J. Immunol. Meth.* **1998**, *220,* 1-17.

63. Robinson, S. C.; Scott, K. A.; Wilson, J. L.; Thompson, R. G.; Proudfoot, A. E.; Balkwill, F. R. A chemokine receptor antagonist inhibits experimental breast tumor growth. *Cancer Res.* **2003**, *63*, 8360-8365.

64. König, J. E.; Senge, T.; Allhoff, E. P.; König, W. Analysis of the inflammatory network in benign prostate hyperplasia and prostate cancer. *Prostate* **2004**, *58*, 121-129.

65. Chensue, W. S. Molecular Machinations: Chemokines Signals in Host-Pathogen Interactions. *Clin. Microbiol. Rev.* **2001**, *14*, 821-835.

66. Ruddon, R. *Cancer Biology;* Oxford University Press: New York, 2007.; Vol. 4th ed.

67. Wu, X.; Lee, V.; Chevalier, E.; Hwang, S. Chemokine Receptors as Targets forCancer Therapy. *Current Pharmaceutical Design* **2009**, *15*, 742-757.

68. Bennett, L.; Fox, J. M.; Signoret, N. Mechanisms regulating chemokine receptor activity. *Immunology* **2011**, *134*, 246-256.

69. Paterlini, M. G. Structure modeling of the chemokine receptor CCR5: implications for ligand binding and selectivity. *Biophys. J.* **2002**, *83*, 3012-3031.

70. deBrevern, A. G.; Wong, H.; Tournamille, C.; Colin, Y.; Le, V. K. C.; Etchebest, C. A structural model of a seven-transmembrane helix receptor: the Duffy antigen/receptor for chemokine (DARC). *Biochim. Biophys. Acta.* **2005**, *1724(3)*, 288-306.

71. Berkhout, T. A.; Blaney, F. E.; Bridges, A. M.; Cooper, D. G.; Forbes, I. T.; Gribble, A. D.; Groot, P. H.; Hardy, A.; Ife, R. J.; Kaur, R.; Moores, K. E.; Shillito, H.; Willetts, J.; Witherington, J. CCR2: characterization of the antagonist binding site from a combined receptor modeling/mutagenesis approach. *J. Med. Chem.* **2003**, *46*, 4070-4086.

72. Castonguay, L. A.; Weng, Y.; Adolfsen, W.; Di Salvo, J.; Kilburn, R.; Caldwell, C. G.; Daugherty, B. L.; Finke, P. E.; Hale, J. J.; Lynch, C. L.; Hwang, S. Binding of 2-aryl-4-(piperidin-1-yl)butanamines and 1,3,4-trisubstituted pyrrolidines to human CCR5: a molecular modeling-guided mutagenesis study of the binding pocket. *Biochemistry* **2003**, *42*, 1544-1550.

73. Reiter, E.; Lefkowitz, R. J. GRKs and beta-arrestins: roles in receptor silencing, trafficking and signaling. *Trends Endocrinol. Metab.* **2006**, *17*, 159-165.

74. Lefkowitz, R. J.; Whalen, E. J. beta-arrestins: traffic cops of cell signaling. *Curr. Opin. Cell Biol.* **2004**, *16*, 162-168.

75. Neel, N. F.; Schutyser, E.; Sai, J.; Fan, G. H.; Richmond, A. Chemokine receptor internalization and intracellular trafficking. *Cytokine Growth Factor Rev.* **2005**, *16*, 637-658.

76. Chensue, W. S. Molecular Machinations: Chemokines Signals in Host-Pathogen Interactions. *Clin. Microbiol. Rev.* **2001**, *14*, 821-835.

77. Jöhrer, K.; Pleyer, L.; Olivier, A.; Maizner, E.; Zelle-Rieser, C.; Greil, R. Tumour-immune cell interactions modulated by chemokines. *Expert Opin. Biol. Ther.* **2008**, *8*, 269-290.

78. Ribeiro, S.; Horuk, R. The clinical potential of chemokine receptor antagonists. *Pharmacol. Ther.* **2005**, *107*, 44-58.

79. Slettenaar, V. I.; Wilson, J. L. The chemokine network: a target in cancer biology? *Adv. Drug Deliv. Rev.* **2006**, *58*, 962-974.

80. Zlotnik, A. Chemokines and cancer. *Int. J. Cancer* **2006**, *119*, 2026-2029.

81. Ben-Baruch, A. Organ selectivity in metastasis: regulation by chemokines and their receptors. *Clin. Exp. Metastasis* **2008**, *25*, 345-356.

82. Raport, C.; Gosling, J.; Schweickart, V.; Gray, P.; Charo, I. Molecular cloning and functional characterization of a novel human CC chemokine receptor (CCR5) for RANTES, MIP-1beta, and MIP-1alpha. *J. Biol. Chem.* **1996**, *271*, 17161-17166.

83. Deng, D.; Liu, R.; Ellmeier, W.; Choe, S.; Unutmaz, D.; Burkhart, M.; DiMarzio, P.; Marmon, S.; Sutton, R.E.; Hill, C.M. *et al.* Identification of a major co-receptor for primary isolates of HIV-1. *Nature.* **1996**, 381, 661-666.

84. Feng, Y.; Broder, C.C.; Kennedy, P.E.; Berger, E.A. HIV-1 entry cofactorfunctional cDNA cloning of a seven-transmembrane G protein–coupled receptor. *Science*. **1996**, 272, 872–877.

85. Field, J.; Nikawa, J.; Broek, D.; MacDonald, B.; Rodgers, L.; Wilson, I. A.; Lerner, R. A.; Wigler, M. Purification of a RAS-responsive adenylyl cyclase complex from Saccharomyces cerevisiae by use of an epitope addition method. *Mol. Cell Biol.* **1988**, *8*, 2159-2165.

86. Oppermann, M. Chemokine receptor CCR5: insights into structure, function, and regulation. *Cellular Signaling* **2004**, *16*, 1201-1210.

87. Aramori, I.; Ferguson, S. S.; Bieniasz, P. D.; Zhang, J.; Cullen, B.; Cullen, M. G. Molecular mechanism of desensitization of the chemokine receptor CCR-5: receptor signaling and internalization are dissociable from its role as an HIV-1 co-receptor. *EMBO J.* **1997**, *16*, 4606-4616.

88. Zhao, J.; Ma, L.; Wu, Y. L.; Wang, P.; Hu, W.; Pei, G. Chemokine receptor CCR5 functionally couples to inhibitory G proteins and undergoes desensitization. *J. Cell. Biochem.* **1998**, *71*, 36-45.

89. Li, Z.; Jiang, H.; Xie, W.; Zhang, Z.; Smrcka, A. V.; Wu, D. Roles of PLC-2 and -3 and PI3K in Chemoattractant-Mediated Signal Transduction . *Science* **2000**, *287*, 1046-1049.

90. Kraft, K.; Olbrich, H.; Majoul, I.; Mack, M.; Proudfoot, A.; Oppermann, M. Characterization of sequence determinants within the carboxyl-terminal domain of chemokine receptor CCR5 that regulate signaling and receptor internalization. *J. Biol. Chem.* **2001**, *276*, 34408-34418.

91. Jones, K.; Maquire, E.; Davenport, A. Chemokine receptor CCR5: from AIDS to atherosclerosis. *British Journal of Pharmacology* **2011**, *162*, 1453-1469.

92. Berger, E. A.; Murphy, P. M.; Farber, J. M. Chemokine receptors as HIV-1 coreceptors: roles in viral entry, tropism, and disease. *Annu. Rev. Immunol.* **1999**, *17*, 657-700.

93. Berkhout, B.; Eggink, D.; Sanders, R. W. Is there a future for antiviral fusion inhibitors? *Curr. Opin. Virol.* **2012**, *1*, 50-59.

94. Littman, D. R. Chemokine Receptors: Keys to AIDS Pathogenesis? *Cell* **1998**, *93*, 677-680.

95. Baba, M.; Takashima, K.; Miyake, H.; Kanzaki, N.; Teshima, K.; Wang, X.; Shiraishi, M.; Iizawa, Y. TAK-652 inhibits CCR5 mediated Human Immunodeficiency Virus Type 1 infection In Vitro and has favorable pharmacokinetics in humans. *Antimicrobial Agents and Chemotherapy* **2005**, *49*, 4584-4591.

96. Palani, A.; Shapiro, S.; Clader, J.; Greenlee, W.; Blythin, D.; Cox, K.; Wagner, N.; Strizki, J.; Baroudy, B.; Dan, N. Biological evaluation and interconversion studies of rotamers of SCH 351125, an orally bioavailable CCR5 antagonist. *Bioorganic & Medicinal Chemistry Letters* **2003**, *13*, 705-708.

97. Shiraishi, M.; Aramaki, Y.; Seto, M.; Imoto, H.; Nishikawa, Y.; Kanzaki, N.; Okamoto, M.; Sawada, H.; Nishimura, O.; Baba, M.; Fujino, M. Discovery of novel, potent, and selective small-molecule CCR5 antagonists as anti-HIV-1

agents: synthesis and biological evaluation of anilide derivatives with a quaternary ammonium moiety. *J. Med. Chem.* **2000**, *43*, 2049-2063.

98. Trkola, A.; Ketas, T. J.; Nagashima, K. A.; Zhao, L.; Cillier, T.; Morris, L.; Moore, J. P.; Maddon, P. J.; Olson, W. C. Potent, Broad-Spectrum Inhibition of Human Immunodeficiency Virus Type 1 by the CCR5 Monoclonal Antibody PRO 140. *J. Virol.* **2001**, *75*, 579-588.

99. Reeves, J. D.; Piefer, A. J. Emerging drug targets for antiretroviral therapy. *Drugs* **2005**, *13*, 1747-1766.

100. Youngs, S. J.; Ali, S. A.; Taub, D.; Rees, R. C. Chemokines Induce Migrational Responses In Human Breast Carcinoma Cell Lines. *Int. J. Cancer* **1997**, *71*, 257-266.

101. Luboshits, G.; Shina, S.; Kaplan, O.; Engelberg, S.; Nass, D.; Lifshitz-Mercer, B.; Chaitchik, S.; Keydar, I.; Ben-Baruch A. Elevated Expression of the CC Chemokine Regulated on Activation, Normal T Cell Expressed and Secreted (RANTES) in Advance Breast Carcinoma. *Cancer Res.* **1999**, *59*, 4681-4687.

102. Vaday, G. G.; Peehl, D. M.; Kadam, P. A.; Lawrence, D. M. Expression of CCL5 (RANTES) and CCR5 in prostate cancer. *Prostate* **2006**, *66*, 124-134.

103. Baba, M.; Nishimura, O.; Kanzaki, N.; Okamoto, M.; Sawada, H.; Iizawa, Y.; Shiraishi, M.; Aramaki, Y.; Okonogi, K.; Ogawa, Y.; Meguro, K.; Fujino, M. A small-molecule, nonpeptide CCR5 antagonist with highly potent and selective anti-HIV-1 activity. *Proc. Natl. Acad. Sci.* **1999**, *88*, 2356-2360.

104. Westby, M.; Van der Ryst, E. CCR5 antagonists: host-targetted antiviral agents for the treatment of HIV infection, 4 years on. *Antiviral Chemistry & Chemotherapy* **2010**, *20*, 179-192.

105. Newman, D. J.; Cragg, G. M.; Snader, K. M. Natural products as sources of new drugs over the period 1981-2002. *J. Nat. Prod.* **2003**, *66*, 1022-1037.

106. Clardy, J. and Walsh, C. Lessons from natural molecules. *Nature* **2004**, *432*, 829-837.

107. Jayasuriya, H.; Herath, K. B.; Ondeyka, J. G.; Polishook, J. D.; Bills, G. F.; Dombrowski, A. W.; Springer, M. S.; Siciliano, S.; Malkowitz, L.; Sanchez, M.; Guan, Z.; Tiwari, S.; Stevenson, D. W.; Borris, R. P.; Singh, S. B. Isolation and structure of antagonists of chemokine receptor (CCR5). *J. Nat. Prod.* **2004**, *67*, 1036-1038.

108. Zhang, X.; Haney, K.; Richardson, A.; Wilson, E.; Gewirtz, D.; Ware, J.; Zehner, Z.; Zhang, Y.; Anibamine, a natural product CCR5 antagonist, as a novel lead for the development of anti-prostate cancer agents. *Bioorganic & Medicinal Chemistry Letters*, **2010**, *20*, 4627-4630.

109. Zhang, X.; Haney, K. M.; Richardson, A. C.; Wilson, E.; Gewirtz, D. A.; Ware, J. L.; Zehner, Z. E.; Zhang, Y. Anibamine, a natural product CCR5 antagonist, as a novel lead for the development of anti-prostate cancer agents. *Bioorg. Med. Chem. Lett.* **2010**, *20*, 4627-4630.

110. Li, G.; Haney, K. M.; Kellogg, G. E.; Zhang, Y. Comparative docking study of anibamine as the first natural product CCR5 antagonist in CCR5 homology models. *J. Chem. Inf. Model.* **2009**, *49*, 120-132.

111. Li, G.; Watson, K.; Buckheit, R. W.; Zhang, Y. Total synthesis of anibamine, a novel natural product as a chemokine receptor CCR5 antagonist. *Org. Lett.* **2007**, *9*, 2043-2046.

112. Haney, K. M.; Zhang, F.; Arnatt, C. K.; Yuan, Y.; Li, G.; Ware, J. L.; Gewirtz, D. A.; Zhang, Y. The natural product CCR5 antagonist anibamine and its analogs as anti-prostate cancer agents**.** *Bioorg. Med. Chem. Lett.* **2011**, *21*, 5159-5163.

113. Schenone, P.; Mosti, L.; Menozzi, G. Reaction of 2-Dimethylaminomethylene-1,3-diones with dinucleophiles. I.Synthesis of 1,5-disubstituted 4-acylpyrazoles. *J. Heterocycl. Chem*. **1982**, *19*, 1355-1361.

114. Menozzi, G.; Schenone, P.; Mosti, L. Reaction of 2-Dimethyaminomethylene-1,3-diones with dinucleophiles. II. Synthesis of 5-(alkyl)(phenyl)-4-acylsoxazoles and 6,7-dihydro-1,2-benisoxazol-4(5*H*)-ones. *J. Heterocycl. Chem*. **1983**, *20*, 645-648.

115. Alberola, A.; Antolin, L. F.; Gonzalez, M. A.; Laguna, M. A.; Pulido, F. J. Base-induced cleavage of 4-functionalized-3-unsubstituted isoxazoles. Synthesis of 5-aminoazoles and 4-cyanoazoles. *J. Heterocycl. Chem*. **1987**, *25*, 393-397.

116. Alberola, A.; Antolin, L. F.; Gonzalez, M. A.; Pulido, F. J. Base-induced cleavage of 4-functionalized-3-unsubstituted isoxazoles. Synthesis of 2-aminopyrimidines and pyrimidine-2-(3*H*)-thiones. *J. Heterocycl. Chem.* **1986**, *23*, 1035-1038.

117. Haley, C. A. C. and Maitland, M. Organic reactions in aqueous solution at room temperature. Part I. The influence of pH on condensations involving the linking of carbon to nitrogen and of carbon to carbon. *J. Chem. Soc.* **1951**, 3155-3174.

118. Mal, P.; Lourderaj, U.; Parveen; Venugopalan, P.; Moorthy, N. J.;Sathyamurthy, N. Conformational control and photoenolization of pyridine-3-carboxaldehydes in the solid state: Stabilization of photoenols via hydrogen bonding and electronic control. *J. Org. Chem.* **2003**, *68*, 3446-3453.

119. Friedman, L. and Shechter, H. Dimethylformamide as a useful solvent in preparing nitriles from aryl halides and cuprous cyanide; improved isolation techniques. *J. Org. Chem.* **1961**, *26*, 2522-2524.

120. Kato, Y.; Okada, S.; Tomimoto, K.; Mase, T. A facile bromination of hydroxyheteroarenes. *Tetrahedron Lett.* **2001**, *42*, 4849-4851.

121. Dahan, A. and Portnoy, M. Synthesis of homo- and heteroprotected furcated units for modular chemistry. *J. Org. Chem.* **2001**, *66*, 6480-6482.

122. Lautens, M. and Yoshida, M. Rhodium-catalyzed addition of arylboronic acids to alkynyl aza-heteraromatic compounds in water. *J. Org. Chem.* **2003**, *68*, 762-769.

123. Heffner, R. J.; Jiang, J. J.; JoulliG, M. M. Total synthesis of (-)-nummularine F. *J. Am. Chem. Soc.* **1992**, *114*, 10181-10189.

124. Han, S.; Kim, Y. Recent development of peptide coupling reagents in organic synthesis. *Tetrahedron* **2004**, *60*, 2447-2467.

125. Jenkins, D. J.; Riley, A. M.; Potter, B. V. L. Chiral cyclopentane-based mimics of D-Myo-Inositol 1,4,5-triphosphate from D-glusoce.

126. Bates, R. W. and Boonsombat, J. The pyridinium reduction route to alkaloids: a synthesis of (±)-tashiromine. *J. Chem. Soc., Perkin Trans.* **2001**, *1*, 654-656.

127. Cell proliferation reagent WST-1. **2011** accessed from www.roche-applied-science.com.

128. Mailman, R. GPCR functional selectivity has therapeutic impact. *Trends. Pharmacol. Sci.* **2007**, *28*, 390-396.